To the Graduate Council:

I am submitting herewith a dissertation written by Robert Alonzo Yokley entitled "The Photochemistry of Polycyclic Aromatic Hydrocarbons Adsorbed on the Surface of Coal Fly Ash." I have examined the final copy of this dissertation for form and content and recommend that it be accepted in partial fulfillment of the requirements for the degree of Doctor of Philosophy, with a major in Chemistry.

Gleb Mamantov, Major Professor

Earl L. Wehry, Major Professor

We have read this dissertation
and recommend its acceptance:

Accepted for the Council:

The Graduate School

# THE PHOTOCHEMISTRY OF POLYCYCLIC AROMATIC HYDROCARBONS ADSORBED ON THE SURFACE OF COAL FLY ASH

A Dissertation

Presented for the

Doctor of Philosophy

Degree

The University of Tennessee, Knoxville

Robert Alonzo Yokley

March 1985

# DEDICATION

To the memory of my father.

# ACKNOWLEDGMENT

The author wishes to express his sincere gratitude and deepest appreciation to Dr. Gleb Mamantov and Dr. Earl L. Wehry for their guidance, advice, and encouragement during the course of this work. Their high level of excellence is a model to be emulated.

Appreciation is also extended to the University of Tennessee for a Teaching Assistantship during three and one half years, and the Department of Energy for financial assistance for the research.

Further, the author expresses his indebtedness to Mr. George McGhee for typing, Mr. Dewey Lee for the porosity measurements, Mr. L. H. Norman and Arthur Pratt of the glassblowing shop, and Mr. Bobby Lay, Mr. Darrell Lay, Mr. Roy Hodge, Mr. Clax Hallman, and Mrs. Teresa Shock of the Chemistry Stores Stockroom. Their help and friendship will always be remembered.

A major project such as this can only be accomplished with the assistance and support of coworkers. Advice from Dr. Arlene Garrison and Dr. Ron Hohmann was invaluable.

Finally, the author wishes to express his love and gratitude to his mother, wife, and daughter. Without the love and encouragement of his wife, the author would never have attended graduate school.

# ABSTRACT

The fate of airborne particulate-associated polycyclic aromatic hydrocarbons is a problem of substantial concern, especially since recent observations indicate that the mutagenicity of organic extracts from sampled airborne particulate matter cannot be related solely to the presence of polycyclic aromatic hydrocarbons (PAHs). Reactions between particulate-associated PAHs and gaseous species, such as $O_2$, $O_3$, $SO_2$, and $NO_2$, either photochemically or non-photochemically, may be responsible for this excess mutagenicity.

The chemical reactivity of the PAHs pyrene and benzo(a)pyrene, adsorbed on coal fly ash surfaces, has been examined. Eight fly ashes, of varying origin and composition, were used as substrates for the adsorbed PAHs. Samples were subjected to micro-soxhlet extraction, before and after illumination by a solar spectrum-simulating lamp, and then quantified by ultraviolet absorption and fluorescence spectroscopy. Some of the samples were stored in the dark and then reextracted while other samples were exposed to $NO_2$ and $HNO_3$, as well as illumination. Many of these samples were subjected to direct-probe mass spectrometry.

Coal fly ash tends to stabilize pyrene and benzo(a)pyrene against photochemical transformations as compared with the same compounds adsorbed on silica gel, alumina, or glass. Non-photochemical transformations are so slow that their environmental significance is negligible. It appears that $HNO_3$ is required, either as a reactant or as a catalyst, for nitration of coal fly ash-associated PAHs,

photochemically or non-photochemically, when the adsorbed PAHs are exposed to $NO_2$.

It appears that carbon content and absorbance (or color) of coal fly ash are significant factors affecting the photochemical behavior of adsorbed PAHs. Furthermore, it appears that ambient atmospheric $HNO_3$ concentrations may be sufficient for nitration of particulate-associated PAHs; many of the nitro-PAHs are extremely mutagenic compounds.

TABLE OF CONTENTS


| CHAPTER | | PAGE |
|---|---|---|
| I. | INTRODUCTION | 1 |
| | A. Formation of Polycyclic Aromatic Hydrocarbons | 1 |
| | B. Carcinogenicity of Polycyclic Aromatic Hydrocarbons | 1 |
| | C. Carcinogenicity and Mutagenicity of Organic Extracts of Airborne Particulate Matter | 4 |
| | D. Sources of PAHs | 5 |
| | E. Atmospheric Gaseous Pollutants | 5 |
| | F. Size Distribution of Coal Fly Ash | 8 |
| | G. Morphology of Coal Fly Ash | 13 |
| | H. Elemental Composition of Coal Fly Ash | 15 |
| | I. Photochemical and Non-Photochemical Behavior of PAHs | 20 |
| | J. Objectives of this Study | 29 |
| II. | EXPERIMENTAL | 31 |
| | A. Polycyclic Aromatic Hydrocarbons | 31 |
| | B. Substrates | 31 |
| | C. Adsorption Apparatus | 36 |
| | D. Irradiation Experiments | 41 |
| | E. Photoreactor | 45 |
| | F. Analytical Methods for PAHs | 48 |
| | 1. Extractions | 48 |
| | 2. Ultraviolet Absorption Spectroscopy | 50 |
| | 3. Fluorescence Spectrometry | 50 |
| | 4. Direct-Probe Mass Spectrometry | 55 |
| | G. pH Measurements | 57 |

CHAPTER PAGE

II. (Continued)

H. Total % Carbon . . . . . 57

I. Porosity and Surface Area Measurements . . . . . 58

J. Diffuse Reflectance Measurements . . . . . 58

K. Techniques for Pollutant Gas Studies . . . . . 58

L. Selected Wavelength Irradiation Experiments . . . . . 63

III. RESULTS AND DISCUSSION OF PHOTOCHEMICAL AND NON-PHOTOCHEMICAL TRANSFORMATIONS . . . . . 64

A. Initial Vapor-Adsorption Experiments . . . . . 64

B. Comparisons of Different Extraction Techniques . . . . . 72

C. Non-Photochemical Transformation . . . . . 78

D. Irradiation Experiments with "PAH-coated" Substrates . . . 87

E. Attempted Identification of Photochemical Products . . . . 95

F. Chemical and Physical Characteristics of Various Substrates . . . . . 122

G. Surface Area and Porosity of Adsorbents . . . . . 130

H. Selected Wavelength Irradiation Experiments . . . . . 159

IV. INTERACTIONS OF PARTICULATE-ASSOCIATED PAH WITH GASEOUS $NO_2$ . 167

A. Non-Photochemical Reactions of Pyrene With $NO_2$ . . . . . 167

B. Non-Photochemical Reactions of Benzo(a)pyrene With $NO_2$ . . 184

C. Photochemical Reactions of Adsorbed PAHs in the Presence of Gaseous $NO_2$ . . . . . 189

V. SUMMARY AND CONCLUSIONS . . . . . 200

LIST OF REFERENCES . . . . . 206

APPENDIX . . . . . 214

VITA . . . . . 218

# LIST OF TABLES

TABLE PAGE

1. Percentage of Benzo(a)pyrene Emissions from various sources . . . . . 6
2. Trace Gaseous Pollutants Identified Spectroscopically in Ambient Southern California Air and Approximate Concentration Ranges Observed in Light to Severe Episodes of Photochemical Air Pollution . . . . . 7
3. Relative Abundance (%) of Morphologic Particle Classes in Four Fly Ash Fractions . . . . . 14
4. The Four Main Phases of Fly Ash . . . . . 16
5. Typical Matrix Element Composition of Some U.S. Coal Fly Ashes Expressed as Weight Percentage of the Oxide . . . . . 17
6. Elemental Composition of Commercial Fly Ash Samples Based on Weight Percentage of Oxide Equivalents . . . . . 33
7. Bulk Composition of Fly Ashes Expressed as Weight Percentage of Oxide Equivalents . . . . . 34
8. Phases Present in Fly Ash Samples . . . . . 35
9. Concentration of Pyrene Solutions Obtained by Bubbling Diffusion Cell Effluent through Toluene . . . . . 65
10. Results of Pyrene Adsorption Capacity of East Tennessee Coal Fly Ash Experiment . . . . . 67
11. Semi-Quantitative Level of Difficulty for "Coating" Various Substrates at the 100 µg/g Level . . . . . 71
12. Extraction Efficiency of Three Techniques . . . . . 75

TABLE PAGE

13. Comparison of Micro-Soxhlet and Sonication Extraction Efficiency . . . . . 77

14. Non-Photochemical Behavior of Pyrene Adsorbed on Various Substrates . . . . . 80

15. Non-Photochemical Behavior of Pyrene Adsorbed on Coal Fly Ashes . . . . . 81

16. Non-Photochemical Behavior of Benzo(a)pyrene Adsorbed on Various Substrates . . . . . 83

17. Non-Photochemical Behavior of Benzo(a)pyrene Adsorbed on Coal Fly Ashes . . . . . 85

18. Qualitative Summary of Non-Photochemical Experiments . . . . . 86

19. Photochemical Behavior of Pyrene Adsorbed on Various Substrates . . . . . 88

20. Quantification (in μg PAH/g Substrate) of Extracts Before and After Rotation Under Vacuum of "PAH-Coated" Substrates in the Dark as Compared to Their Photochemical Behavior . . . . 90

21. Photochemical Behavior of Pyrene Adsorbed on Coal Fly Ashes . . . . . 91

22. Photochemical Behavior of Benzo(a)pyrene Adsorbed on Various Substrates . . . . . 92

23. Photochemical Behavior of Benzo(a)pyrene Adsorbed on Coal Fly Ashes . . . . . 93

24. Qualitative Summary of Photochemical Experiments . . . . . 94

TABLE PAGE

25. Mass and Relative Abundance of Each Ion Obtained From the Mass Spectrum of Texas Lignite Coal Fly Ash (Sieved To $\leq$ 45 μm) . . . . . 96

26. Mass and Relative Abundance of Each Ion Obtained from the Mass Spectrum of Degassed (24 hr) Texas Lignite Coal Fly Ash . . . . . 97

27. Mass and Relative Abundance of Each Ion Obtained from the Mass Spectrum of "Pyrene-Coated" Texas Lignite Coal Fly Ash . . . . . 99

28. Mass and Relative Abundance of Each Ion Obtained from the Mass Spectrum of Irradiated "Pyrene-Coated" Texas Lignite Coal Fly Ash . . . . . 100

29. Mass and Relative Abundance of Each Ion Obtained from the Mass Spectrum of "Pyrene-Coated" Alumina . . . . . 102

30. Mass and Relative Abundance of Each Ion Obtained from the Mass Spectrum of Irradiated "Pyrene-Coated" Alumina . . . . . 103

31. Mass and Relative Abundance of Each Ion Obtained from the Mass Spectrum of "Benzo(a)pyrene-Coated" New Mexico Subbituminous Coal Fly Ash . . . . . 110

32. Mass and Relative Abundance of Each Ion Obtained from the Mass Spectrum of Irradiated "Benzo(a)pyrene-Coated" New Mexico Subbituminous Coal Fly Ash . . . . . 111

33. Mass and Relative Abundance of Each Ion Obtained from the Mass Spectrum of "Benzo(a)pyrene-Coated" Alumina . . . . . 112

TABLE PAGE

34. Mass and Relative Abundance of Each Ion Obtained from the Mass Spectrum of Irradiated "Benzo(a)pyrene-Coated" Alumina . . . . . 113

35. Mass and Relative Abundance of Each Ion Obtained from the Mass Spectrum of "Benzene(a)pyrene-Coated" Texas Lignite Coal Fly Ash . . . . . 114

36. Mass and Relative Abundance of Each Ion Obtained from the Mass Spectrum of Irradiated "Benzo(a)pyrene-Coated" Texas Lignite Coal Fly Oil . . . . . 115

37. Mass and Relative Abundance of Each Ion Obtained from the Mass Spectrum of "Benzo(a)pyrene-Coated" Commercial Fly Ash (Lot No. 720-1) . . . . . 117

38. Mass and Relative Abundance of Each Ion Obtained from the Mass Spectrum of Irradiated "Benzo(a)pyrene-Coated" Commercial Fly Ash (Lot No. 720-1) . . . . . 118

39. Chemical and Physical Characteristics of Various Substrates . . 123

40. Absorbance of Various Substrates Listed in 5 nm Increments Over the 400 to 250 nm Range as Determined by Diffuse Reflectance Spectroscopy . . . . . 127

41. The Specific Surface Area and c Constant as Determined by the BET Gas Adsorption Method . . . . . 144

42. The Various Types of Adsorption-Desorption Isotherms for Various Substrates as Determined by the BET Gas Adsorption Method . . . . . 147

TABLE PAGE

43. Adsorption Pore Volume Distribution and Pore Volume Maxima of Various Substrates Subjected to the BET Gas Adsorption Method . . . . . 155

44. Surface Characteristics of Various Substrates as Evaluated from the Observed Experimental Data . . . . . 157

45. The Results of Micro-Soxhlet Extraction Results for "Benzo(a)pyrene-Coated" Cobalt Glass and Controlled Porosity Glass Substrates Before and After Illumination at 365 and 284 Nanometers . . . . . 164

46. Results of Micro-Soxhlet Extractions of "PAH-Coated" Substrates Before and After Exposure to 95 ppm $NO_2$ ($HNO_3$ Present) for 20 Minutes . . . . . 168

47. Mass Versus Relative Abundance Data Obtained from the Mass Spectrum of "Pyrene-Coated" Texas Lignite Coal Fly Ash After Exposure to $NO_2$ ($HNO_3$ Present) . . . . . 170

48. Isotopic Abundance Calculations for Selected Data from the Mass Spectrum of "Pyrene-Coated" Texas Lignite Coal Fly Ash that had been Exposed to 95 ppm $NO_2$ ($HNO_3$ Present) for 20 Minutes . . . . . 171

49. The Mass and Relative Abundance Data Obtained from the Mass Spectrum of Pure 1-Nitropyrene . . . . . 172

50. The Mass and Relative Abundance Data Obtained from the Mass Spectrum of Pure 3-Nitropyrene . . . . . 173

TABLE PAGE

51. Mass and Relative Abundance of Ions of Interest from the Mass Spectra of "Pyrene-Coated" Texas Lignite Coal Fly Ash, 1-Nitropyrene, and 3-Nitropyrene . . . . . 175

52. Results of Extracting and Analyzing Nylon Filters for the Presence of Nitrate After a One Hour Exposure to 95 ppm $NO_2$ . . . . . 182

53. Results of Extracting and Analyzing Nylon Filters that have not been Exposed to $NO_2$ . . . . . 183

54. Micro-Soxhlet Extraction Results of "PAH-Coated" Substrates Before and After Exposure to 95 ppm $NO_2$ ($HNO_3$ Absent) in the Dark for One Hour . . . . . 185

55. Results of Micro-Soxhlet Extraction of "Pyrene-Coated" Substrates Before and After Exposure to 12 ppm $NO_2$ ($HNO_3$ Absent) and Illumination for 24 Hours . . . . . 190

56. The Mass and Relative Abundance of Each Ion Obtained from the Mass Spectrum of Irradiated "Pyrene-Coated" Silica Gel Exposed to 12 ppm $NO_2$ ($HNO_3$ thought not to be present) . . . 192

57. The Mass and Relative Abundance of Each Ion Obtained from the Mass Spectrum of Illuminated "Pyrene-Coated" Silica Gel in the Presence of 12 ppm (fresh nylon wool so $HNO_3$ is not present) . . . . . 197

58. The Results of Micro-Soxhlet Extraction of "Benzo(a)Pyrene-Coated" Substrates Before and After Exposure to 12 ppm $NO_2$ ($HNO_3$ absent) and Illumination for 24 Hours . . . . . 198

# LIST OF FIGURES

FIGURE PAGE

1. The Action of Mixed Function Oxidases on Benzo(a)pyrene to Form the Carcinogenic Metabolite 7,8-diol-9,10-epoxide . . . 3
2. (Left). Summary of Differential Size Distributions at the Outlets of Six Utility Boilers..(Right). Expanded View of the Submicrometer Mode Region of Figure on Left . . . . . 10
3. Plot of Particle Diameter Versus Fraction Deposited for Three Different Areas of the Lungs . . . . . 12
4. Ion Microprobe Depth Profiles for Pb and Tl in Unleached and Leached Fly Ash Samples . . . . . 19
5. The Polycyclic Aromatic Hydrocarbons Studied in this Work . . . 21
6. Block Diagram of the Vapor-Deposition Apparatus . . . . . 37
7. Generator and Diffusion Tube . . . . . 39
8. Expanded Bed Reactor . . . . . 40
9. Cermax Lamp Output (Manufacturer's Literature) . . . . . 42
10. Spectrum of Sunlight . . . . . 43
11. Quartz Irradiation Cell . . . . . 44
12. Block Diagram of Irradiation Apparatus . . . . . 46
13. Photoreactor . . . . . 47
14. Absorption Spectrum for Pyrene (0.65 ppm) Dissolved in Methanol . . . . . 51
15. Absorption Spectrum for Benzo(a)pyrene (0.48 ppm) Dissolved in Methanol . . . . . 52
16. Beer's Law Plot for Pyrene Dissolved in Methanol . . . . . 53
17. Beer's Law Plot for Benzo(a)pyrene Dissolved in Methanol . . . 54

FIGURE PAGE

18. Fluorescence Spectrum of Pyrene Dissolved in Toluene . . . . . 56

19. Block Diagram of Pollutant Gas Experiments Using the Photoreactor . . . . . 60

20. Plot of Pyrene Extract Concentration Versus Time . . . . . 69

21. Plot of Logarithim of Percentage Recovery versus Percentage of HF . . . . . 74

22. Ultraviolet-Visible Adsorption Spectra of the Concentrated Micro-Soxhlet Extracts (in Acetonitrile) of "Pyrene-Coated" Alumina (a) After and (b) Before Irradiation . . . . 107

23. Ultraviolet-Visible Adsorption Spectra of the Concentrated Micro-Soxhlet Extracts (in Acetonitrile) of "Pyrene-Coated" Texas Lignite Coal Fly Ash (a) After and (b) Before Irradiation . . . . . 108

24. Absorption Spectra of (a) Benzo(a)pyrene, (b) Irradiated (24 hr) "Benzo(a)pyrene-Coated" Controlled Porosity Glass, and (c) Unirradiated "Benzo(a)pyrene-Coated" Controlled Porosity Glass . . . . . 120

25. Diffuse Reflectance Spectrum of Silica Gel . . . . . 125

26. Graphical Representation of Data obtained from the Diffuse Reflectance Spectra of (a) Western Kentucky Bituminous, (b) Kaneb, (c), East Tennessee Bituminous, (d) New Mexico Subbituminous, and (e) Texas Lignite Coal Fly Ashes and, (f) Silica Gel . . . . . 129

27. Adsorption Isotherm Curves of $n/n_m$ versus $P/P^0$. (A) c=1; (B) c=11; (C) c=100; (D) c=10,000 . . . . . 136

FIGURE PAGE

28. The Six Types of Adsorption Isotherms According to the classification of Brunauer, Deming, Deming, and Teller (BDDT) . . . . . 138

29. Types of Hysteresis Loops . . . . . 140

30. The Adsorption-Desorption Isotherm for Controlled Porosity Glass Obtained by Plotting Data Collected by the BET Method . 148

31. The Adsorption-Desorption Isotherm for Texas Lignite Coal Fly Ash, Obtained by Plotting Data Collected by BET Method . 149

32. "T-Plots" for (a) East Tennessee Bituminous and (b) Texas Lignite Coal Fly Ashes, Obtained by Plotting Data Collected by the BET Method . . . . . 151

33. "T-Plots" for (a) Controlled Porosity Glass and (b) Brown Glass Bottle, Obtained by Plotting Data Collected by the BET method . . . . . 152

34. The Adsorption Pore Volume Distribution of (a) Controlled Porosity Glass and (b) Texas Lignite Coal Fly Ash, Obtained by Plotting Data Collected by the BET Method . . . . . 154

35. (a) Transmittance Spectrum of a Cobalt Glass Plate (2 mm thick that had not been pulverized) and, (b) Absorption Spectrum of Benzo(a)pyrene Dissolved in Methanol. Arrows refer to the two wavelengths used in the Selected Wavelength Irradiation Experiment . . . . . 160

FIGURE PAGE

36. Bar Graph of Direct-Probe Mass Spectral Data (From Mass 10 to Mass 320) Collected for (a) 1-Nitropyrene, (b) 3-Nitropyrene and, (c) "Pyrene-Coated" Texas Lignite Coal Fly Ash after exposure to 95 ppm $NO_2$ ($HNO_3$ Present) for 20 min in the dark . . . . . 176

37. Absorption Spectrum of a Micro-Soxhlet Extract of "Pyrene-Coated" Texas Lignite Coal Fly Ash after a 20 min exposure to $NO_2$ and $HNO_3$ . . . . . 177

38. Absorption Spectrum of 1-Nitropyrene Dissolved in Methanol (about 14 ppm) . . . . . 179

39. Absorption Spectrum of 3-Nitropyrene Dissolved in Methanol (about 15 ppm) . . . . . 180

# CHAPTER I

# INTRODUCTION

## A. Formation of Polycyclic Aromatic Hydrocarbons

Polycyclic aromatic hydrocarbons (PAH) are one of several classes of compounds which, when associated with environmental samples, are collectively known as "polycyclic organic matter" (POM). POM is formed during the incomplete combustion of organic matter and the chemical reactions leading to its formation are thought to proceed by free-radical pathways.[1,2] Radical chain propagation is enhanced by the presence of a chemically reducing atmosphere (common in the center of flames) and leads to the buildup of a complex PAH molecule.[3] Pyrolysis of low-molecular-weight hydrocarbons, such as methane, can lead to the formation of complex hydrocarbons, but yields are enhanced when higher-molecular-weight starting materials, such as coal, are used.[4]

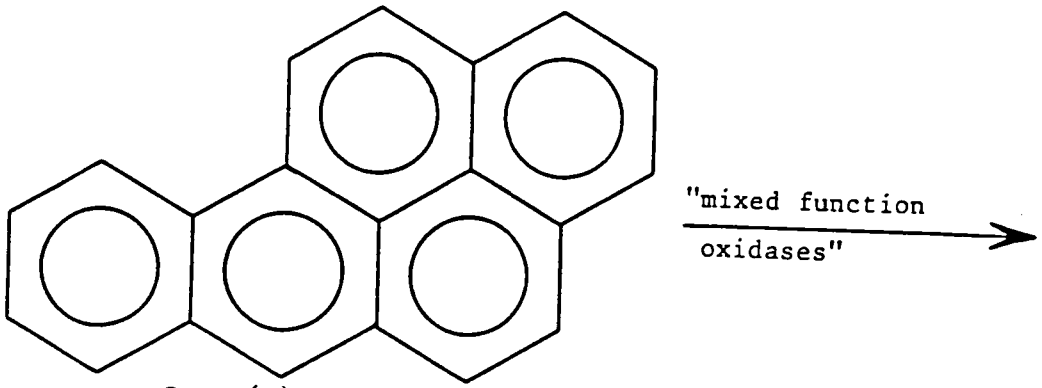
## B. Carcinogenicity of Polycyclic Aromatic Hydrocarbons

The carcinogenic PAHs have been studied for a long time and are some of the most potent carcinogens known. In 1775, Pott[5] suggested that the high incidence of scrotal cancer in chimney sweeps was a result of their occupational exposure to soot. Since that time there has been increasing interest in determining the mode of action of PAH in causing human cancer.

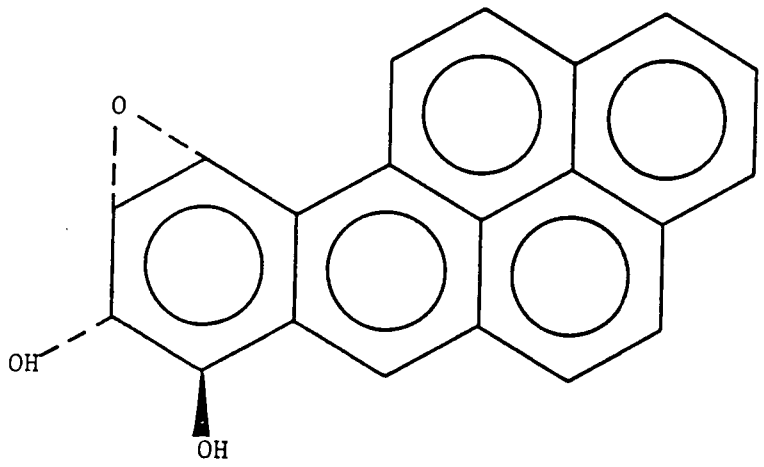
There is considerable evidence that metabolism is required for the expression of carcinogenic potential of PAH (i.e., the PAH is actually a precursor of the actual carcinogen). The primary product of

PAH metabolism is initially an epoxide or, in the case of alkyl-substituted PAH, direct introduction of a hydroxyl group on a saturated carbon atom of the substituent.[6] Carcinogenic activity is related to the structure of the parent carcinogen, since the carcinogenic process is initiated by converting the parent compound to a reactive metabolite. Sims, et al.,[7] were able to formulate the DNA-binding metabolite of benzo(a)pyrene as a 7,8-dihydrodiol-9,10-epoxide (Figure 1). Their results indicate that an isolated double bond in the 9,10-position of benzo(a)pyrene leads to the metabolic formation of a 9,10-epoxide and the epoxide formed in this position reacts effectively with cellular DNA. The dihydrodiols that are precursors of this type of epoxide are common hydrocarbon metabolites. In the case of twelve PAHs (including benzo(a)pyrene) for which the mutagenic activity of appropriate dihydrodiols has been monitored, the dihydrodiol exhibits Ames assay activity equal to or greater than that of the parent hydrocarbon for ten of the compounds.[7] The Ames test is essentially a determination of the number of mutations resulting from the addition of the chemical agent to be studied to a mutant-free bacterial cell culture, and is now generally recognized as a useful screening test for chemical mutagens in complex environmental samples.

It is possible that another metabolite, in addition to the bay-region (unusual chemical reactivity associated with the benzylic position of a saturated angular benzo-ring) dihydrodiol-epoxide or some specific reactive metabolite precursor, such as a carbonium ion,[8] may be required for tumor initiation. It would be particularly beneficial if the bay-region dihydrodiol-epoxide route of metabolism could be




Benzo(a)pyrene




7,8-diol-9,10-epoxide

Figure 1. The Action of Mixed Function Oxidases on Benzo(a)pyrene to Form the Carcinogenic Metabolite 7,8-diol-9,10-epoxide.[7]

circumvented by, for example, some, as yet, unknown dietary factor.[9] Obviously, further documentation is needed to fully understand the mechanisms by which PAHs induce tumors, but it appears clear that oxygenated derivatives of many PAHs may be especially hazardous compounds.[10-13]

## C. Carcinogenicity and Mutagenicity of Organic Extracts of Airborne Particulate Matter

Interest in the fate of airborne POM has increased due to observations that the mutagenicity and carcinogenicity of organic extracts from sampled airborne particulate matter cannot be related solely to the presence of adsorbed PAHs.[14-16] This "excess" mutagenic and carcinogenic behavior implies that compounds other than PAHs, as yet uncharacterized, must also be present as adsorbates on some (if not all) airborne particulate samples. Furthermore, it is now known that extracts of ambient POM contain direct-acting mutagens[17-19] (i.e., species that exhibit mutagenic activity in the absence of metabolic activation). The identities of these direct-acting mutagens in combustion-generated POM are either unknown or only tentatively established. Some PAHs, such as benzo(a)pyrene, are extremely potent carcinogens, but (as described above) these compounds require metabolism to express carcinogenicity.

Because of the "excess" mutagenicity of organic extracts of sampled airborne particulate matter, it will be useful to examine the sources of PAHs, as well as other possible airborne pollutants.

## D. Sources of PAHs

There are many sources of PAHs, including stationary and non-stationary sources. The major sources of PAHs are combustion of fossil fuel for heat and power production,[20,21] coke production,[22] transportation (motor vehicles),[23] and open refuse burning.[7] Table 1 shows estimated percentages of benzo(a)pyrene emissions from each source.[9] Since the combustion of coal produces about 20-25% of all particulate matter released into the atmosphere in the United States, the use of coal for heat and power production is expected to represent a significant source of PAHs associated with particulate matter. By 1995 the utility demand for coal is expected to increase by 900 million tons per year to supply fuel for 337,000 megawatts of new electrical generating capacity.[24] The significance of PAH emission as a result of coal combustion is even more pronounced when one considers that almost all airborne PAHs consisting of four fused rings or more, e.g. benzo(a)pyrene, are associated with particulate matter, such as soot, diesel exhaust, and coal fly ash, rather than existing in the gaseous state.[25-27]

## E. Atmospheric Gaseous Pollutants

Along with the emission of coal fly ash and particle-associated PAHs during coal combustion there also are produced various nitrogen-containing pollutants. Some of these gaseous pollutants and their approximate atmospheric concentrations are listed in Table 2.[23] These concentrations can be higher in highly industrialized areas and under

TABLE 1

PERCENTAGE OF BENZO(a)PYRENE EMISSIONS FROM VARIOUS SOURCES[9]

| | |
|---|---|
| Heat and Power Generation | 37 to 38% |
| Open Refuse Burning | 42 to 46% |
| Coke Production | 15 to 19% |
| Motor Vehicles | 1 to 1.5% |

TABLE 2

TRACE GASEOUS POLLUTANTS IDENTIFIED SPECTROSCOPICALLY IN AMBIENT SOUTHERN CALIFORNIA AIR AND APPROXIMATE CONCENTRATION RANGES OBSERVED IN LIGHT TO SEVERE EPISODES OF PHOTOCHEMICAL AIR POLLUTION[23]

| Compound | Range of Peak Concentrations | Time of Peak Concentrations |
|---|---|---|
| Nitric acid ($HONO_2$) | 1-50 ppb | Midafternoon |
| Peroxyacetylnitrate (PAN) | 1-40 ppb | Midafternoon |
| Nitrous acid (HONO) | 1-8 ppb | Early morning (before sunrise) |
| Nitrate radical ($NO_3$) | 5-350 ppt | Night |
| Formaldehyde (HCHO) | 1-80 ppb | Midafternoon |
| Formic acid (HCOOH) | 1-20 ppb | Midafternoon |
| Nitrogen dioxide ($NO_2$) | 0.1-0.8 ppm | Morning/ afternoon |

atmospheric conditions conducive to higher concentrations, such as stagnant pockets of air.

As a result of the combustion of sulfur-containing coal, sulfur oxides are also released into the atmosphere. The original species formed are largely $SO_2$ and, to a lesser extent, $SO_3$.[28] Although the $SO_2$ concentration of clean dry air is only about 2 ppb (parts per billion),[27] highly industralized areas experience considerably higher concentrations. Sulfur oxides have been linked to the acid-rain problem.

Although ozone ($O_3$) is not considered a pollutant, its possible reactions with PAHs adsorbed on airborne particulate matter cannot be eliminated as a possible source for carcinogenic and mutagenic compounds, since these reactions lead to oxidized PAHs. The $O_3$ concentration of clean dry air is typically about 20 ppb.[29]

Pitts[23] has stated his belief that "either directly or through complex chemical and biological interactions, certain of these gaseous pollutants may contribute to both the nononcogenic and oncogenic (tumor producing) health impacts of primary exhaust systems and of ambient smog."

## F. Size Distribution of Coal Fly Ash

Since most of the PAHs emitted from a coal-fired power plant are presumed to deposit on the surface of fly ash (coal typically contains 2 to 30% noncombustible mineral material which leads to the by-product fly ash), it is necessary that the interactions between the PAHs and fly ash be more fully understood. If the interactions between PAHs and

fly ash can be correctly elucidated, it may become possible to develop the control technology necessary to reduce the release of fly ash and the associated PAHs into the atmosphere. It will, therefore, be necessary to consider some of the physical and chemical characteristics of fly ash.

Figure 2 summarizes the particle size distribution for fly ash emitted from six utility boilers of various configurations.[24] In this work, cascade impactors were used to measure size distributions of particles above about 0.3 micrometer in diameter and electrical aerosol analyzers were used to measure size distributions of particles below 0.5 micrometer in diameter. It appears from this plot that, regardless of the design or megawatt output of the boilers, the particle-size distribution tends to be bimodal. The maxima in the particle-size distribution tend to fall into one of two categories: either a submicrometer mode (particles approximately 0.1 μm in diameter) or a large-particle mode (particle sizes greater than 0.5 μm). Most of the mass of the coal fly ash (97.8 to 99.8%) is collected in the hopper and/or the electrostatic precipitator or other stack particle collection device. However, over 80% of the particles on a numerical basis have diameters equal to or less than 1 micrometer; these particles tend to escape into the atmosphere since the collection efficiencies of control devices for submicrometer particles are at a minimum. These submicrometer particles also have a longer residence time (4 to 40 days in dry air) in the atmosphere than do the larger, 1-10 micrometer diameter particles (0.5 to 4 days in dry air).[30]

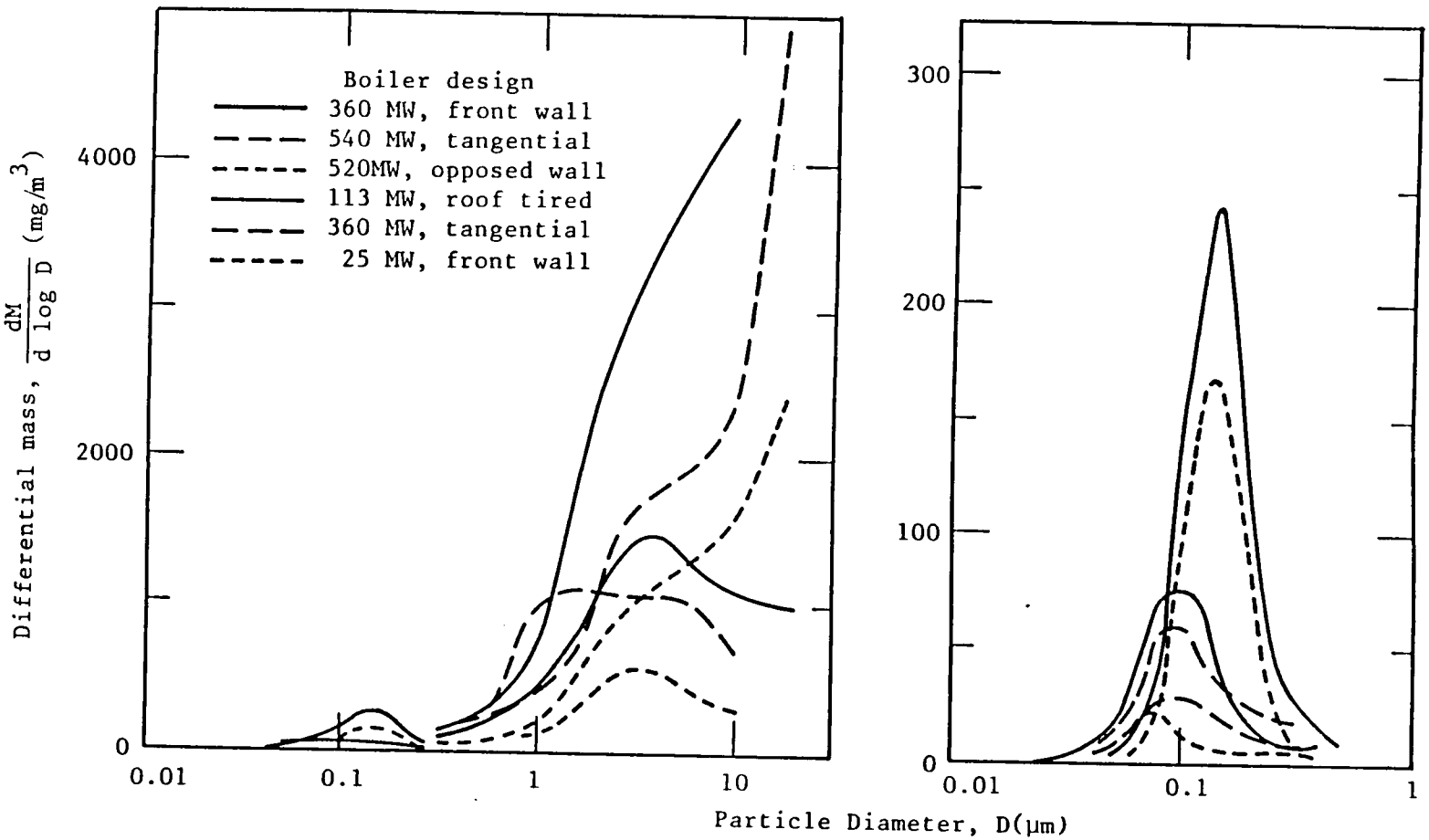



Figure 2. (Left). Summary of Differential Size Distributions at the Outlets of Six Utility Boilers. (Right). Expanded View of the Submicrometer Mode Region of Figure on Left.[24]

Figure 3 shows how particles are distributed into the lungs upon inhalation, as a function of particle diameter. Particle size is presented in terms of the diameter of an equivalent spherical particle of unit density. This means that the particle diameters plotted in Figure 3 do not correspond to a physical diameter as determined by a Coulter counter or an electron microscope.[31] From Figure 3 one can see that a larger fraction of particles are deposited into the pulmonary and tracheobronchial regions of the lungs for particles of small diameter.

Particles that are deposited in the nasopharyngeal and tracheobronchial regions of the respiratory tract do not remain there for extended periods of time since such particles are normally removed to the pharynx and swallowed within a matter of hours. The extraction of any toxic species, therefore, will take place predominantly in the stomach where their residence time is short.[32] Particles deposited in the pulmonary regions, however, may remain there for weeks or even years.[33] There is, therefore, a higher probability of extracting any organic and/or inorganic species associated with the smaller particles into the physiological fluids of the human body. The health effects would, of course, depend on the species associated with the smaller particles, and the concentration of those species. Since the smaller particles have higher specific surface areas (surface area per unit mass) than the larger particles, the smaller particles may have higher concentrations of species adsorbed on their surface, and also greater exposure of the adsorbed species to physiological fluids may occur.

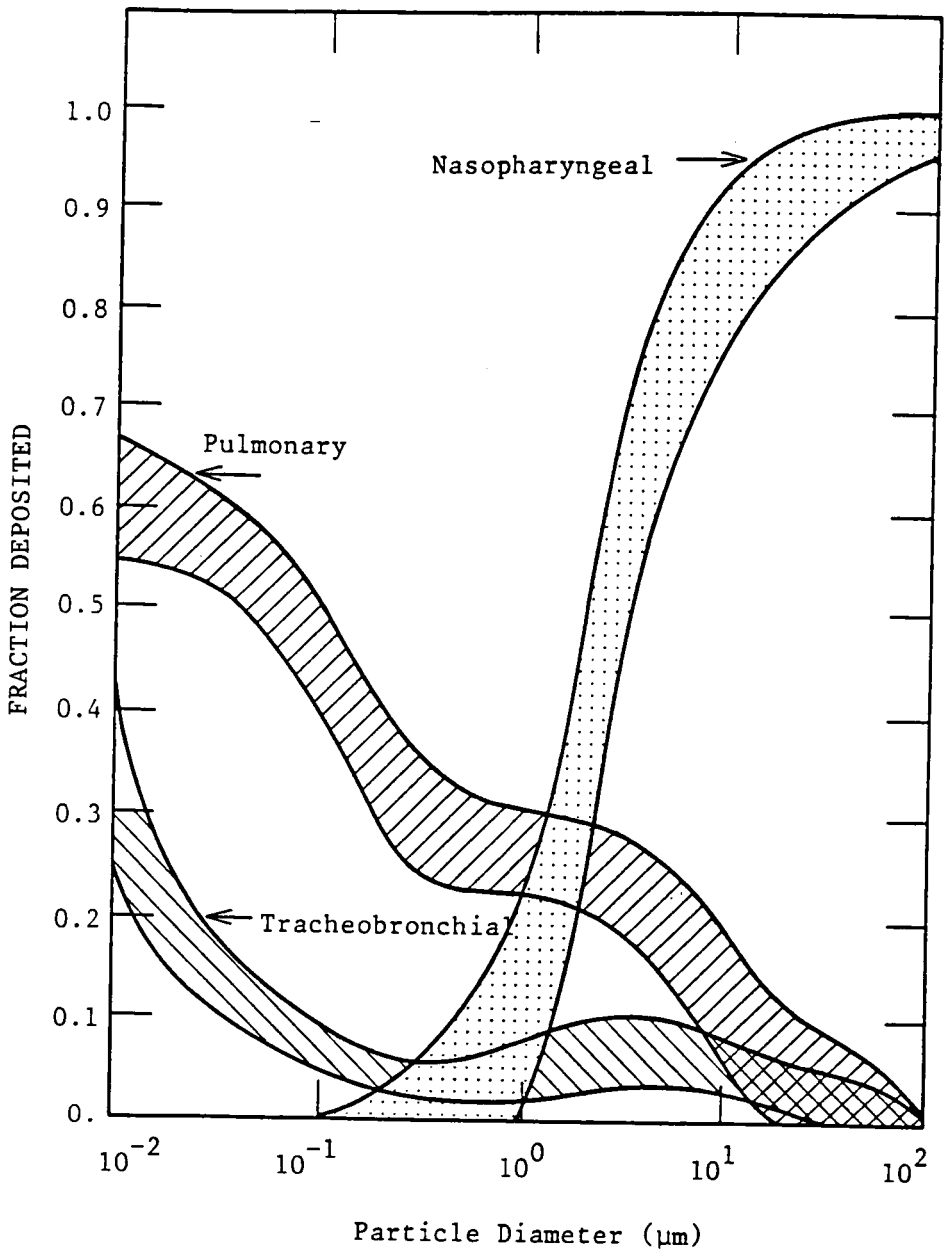



Figure 3. Plot of Particle Diameter Versus Fraction Deposited for Three Different Areas of the Lungs.[31]

Because of the major implications associated with respirable particles, the Environmental Protection Agency has recently proposed to change the focus of the particulate matter standard from controlling all airborne particles to controlling inhalable particles (diameters of 10 micrometer or less).[34] This proposed regulatory change has engendered considerable controversy.

## G. Morphology of Coal Fly Ash

Scanning electron microscopy (SEM) has revealed that coal fly ash is a very complex, inhomogeneous mixture of a wide variety of particle shapes, sizes, and colors.[35,36] Light microscopy (LM)[37] has been used to define eleven major classes of coal fly ash particles which are listed in Table 3. These classes of coal fly ash particles were defined by the characteristics of opacity, shape, and type of inclusions, and the relative abundances shown in Table 3 were determined by LM counting to assess the relative contribution of each morphologic class to the respective size fraction.

Spherical particles make up most of the fly ash, especially in the small particle diameter portions (see Table 3). These spheres are glassy and mostly transparent. Some of the spheres are hollow ("cenospheres"), and some are filled with other spheres ("plerospheres"), amorphous particles, and/or crystals. The few opaque spheres are mostly magnetite or other iron oxide particles. The variation in color of coal fly ash particles is presumably due to varying concentrations of iron oxides and carbon. Particles with similar morphologies may,

TABLE 3

RELATIVE ABUNDANCE (%) OF MORPHOLOGIC PARTICLE CLASSES IN FOUR FLY ASH FRACTIONS[37]

| Particle class | Fraction 1 (Range)[a] | 2 (Range) | 3 (Range) | 4 (Range) |
|---|---|---|---|---|
| A. Amorphous, nonopaque | 7.25(5.62) | 2.13(0.95) | 0.79(0.50) | 0.33(0.52) |
| B. Amorphous, opaque | 0.42(0.13) | 0.18(0.20) | • • • | • • • |
| C. Amorphous, mixed opaque and nonopaque | 0.77(0.71) | 0.09(0.20) | • • • | • • • |
| D. Rounded, vesicular, nonopaque | 12.39(2.61) | 6.67(3.00) | 2.91(0.10) | 2.99(1.58) |
| E. Rounded, vesicular, mixed opaque and nonopaque | 2.27(0.40) | 0.24(0.09) | • • • | 0.03(0.10) |
| F. Angular, lacy, opaque | 1.34(0.33) | 0.57(0.51) | 0.27(0.14) | 0.33(0.10) |
| G. Nonopaque, cenosphere | 41.41(6.36) | 26.22(3.50) | 13.20(5.44) | 7.91(2.02) |
| H. Nonopaque, plerosphere | 0.51(0.27) | 0.21(0.34) | • • • | • • • |
| I. Nonopaque, solid sphere | 25.58(0.34) | 56.01(0.67) | 79.16(6.02) | 86.99(4.76) |
| J. Opaque sphere | 1.56(0.83) | 0.90(0.96) | 0.33(0.12) | 0.24(0.21) |
| K. Nonopaque sphere with crystals | 6.80(3.64) | 6.79(1.25) | 3.18(0.05) | 0.95(1.44) |
| L. Combined particle classes B and F[b] | • • • | • • • | 0.15(0.09) | 0.24(0.19) |

[a]Range of average abundance from three samples.

[b]Combined due to inability to distinguish between these classes for the finer particles.

however, have dramatically different elemental morphologies may, compositions.

Table 4 lists the four "main" phases of coal fly ash and their characteristic empirical formulas, distinguished experimentally[35] by their solubility in varying concentrations of HF and HCl. The magnetic spinel phase can be separated from the rest of the fly ash by using a magnet, and has a high Fe content. The carbon phase is usually the result of inefficient combustion and will, of course, vary in concentration depending on the combustion parameters of temperature and exposure time. The glass phase is almost entirely composed of $SiO_2$, but there are varying concentrations of other species such as almost all group I and II elements. The mullite-quartz phase is composed of aluminum oxides as well as the silicon oxides.

## H. Elemental Composition of Coal Fly Ash

Table 5 shows the typical bulk composition of coal fly ash as reported by several workers.[38-40] Several instrumental techniques have been used to characterize coal fly ash, including neutron activation analysis (NAA), x-ray fluorescence (XRF), atomic absorption spectroscopy (AAS) after dissolution of the fly ash, secondary ion mass spectrometry (SIMS), electron spectroscopy for chemical analysis (ESCA), and Auger electron spectroscopy (AES).[41-48] Coal fly ash contains almost every element in the periodic table. The most dominant elements are Al, Fe, Si, O, and C along with significant concentrations of Ca, K, Mg, Na, and Ti.[31]

TABLE 4

THE FOUR MAIN PHASES OF FLY ASH[35]

| Phase | Formula | Solubility |
|---|---|---|
| Carbon | C | Insoluble in HF |
| Glass | $SiO_2$ | Soluble in 1% HF |
| Magnetic Spinel | $Fe_{2.3}Al_{0.7}O_4$ | Soluble in Concentrated HCl |
| Mullite-Quartz | $2Al_2O_3 \cdot SiO_2$ to $3Al_2O_3 \cdot 2SiO_2$ | Soluble in 48% HF after several days |

TABLE 5

TYPICAL MATRIX ELEMENT COMPOSITION OF SOME U.S. COAL FLY ASHES EXPRESSED AS WEIGHT PERCENTAGE OF THE OXIDE[38]

| $Al_2O_3$ | $SiO_2$ | $Fe_2O_3$ | CaO | $K_2O$ |
|---|---|---|---|---|
| 14-30 | 22-60 | 3-21 | 0.5-31 | 0.2-3.5 |

Spectroscopic analysis has provided evidence that some trace elements (e.g. As, Pb, Se) tend to increase in concentration with decreasing particle size.[43,49] Most of the mass of these elements is concentrated in the particle size range 0.5 to 10.0 micrometer. Some trace elements (e.g. Cr, Pb, Tl) are more concentrated at the particle surface than in the bulk of the particle.[48] Surface analytical techniques such as ion microprobe mass spectrometry (IMMS) and AES were used to obtain depth profiling information while spark source mass spectrometry (SSMS) and solvent leaching were used to obtain bulk concentrations of various coal fly ash particles. Figure 4 shows a plot of relative intensity versus depth (Å) obtained by IMMS (depth increased with time). It appears from these data that the concentrations of Pb and Tl decrease dramatically only a few Ångstroms into the particle. The combination of these techniques for analyses of coal fly ash particles showed that Pb and Tl were present at concentrations of only 620 and 30 ppm on the basis of bulk analysis but reached respective concentrations of 4% and 4500 ppm near the particle surfaces.

The fact that the smaller particles have a longer residence time in the atmosphere, a higher specific surface area, and an increased concentration of some toxic metals at the surface of the particles, leads one to believe that the possible adverse health effects of the smaller particles are much more pronounced than previously thought (based on bulk analysis). Furthermore, the smaller particles have a higher fraction deposited into the pulmonary region of the lungs which increases the efficiency of extraction of the toxic metals into the physiological fluids of the body.

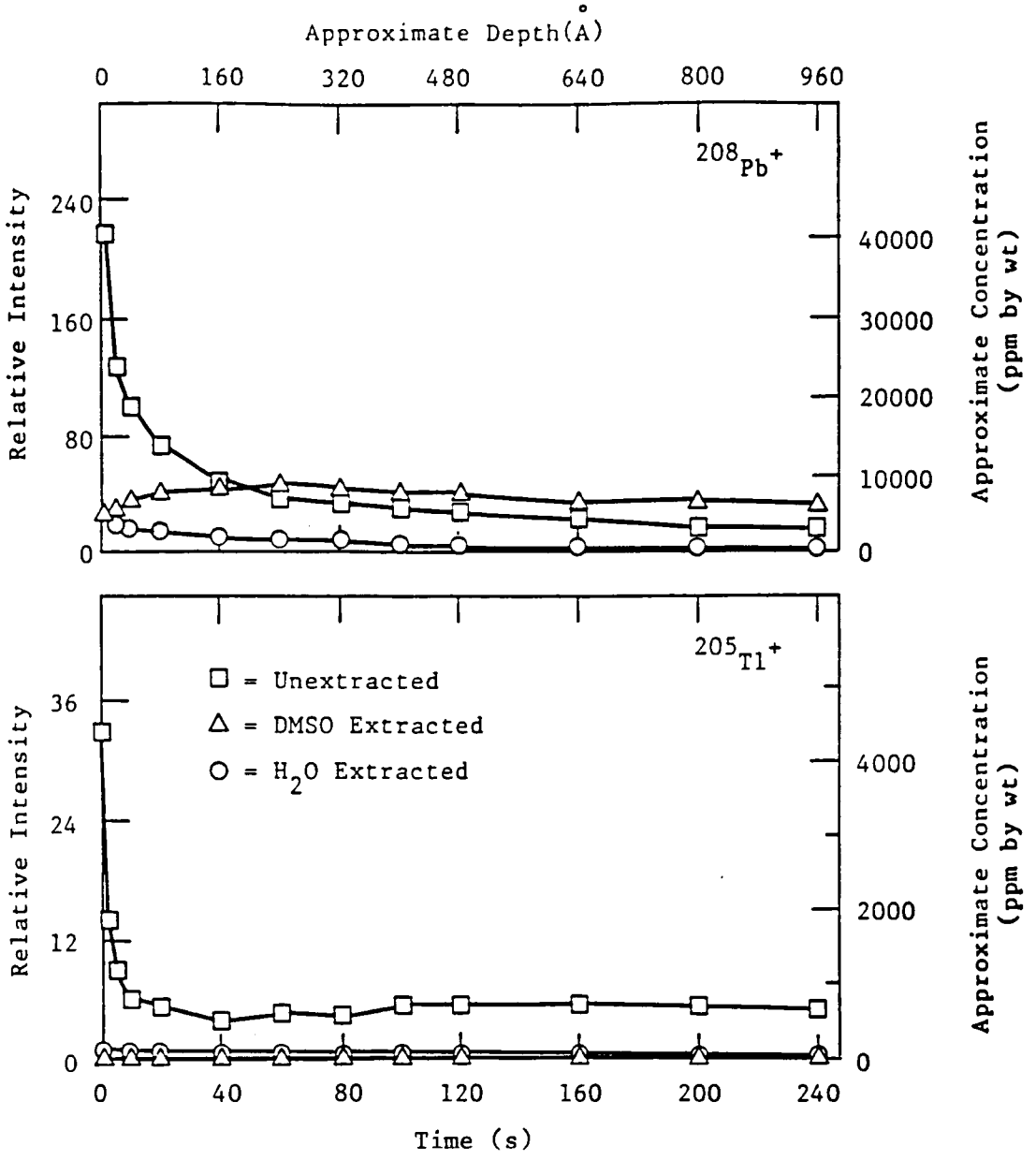
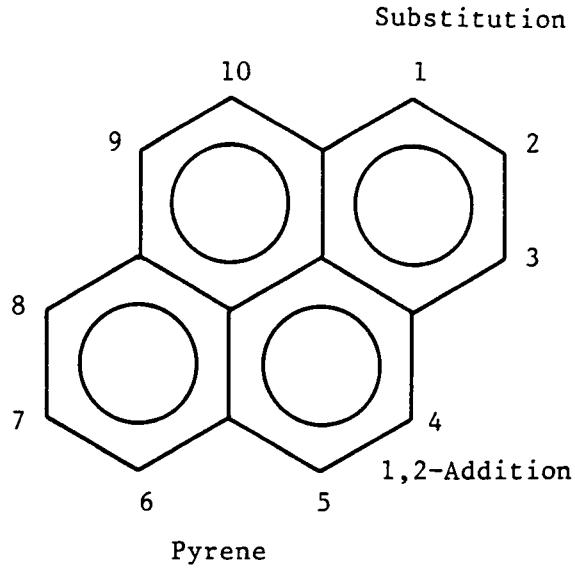



Figure 4. Ion Microprobe Depth Profiles for Pb and Tl in Unleached and Leached Fly Ash Samples.[48]

Since PAHs are adsorbed on the surface of coal fly ash,[20,50-54] the possibility also exists for extraction of the PAHs into the physiological fluids of the body. One must also consider that the uncharacterized "excess" mutagens and carcinogens are also extracted. It is, therefore, necessary to understand the interactions between PAHs and coal fly ash as well as the interactions between PAHs adsorbed on fly ash and other atmospheric constituents. To make an accurate assessment of these interactions, it will also be necessary to learn the extent to which coal fly ash surfaces affect the photochemical and non-photochemical behavior of PAHs. The presence of water vapor, sunlight, and chemical species such as $NO_2$, $SO_2$, and $O_3$, leads to reactions of PAHs, some of which are photochemical and some thermal in nature.

## I. Photochemical and Non-Photochemical Behavior of PAHs

Figure 5 shows the structures of pyrene and benzo(a)pyrene as well as the positions where certain types of chemical reactions are most likely to occur. Many PAHs, when in solution, undergo photochemical change upon irradiation.[55] Benzo(a)pyrene, dissolved in benzene in the presence of $O_2$, undergoes photodecomposition leading to the products 6,12-benzo(a)pyrenequinone, 1,6-benzo(a)pyrenequinone, and possibly 3,6-benzo(a)pyrenequinone when irradiated with an ultraviolet light source of wavelength greater than 280 nanometers.[56] In the presence of ozone, benzo(a)pyrene, dissolved in methylene chloride and methylene chloride-methanol (3:1) mixtures, photodecomposes to form 1,6-benzo(a)pyrenequinone, 3,6-benzo(a)pyrenequinone, and 4,5-benzo(a)-pyrenequinone.[57] The photochemical products of pyrene in solution



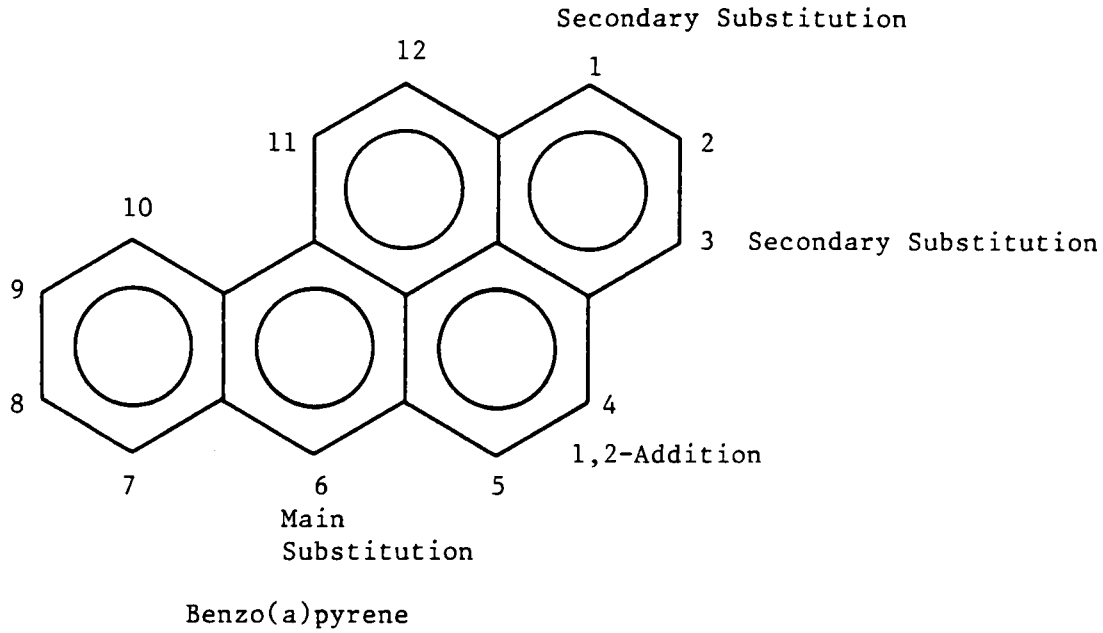




Figure 5. The Polycyclic Aromatic Hydrocarbons Studied in this Work.

have been reported to be quinones,[20] although no experimental evidence was cited.

Photochemical changes of PAHs have also been observed when they were adsorbed on the surface of substrates such as alumina and silica gel while the substrate was in the form of a thin-layer chromatographic plate (an example of a "solution-deposited" sample).[58,59] "Solution-deposited" fly ash samples are samples of fly ash that have been covered with a particular PAH in an organic solvent (e.g., methylene chloride). Evaporation of the solvent should leave the PAHs adsorbed to the surface of the fly ash. Numerous products were found after irradiating pyrene adsorbed on silica gel G, including 1,6-pyrenedione and 1,8-pyrenedione.[60]

Benzo(a)pyrene, solution-deposited onto glass fiber filters, was reported to undergo photochemical transformation.[61] The non-photochemical half-time was about five times as long as the photochemical half-time and the products were not identified. Blau and Güsten[62] reported the quantum yield for the photodegradation of benzo(a)pyrene adsorbed on silica gel to be $5.3 \times 10^{-5}$.

It has been found that many (but not all) fly ash substrates stabilize PAHs with respect to photochemical degradation.[63] This work demonstrated that studies of PAH photodecomposition in solution, as of PAHs solution-deposited on fly ash surfaces, could not be used as direct models for the environmental degradation of PAHs adsorbed on coal fly ash.

It is now quite evident that the photochemical and non-photochemical behavior of PAHs vapor deposited onto the surface of fly ash

may be significantly different from the behavior of PAHs in solution or when solution-deposited onto the surface of fly ash.[63-66] Furthermore, the adsorption mechanism for PAHs on fly ash that have been solution-deposited may be considerably different than that taking place in the stack of a fossil-fueled steam plant.[66] It is, therefore, much more environmentally significant to study vapor-deposited PAHs on the surface of fly ash.

The photochemical behavior of a particular PAH on one substrate may be different from that observed when the PAH is adsorbed on another substrate. For example, benzo(a)pyrene, solution-deposited onto alumina, has been reported to undergo 50% photodecomposition with an 80-minute exposure to an unfiltered 150-watt xenon lamp; under identical conditions, benzo(a)pyrene adsorbed onto fly ash exhibited only 15% decomposition.[57] Previous solution and solution-deposition work would lead one to believe that the half-lives of PAHs adsorbed on coal fly ash are on the order of hours to days.[57,58,60,67] It is now known, however, that particle-associated PAHs may remain in the atmosphere for much longer periods of time.

The extent of photochemical degradation has been observed to be greater for pure solid PAHs than for PAHs adsorbed on soot.[68] This stabilization towards photochemical change may be due in part to the porosity of the soot particles. If a PAH molecule can be "screened" from the incoming radiation, by depositing into a pore of the (opaque) particulate matter, there is less probability for absorption of incident radiation by that molecule. Presumably, the PAH molecule must be excited to a higher electronic state before a photochemical reaction can occur.

Another important point to consider is whether or not PAHs are adsorbed on the fly ash at a concentration large enough to distribute into a multilayer of molecules rather than a monolayer (i.e., no PAH molecules adsorbed onto the "top" of other PAH molecules). In heterogeneous reactions the outer layer(s) is protected from further reaction by the initially formed products. Furthermore, during irradiation, only the outer layer will be photochemically excited. This question may be extremely difficult to answer due to the inhomogeneity of most fly ash surfaces, implying that PAHs may tend to be adsorbed in "clusters" at especially active surface adsorption sites rather than distributing themselves uniformly over the surface.

The suppression of photochemical degradation of PAHs adsorbed on coal fly ash may be due in part to quenching of electronically excited PAH molecules by surface species. The excited-state lifetime of a PAH molecule may be significantly decreased if the PAH molecule forms a $\pi$ complex with either a carbon (polymeric or graphitic)[69] or an inorganic, mineral portion of the fly ash.[70] Particles of soot that have a high carbon content tend to adsorb and retain PAHs quite strongly.[71-73] This high affinity for carbon is confirmed by the long extraction times and high extraction temperatures needed to quantitatively recover PAHs deposited onto carbonaceous materials, and the fact that quantitative recoveries often cannot be achieved at all. It is highly likely that different surface characteristics are responsible for the differing photocatalytic properties of different coal fly ashes.[74]

Some PAHs appear to undergo non-photochemical transformations more rapidly on coal fly ash than on more "conventional" substrates.[63] For example, fluorene (and several other PAHs), when in solution or when vapor-deposited onto alumina and silica gel, did not exhibit any detectable non-photochemical degradation when stored in the dark. Fluorene, however, was reported to undergo a "dark" oxidative transformation when adsorbed on coal fly ash, graphite and activated charcoal. The product of this non-photochemical transformation was identified as 9-fluorenone.

PAHs adsorbed on the surface of coal fly ash will not only be subjected to sunlight and water vapor, but also nitrogen oxides, sulfur oxides, oxygen, and ozone. A realistic evaluation of the impact of particle-associated PAHs on the environment must also consider the possibility of PAHs reacting with these species.

Ozone reacts rapidly with solid benzo(a)pyrene when this PAH is deposited into petri dishes[75] or glass fiber filters,[11] and the reaction takes place more rapidly in the presence of light. The major reaction products appear to be ring-opened compounds including dialdehydes, dicarboxylic acids, and ketocarboxylic acids. The benzanthrone structure is the major skeleton remaining after the oxidation of benzo(a)pyrene. The reaction mixture obtained from the reaction of benzo(a)pyrene and ozone showed direct mutagenic activity in the Ames test (benzo(a)pyrene itself requires metabolic activation to exhibit mutagenicity). Although 1,6-; 3,6-; and 6,13-benzo(a)pyrenequinones are major products of benzo(a)pyrene ozonolysis, they are only slightly mutagenic.[61] The most highly mutagenic species was identified as benzo(a)pyrene-4,5-oxide.

PAHs present in diesel particulate matter are highly reactive toward ppm levels of $O_3$ in air, and the reaction rate is reported to be independent of exposure to light. The reaction mixture obtained is very complex and no reaction products appear thus far to have been identified. It is not known whether the microbiological testing of diesel soot extracts exposed to $O_3$ would yield significantly more direct-acting mutagenic activity in the Ames test, as compared with that detected using the extract prior to exposure to $O_3$.[76]

When benzo(a)pyrene, perylene, and 1-nitropyrene were exposed to 100 ppb $O_3$ in the dark while adsorbed on glass or Teflon filters as well as on glass or Teflon filters loaded with fly ash, no reaction was observed. It appears that some PAHs are resistant to ozonation in the dark.[77]

Gaseous pollutants such as $SO_2$ and $SO_3$ are also present in the atmosphere as a result of the sulfur content of various fuels such as oil and coal. Pyrene reacts with $H_2SO_4$ in solution to produce disulfonic acids.[78] No products have been identified, however, when pyrene was adsorbed on the surface of soot particles and then exposed to various concentrations of $SO_2$ while being irradiated[79] even though the pyrene concentration appeared to decrease, which would lead one to believe that a chemical reaction had occurred.

Other workers exposed pyrene and benzo(a)pyrene, solution-deposited on fly ash and alumina, to 10% $SO_2$ in air.[62] They isolated pyrene-1-sulfonic acid, pyrenedisulfonic acid, and benzo(a)pyrenesulfonic acid as reaction products. When PAHs were vapor-deposited onto fly ash and exposed to 10% $SO_2$ in air,[62] a reaction occurred but no

products were identified. In another experiment,[80] PAHs on soot particles were exposed to air containing 5 ppm $SO_2$ for months (3 to 4) without significant loss. No products, including the PAH sulfonic acids, have been identified on environmentally significant (i.e., vapor-deposited) samples of coal fly ash. The health risks associated with PAH sulfonic acids appear to be orders of magnitude less than those of the PAH-$NO_2$ derivatives.[81] However, it is not really known what PAH-$SO_2$ products might be present on airborne particulate matter and the health risk of such compounds, if they are found in appreciable quantities in the atmosphere, may be significant.

Whether or not coal fly ash stabilizes PAHs with respect to nitration reactions is not clear. It has been reported that benzo(a)-pyrene, adsorbed on glass filters, reacts with $NO_2$[82] to form a nitro-benzo(a)pyrene. Other reports indicate that $HNO_3$, as an impurity, in $NO_2$ gas cylinders may be responsible for catalyzing the nitration reaction.[83,84] It is claimed that PAHs solution-deposited on coal fly ash and then exposed to ppm levels of $NO_2$ undergo no measurable decomposition if the $NO_2$ is first purged of $HNO_3$.[77]

It appears that some nitro-PAHs (e.g., nitro derivatives of benzo(a)pyrene) will degrade in solution to quinones upon irradiation.[85] When benzo(a)pyrene adsorbed on glass fiber filters was exposed to 0.25 ppm $NO_2$ (a concentration often exceeded in ambient air in downtown Los Angeles) and a trace quantity of $HNO_3$, the reaction products obtained were 1-, 3-, and 6-nitrobenzo(a)pyrene. The 1- and 3-nitrobenzo(a)pyrenes appear to be photostable and are also strong direct mutagens.[86] The 6-nitrobenzo(a)pyrene, which is reported to

be at least weakly mutagenic, undergoes efficient photodegradation to a benzo(a)pyrenequinone.[87] Overall, the transformation rates of nitro-PAHs appear to be slower than those of the corresponding PAHs.[88] The formation rates of 1-nitropyrene and 6-nitrobenzo(a)-pyrene have been observed to be much lower when pyrene and benzo(a)-pyrene were adsorbed (solution-deposited) on carbonaceous deposits than when the substrate was alumina, silica gel, or coal fly ash.[89]

If coal fly ash stabilizes the nitro-PAHs with respect to further degradation, then possible nitration reactions of particle-associated PAHs in the atmosphere could have significant environmental health risks. Furthermore, 6-nitrobenzo(a)pyrene, which is only weakly mutagenic, is susceptible to degradation while the 1- and 3-nitro-benzo(a)pyrenes, which are much more strongly mutagenic, appear much more stable. Thus, particles of respirable size may be coated with extremely mutagenic compounds. Dinitro-PAHs tend to be even more mutagenic than mononitro-PAHs and have been tentatively identified by mass spectrometry in samples of diesel POM.[90] The stability of the dinitro-PAH compounds is not known. It is obvious that the mutageni-city of an extract depends strongly on the identities and amounts of PAHs present and their ability to react with $NO_2$ in the atmosphere.

It is clear that the presence of PAHs adsorbed on the surface of respirable coal fly ash particles is of major concern to environmental chemists. The mutagenicity of nitro-PAHs as well as the mutagenicity and carcinogenicity of oxidized PAHs may increase the health risks associated with inhalation of particulate matter even when produced in small yield. The unravelling of the product identities and

mechanism(s) of atmospheric reactions between particle-associated PAHs and gaseous pollutants (especially $NO_2$) is highly desirable.

## J. Objectives of this Study

The objectives of this study are to determine the extent to which coal fly ash surfaces modify the photochemical and non-photochemical behavior of PAHs in the absence and presence of other major atmospheric pollutants (e.g., $NO_2$). Furthermore, it would be significant if correlations could be established between the behavior of adsorbed PAHs and the physical and chemical characteristics of the fly ash surfaces. Ultimately, the goal of this research is to assess the environmental relevance of the influence of fly ash surfaces upon the chemistry of PAHs.

Pyrene and benzo(a)pyrene will be vapor-deposited onto the surfaces of adsorbents such as alumina, silica gel, and flaked graphite, and onto eight well-characterized fly ash samples that have been collected from the hoppers of electrostatic precipitator collection devices.

Adsorbent samples that have been "coated" with a particular PAH will be illuminated by an intense light source that simulates the solar spectrum. Micro-soxhlet extractions of these samples before and after irradiation will be used to determine if a photochemical change occurs. Precautions will be taken to prevent or minimize thermal degradation of adsorbed PAHs.

For cases in which PAHs adsorbed on fly ash appear to undergo significant photodecomposition, attempts to identify photochemical

products will be made by the use of direct-probe mass spectrometry and ultraviolet absorption spectroscopy. Attempts will be made to rationalize differences in the photochemical behavior of pyrene and benzo(a)pyrene on solid surfaces on the basis of differences in the physical and chemical characteristics of the adsorbents under study.

Experiments will also be performed to determine the effect of exposing adsorbents, that have been "coated" with a particular PAH, to $NO_2$. The effect of this exposure to $NO_2$ will be examined in both the presence and absence of light. Identification of potential products (e.g. nitro derivatives of PAHs) will be attempted by direct-probe mass spectrometry.

Attempts will also be made to establish correlations between the behavior of PAHs adsorbed on the surfaces of adsorbents and the presence of the atmospheric pollutant, $NO_2$.

# CHAPTER II

# EXPERIMENTAL

## A. Polycyclic Aromatic Hydrocarbons

The two PAHs used in this study, pyrene and benzo(a)pyrene, were obtained from Eastman (lot no. B8C) and Aldrich (lot no. 072077), respectively. The pyrene had been assayed by Eastman using UV-visible absorption spectroscopy and was stated to be at least 95% pure. Further purification was carried out in this laboratory by using vacuum sublimation techniques. The benzo(a)pyrene was stated by Aldrich to be 99+% pure and was used as received. The solid PAHs were stored in the dark in a dry box at room temperature.

## B. Substrates

Several different substrates were "coated" with pyrene and benzo(a)pyrene using a vapor-deposition apparatus (to be described in Section C). Some of these substrates were obtained from coal-fired power plants and, therefore, represent "real" samples. Other substrates used in this study were adsorbents that are typically found in most laboratories. The following adsorbents were used:

1. Alumina: Neutral, Brockmann Activity I, 80-200 mesh, obtained from Fisher Scientific Company (lot no. 755945).

2. Silica Gel: 70-230 mesh, obtained from Brinkman Instruments, Inc., Westbury, New York (lot no. 4953813).

3. Carbon: Flaked graphite (lot no. 1645) obtained from Southwestern Graphite Company, Burnet, Texas; sieved to pass a 45 micrometer screen.

4. Commercially Available Fly Ash: These fly ash samples were obtained from Alpha Resources, Inc., Stevensville, Michigan.

a. Fly Ash (lot no. 720-1).

b. Fly ash (lot no. 720-2).

Table 6 shows the major elements reported to be in these two fly ash samples, based on oxide equivalents.[91] The type of coal from which this ash was produced is not known. These fly ash samples were sieved to pass a 45 micrometer screen.

5. Coal Fly Ash.

Several coal fly ash samples were obtained from Oak Ridge National Laboratory, Metals and Ceramics Division. Table 7 shows the major elements present in these samples, based on oxide equivalents.[92,93] Table 8 lists the major and minor phases present in these fly ash samples.

One coal fly ash sample (Kaneb) was obtained from a coal-fired power plant in Florida, that was having combustion problems at the time this fly ash was collected. This particular sample was expected to be high in % carbon because of inefficient combustion. An uncharacterized coal fly ash sample, Crawford coal fly ash, was also obtained from Oak Ridge National Laboratory.

Each of these fly ash samples was sieved to pass through a 45 micrometer screen before any experiments were performed and was stored in the dark in glass vials.

TABLE 6

ELEMENTAL COMPOSITION OF COMMERCIAL FLY ASH SAMPLES BASED ON WEIGHT PERCENTAGE OF OXIDE EQUIVALENTS

| Lot No. | $SiO_2$ | $Al_2O_3$ | $Fe_2O_3$ | CaO | MgO | $SO_3$ | $Na_2O$ | $K_2O$ | $P_2O_5$ | $TiO_2$ |
|---|---|---|---|---|---|---|---|---|---|---|
| 720-1 | 62.1% | 21.6% | 5.72% | 4.1% | 1.21% | 1.57% | 1.08% | 1.2% | .13% | 1.26% |
| 720-2 | 69.9% | 21.9% | 6.15% | 4.8% | 1.34% | 1.35% | .9% | 1.26% | .08% | .73% |

TABLE 7

BULK COMPOSITION OF FLY ASHES EXPRESSED AS WEIGHT PERCENTAGE OF OXIDE EQUIVALENTS[92,93]

| Component | Western Kentucky Bituminous Coal (WK) | Illinois Bituminous Coal (IL) | New Mexico Subbituminous Coal (NM) | Texas Lignite (TX) | Eastern Appalachian Bituminous Coal (EA) | East Tennessee Bituminous Coal (ET) |
|---|---|---|---|---|---|---|
| $SiO_2$ | 50.0% | 48.6% | 60.1% | 55.0% | 50.1% | 30.0% |
| $Al_2O_3$ | 19.0% | 17.2% | 24.7% | 14.2% | 25.7% | 15.5% |
| $Fe_2O_3$ | 24.1% | 23.6% | 3.6% | 4.9% | 15.6% | 1.7% |
| CaO | 1.8% | 3.4% | 5.9% | 20.3% | 1.4% | 0.2% |
| MgO | 0.7% | 1.0% | 1.1% | 3.2% | 1.3% | 1.8% |
| $Na_2O$ | 0.3% | 2.3% | 1.9% | 0.6% | 0.4% | 0.2% |
| $K_2O$ | 2.6% | 1.9% | 0.7% | 0.6% | 2.9% | 2.0% |

TABLE 8

PHASES PRESENT IN FLY ASH SAMPLES[92,93]

| Phase | Fly Ash[a] East Tennessee Bituminous Coal | Western Kentucky Bituminous Coal | Illinois Bituminous Coal | New Mexico Subbituminous Coal | Texas Lignite |
|---|---|---|---|---|---|
| Glass | M | M | M | M | S |
| Spinel | S | M | M | | |
| Mullite | M | S | S | | |
| Quartz | M | S | S | M | M |
| $Fe_2O_3$ | S | M | M | | S |
| $CaFe_2O_4$ | | | | S | S |
| $Ca_2Al_2SiO_7$ | | | | S | |
| $CaFeO_2$ | | | | M | |
| $Al_2O_3$ | | | | S | S |
| $FeAlO_3$ | | | | S | |
| $Ca_2SiO_4$ | | | | | M |
| $CaF_2$ | | | | | S |
| $CaSiO_3$ | | | | | S |

[a]M = major constituent.

S = minor constituent.

6. Controlled Porosity Glass: 37-74 micrometer particle size, 100 Å average pore radius, obtained from Pierce Chemical Company, Rockford, Illinois (lot no. 24830).

7. Glass.

a. A brown glass bottle of the type used to store light-sensitive chemicals was pulverized using a ball mill.

b. Cobalt glass plates of the type used in general chemistry flame tests to filter out ultraviolet radiation were also pulverized using a ball mill.

Both samples of glass were sieved to pass through a 45 micrometer screen.

## C. Adsorption Apparatus

Figure 6 shows a block diagram of the vapor-deposition apparatus. This apparatus was used to vapor-deposit PAHs onto the surface of various substrates and was a modification of the design used by Miguel[94,95] and Korfmacher.[63]

The adsorption apparatus consisted of two gas chromatographic ovens, each having its own temperature controller, heater coil, thermocouple, and fan (to obtain a uniform distribution of heat). The carrier gas used for this work was nitrogen (prepurified) obtained from Matheson Gas Products, Morrow, Georgia or from Burdett Gas Products, Chattanooga, Tennessee, which was passed through an oxy-trap filter obtained from Alltech Associates, Atlanta, Georgia, to remove oxygen before entering the vapor deposition apparatus. Temperature control was typically to within ±1°C.

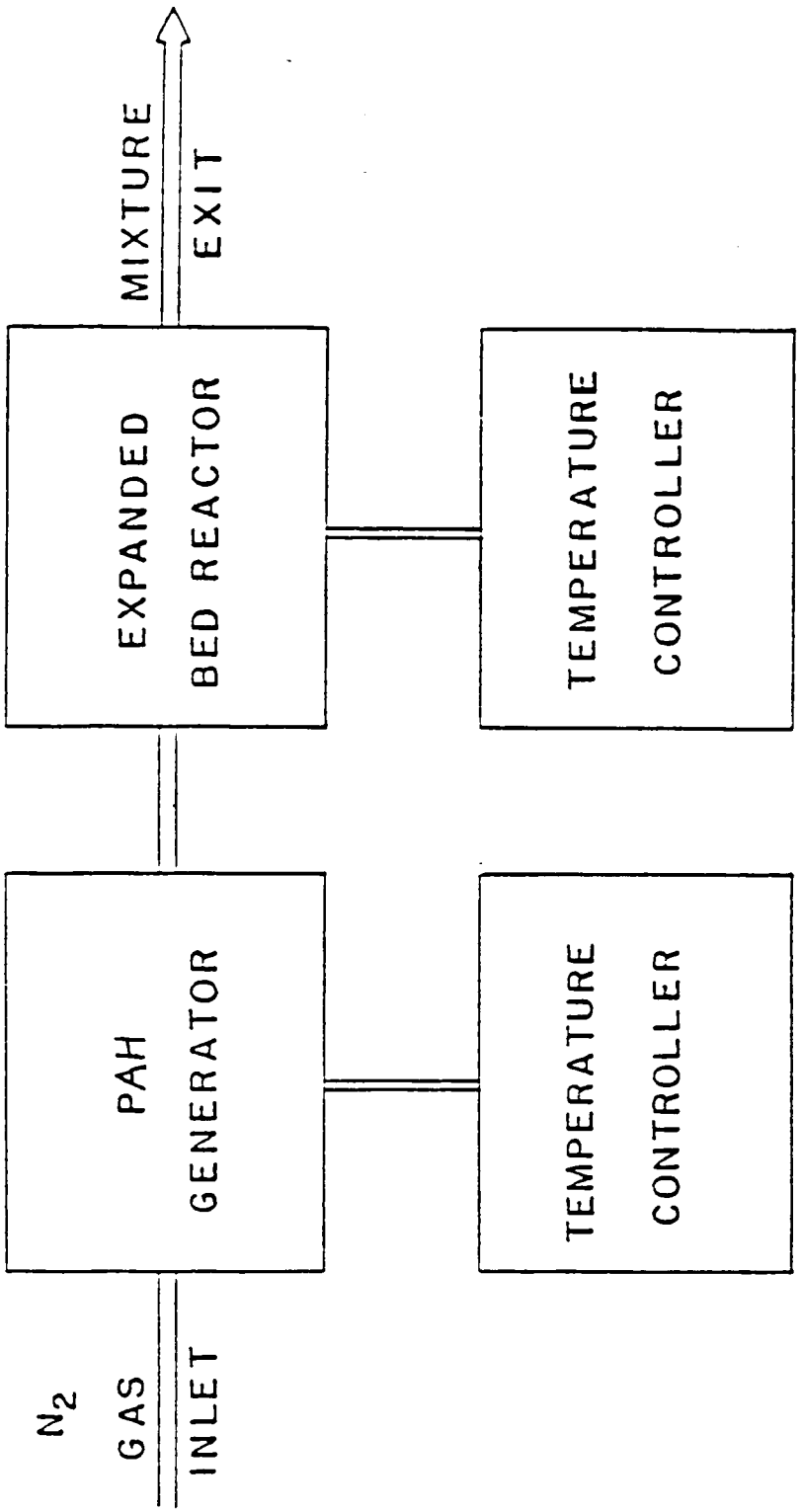



Figure 6. Block Diagram of the Vapor-Deposition Apparatus.

Figure 7 shows the PAH generator. The PAH to be studied was placed in a removable diffusion tube and the generator temperature was set such that the oven temperature was about 5°C below the melting point of the particular PAH under study. This system generated PAH in the vapor phase with a nitrogen gas diluent which then passed from the first oven (generator) through a heated transfer line into the second oven (expanded bed reactor).

Figure 8 shows the expanded bed reactor. Adjustment of the 4-port, 2-way switching valve (Valco Instruments Company, Houston, Texas, model V-4-HT) allowed passage of the PAH/nitrogen mixture through the expanded bed reactor or to by-pass the expanded bed reactor. This feature allowed one to monitor the PAH vapor phase concentration (via a flame ionization detector or collection of extracts by bubbling the output through a liquid solvent) or allowed temperature equilibration of the first oven before passing the PAH/nitrogen mixture through the substrate to be studied. The valve was mounted on the inside of the oven wall such that the handle to the valve could be manipulated from outside the oven. The extra coarse frit at the bottom of the expanded bed reactor was used as a support for the substrate under study and the upper coarse glass frit prevented substrate particles from escaping from the reactor.

The temperature of the glass tubing connecting the two ovens as well as the temperature of the second oven was controlled at 5 to 7°C above the melting point of the PAH being studied. This difference in temperature between the two ovens served the purpose of preventing condensation of the PAH during its passage through the line connecting

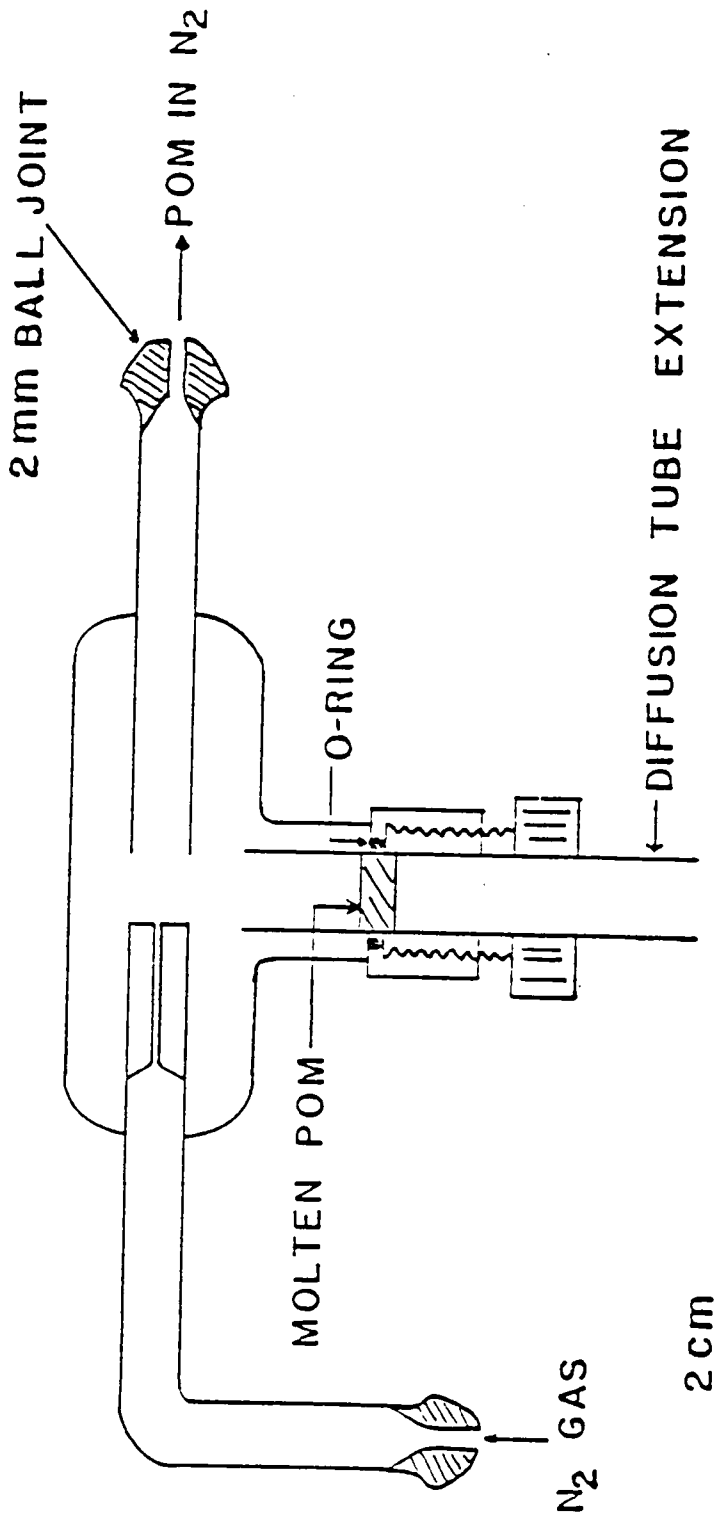



Figure 7. Generator and Diffusion Tube.

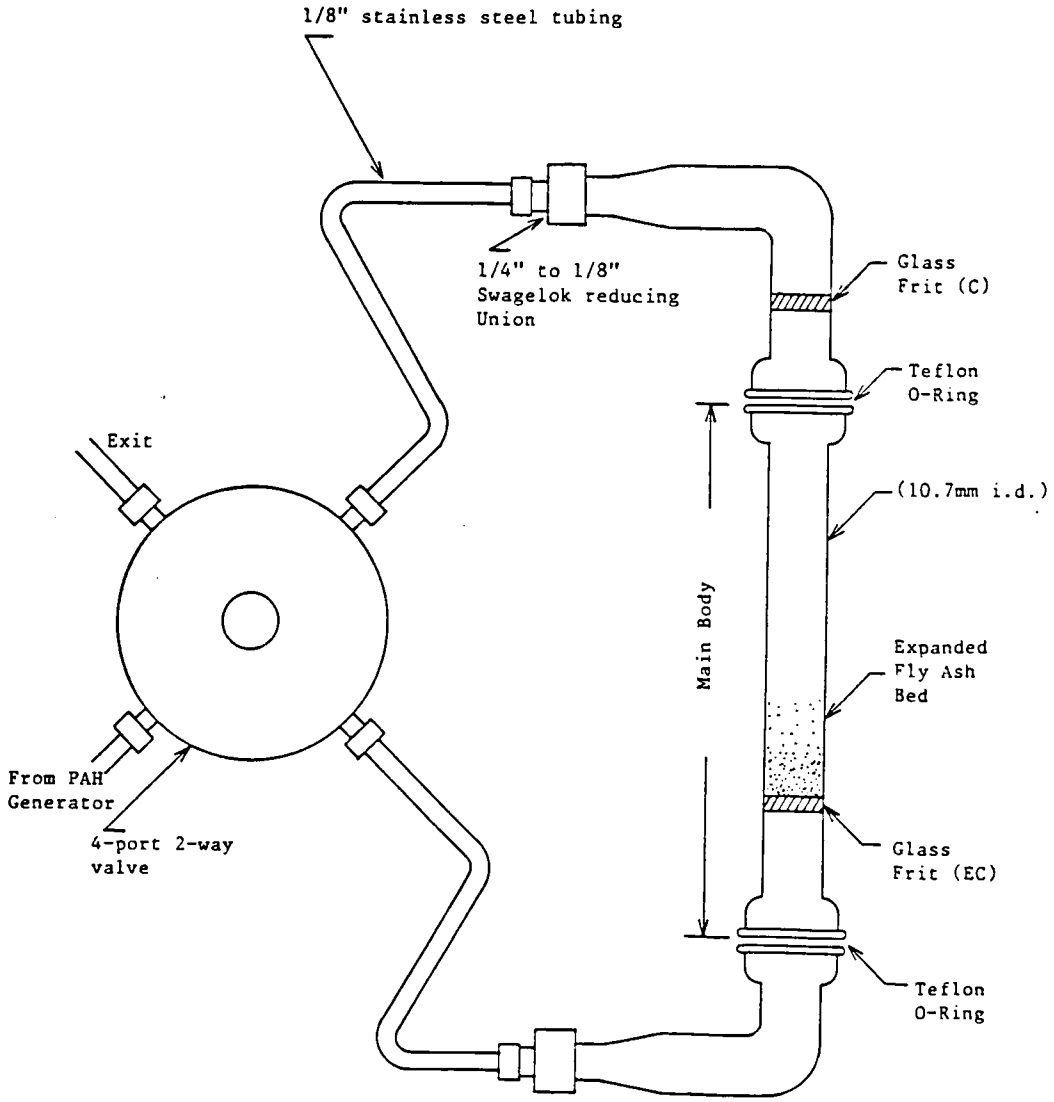



Figure 8. Expanded Bed Reactor.

the two ovens and anywhere in the second oven except on the substrate of interest. In each oven, preceeding the generator and expanded bed reactor, was about 6 feet of coiled glass 1/4 inch tubing. This tubing served the purpose of temperature equilibration for either the $N_2$ or the PAH/$N_2$ as the gases entered each respective oven.

## D. Irradiation Experiments

The irradiation source used in this work was an ultraviolet enhanced output lamp (Cermax Xenon Illuminator, ILC Technology, Sunnyvale, California, model LX300UV) powered by a Cermax PS300-1 power supply (lamp power of 180 to 320 W). Typical lamp currents used during the irradiation experiments were about 18 A dc. The spectral output of this lamp is shown in Figure 9. One can compare Figure 9 with the spectrum of normal sunlight[96] shown in Figure 10.

The output of the irradiation source was filtered by a cell (20 cm path length) containing water. The ends of the cell were made of quartz so that the ultraviolet radiation or actinic region of the spectrum could pass. Water was used in the cell so that the near infrared output of the irradiation source would be attenuated since it was important not to induce thermal changes in the PAHs studied.

The irradiation cell used in this study was made of quartz and is shown in Figure 11. A solid quartz rod was connected to one side so that the substrate was mixed during rotation of the cell. The cell was attached via a ground glass joint to the end of a rotary evaporator motor and a slight vacuum (via a water aspirator) was applied. The cell was rotated at about 60 cycles per minute and was typically about 34 centimeters from the source.

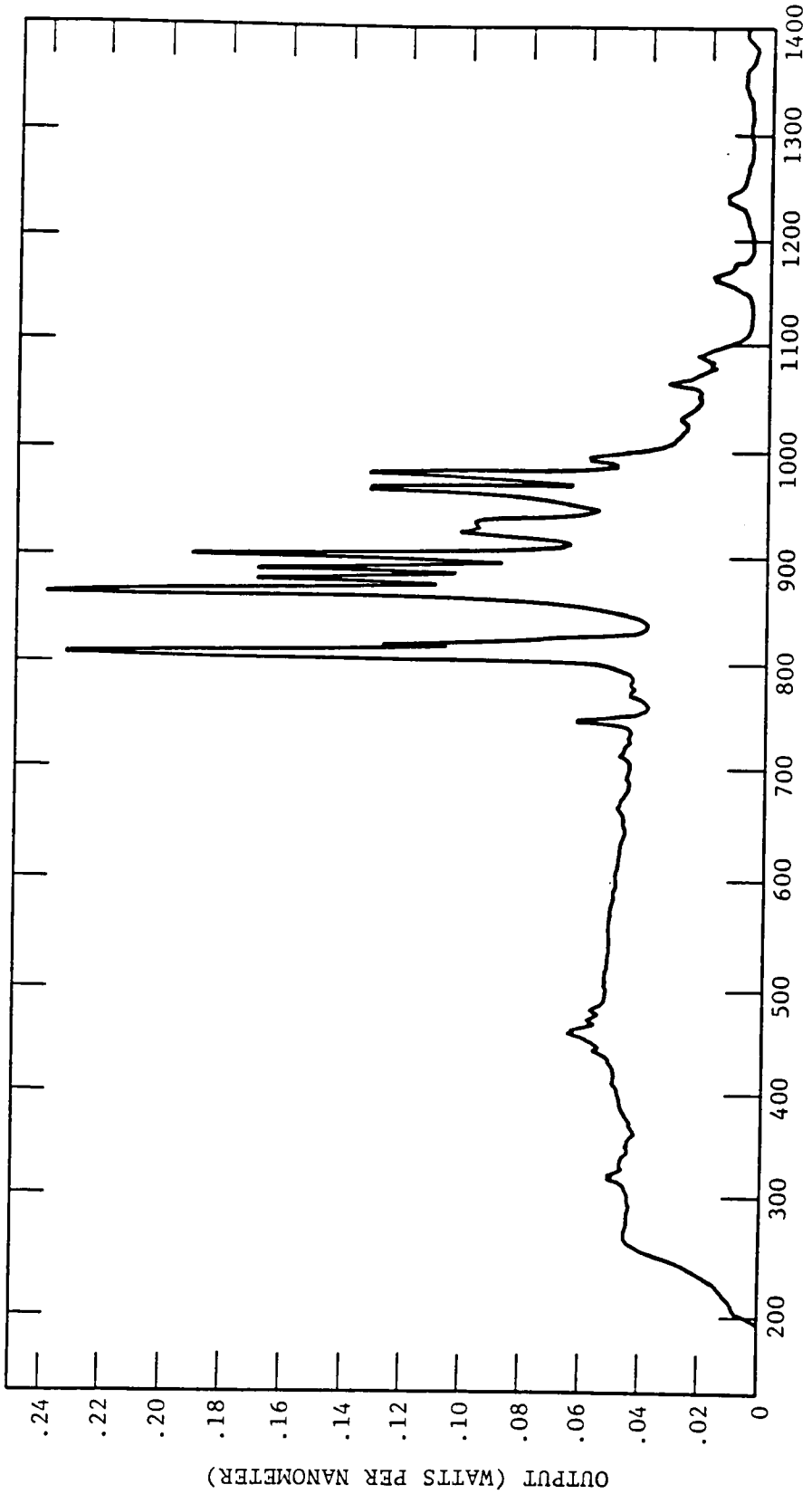



Figure 9. Cermax Lamp Output (Manufacturer's Literature).

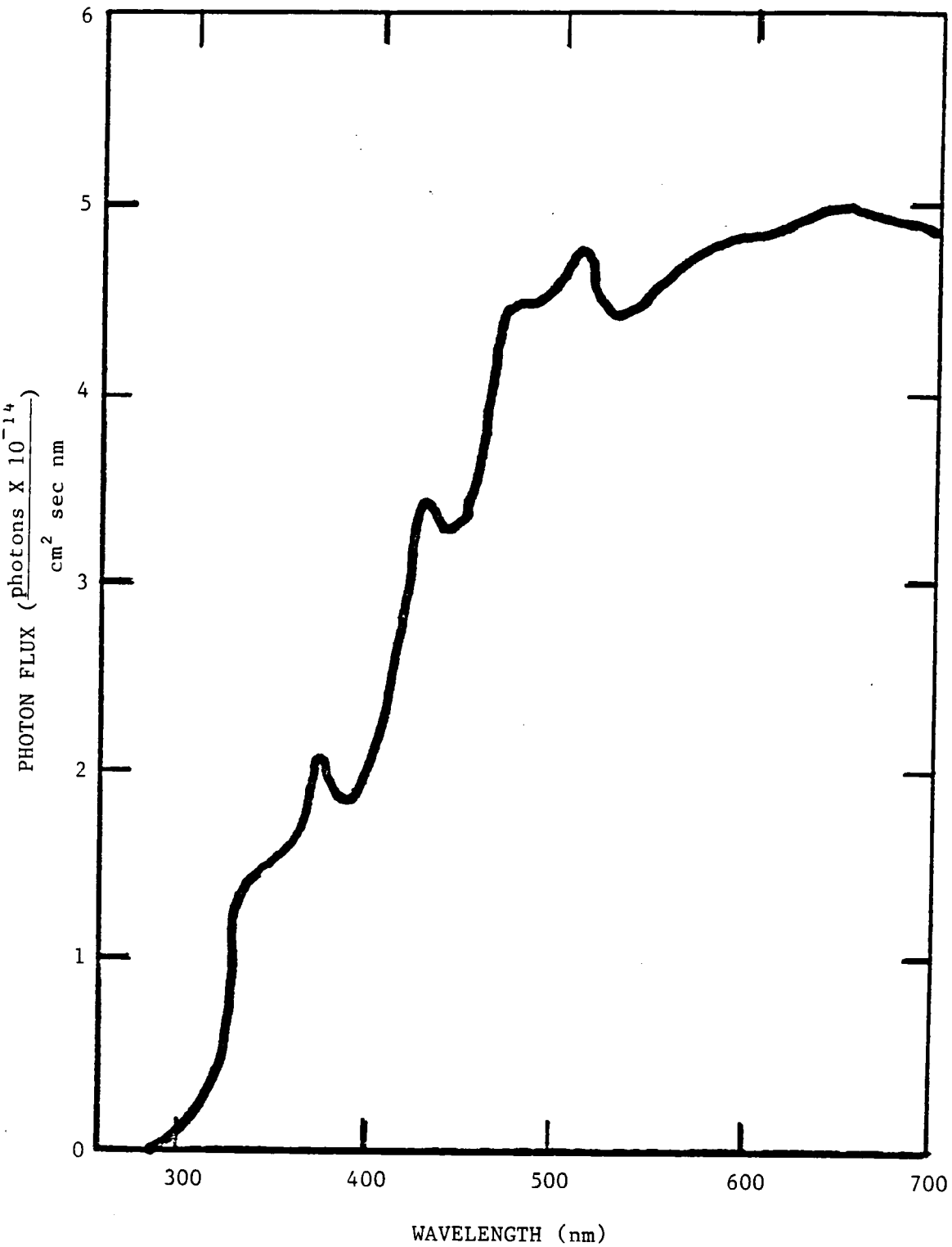



Figure 10. Spectrum of Sunlight.[96]

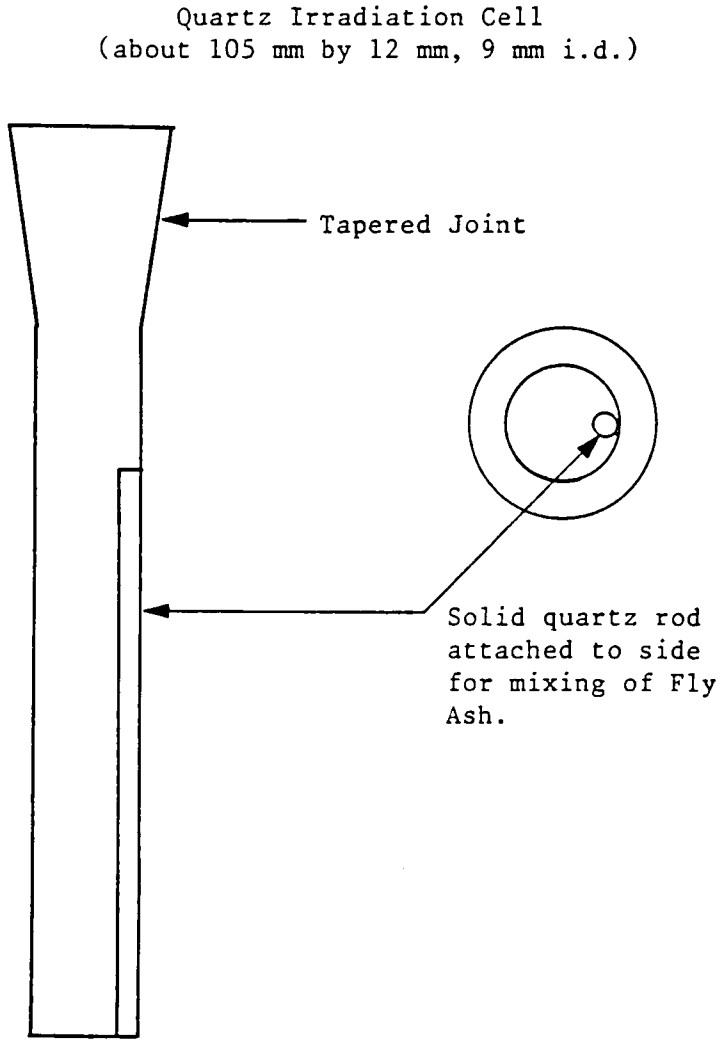



Figure 11. Quartz Irradiation Cell.

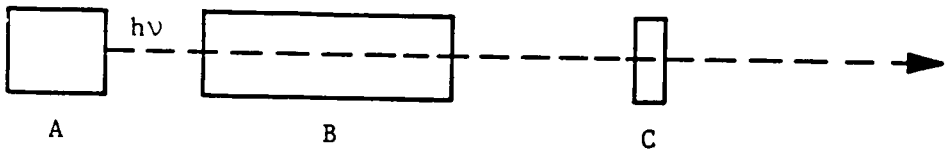
The irradiation apparatus is shown in Figure 12 as a block diagram. The temperature of the substrate in these experiments, as sensed by an Fe-constantan thermocouple, was typically 30°C.

## E. Photoreactor

The photoreactor used in this work is shown in Figure 13 and is a modification of the design used by Daisey, et al.[97] This apparatus allowed the irradiation of a PAH "coated" substrate while the substrate was suspended in a flowing stream of carrier gas (or pollutant gas). The irradiation of substrate particles in this manner should have more environmental significance than irradiating particles in the quartz cell mentioned in the previous section since the photoreactor more closely simulates conditions that substrate particles would actually experience in the atmosphere.

Nitrogen carrier gas was used in the initial experiments so that comparisons could be made between irradiations performed in the photoreactor and in the quartz irradiation cell. Later experiments involved $NO_2$ diluted in a $N_2$ matrix gas (typically 95 parts per million $NO_2$). At gas flow rates of 150 ml/minute ($NO_2/N_2$) and 1.0 l/min ($N_2$), the substrate particles were suspended into the quartz region of the photoreactor so that the particles could be irradiated by the Cermax lamp. This mixture of the two gas streams resulted in a $NO_2$ concentration of about 12 ppm. These experiments are described in more detail in Section K.

A charcoal filter was used to capture organic compounds that may possibly have escaped the photoreactor. The lower fritted disc was




A CERMAX Irradiation Source

B Water Filters (20 cm)

C Irradiation Cell (turned by rotary evaporator motor while under slight vacuum of water aspirator)

Figure 12. Block Diagram of Irradiation Apparatus.

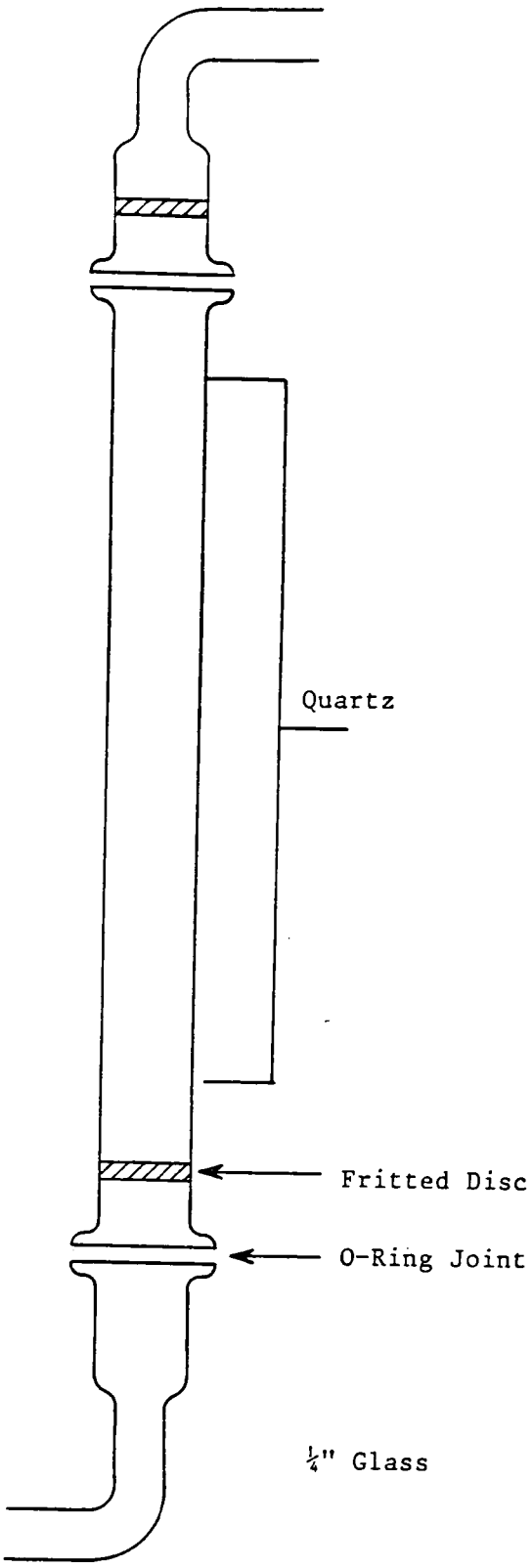



Figure 13. Photoreactor.

used as a support for the substrate under study and the upper fritted disc was used to prevent particles from escaping the photoreactor. Two stainless steel filter holders (Fisher Scientific Company) were placed in the line between the $NO_2/N_2$ gas cylinder and the photoreactor. These filter holders contained 47 mm diameter nylon filters (Membrana Inc., Pleasanton, California) to absorb $HNO_3$. A large tube made of plastic with metal screw cap lids and rubber o-rings (6.5 cm in diameter and 20 cm long) was packed with about 60 g nylon wool (Atlas Electric Devices, Co., Chicago, Illinois) and incorporated in the line before the nylon filters and the photoreactor. This was also used to absorb $HNO_3$. A radioactive ionizing unit (Cahn Instruments, Inc., Cerritos, California) was taped to the outside of the photoreactor to reduce static charge build-up (due to the particles rubbing against each other and the sides of the photoreactor). This ionizing unit was the same kind of device used in delicate balances to reduce static charge that might affect the accuracy of weighings.

## F. Analytical Methods for PAHs

### 1. Extractions

After a particular substrate had been "coated" with a particular PAH, it was necessary to determine the PAH concentration on the surface of the substrate. The extraction technique used was a micro-soxhlet extraction using cellulose thimbles (Fisher Scientific Company). Extractions were performed for 24 hours in either triplicate or quadruplicate so that confidence intervals could be calculated at the 95% confidence level using t-tables. These extractions were performed in a darkened hood so as to minimize exposure to room light.

The solvents used for the micro-soxhlet extractions were either toluene or methanol obtained from Fisher Scientific Company, and were HPLC grade. Toluene, rather than benzene, was originally used for the extraction of pyrene (benzene is a known carcinogen) and was compatible with both fluorescence and ultraviolet absorption spectroscopy. The quantitation of benzo(a)pyrene in toluene by ultraviolet absorption spectroscopy, however, was hindered by the proximity of the toluene absorption cutoff wavelength and the absorption peak of benzo(a)pyrene most desirable for quantitation. Furthermore, the possibility of extracting photochemical products was increased if a more polar solvent was used and for these reasons methanol became the extraction solvent most often used. Although fluorescence spectrometry was used more frequently for quantitative purposes in the early work, ultraviolet absorption spectroscopy later became the "workhorse" method for analysis of substrate extracts. This was due primarily to the ease with which one could change sensitivity scales on the ultraviolet absorption spectroscopy instruments as compared with the fluorescence instruments. If extracts were being quantitated that varied considerably in solute concentration, then one had to repeatedly reset instrument parameters for each concentration range when analyses were performed by fluorescence spectrometry. A simple change of the absorbance range switch on the ultraviolet instrument would suffice. Fluorescence measurements, however, were useful when lower detection limits were required.

2. Ultraviolet Absorption Spectroscopy

Ultraviolet absorption spetroscopy was performed with a Varian Cary 219 spectrophotometer which consisted basically of tungsten-halogen and deuterium lamps, a double-pass monochromator, and a photomultiplier tube. Analyses were performed using 1-centimeter fused-silica (quartz) cells with teflon stoppers. Samples and standards were analyzed the same day.

A solvent background correction was attained and stored in the Cary 219 microprocessor memory using solvent (toluene or methanol) in both the reference and sample compartments. After some of the extract was transferred to a quartz cuvette, an absorbance measurement was made over a 30 to 50 nanometer range so as to include the peak to be quantified. The same procedure was followed for standards (prepared by weighing the desired PAH into a 100 ml volumetric flask and then making the appropriate dilutions to obtain the desired concentration). Figures 14 and 15 show the absorption spectra for pyrene and benzo(a)-pyrene in methanol (the peaks used for quantification were at 334 and 298 nm, respectively) and Figures 16 and 17 show Beer's-law plots for pyrene and benzo(a)pyrene, respectively. It can be seen in Figures 16 and 17 that the absorbance versus concentration plots for these two PAHs were linear over the concentration range of interest. A typical calculation involved a linear regression analysis of peak height versus concentration for quantitation of these compounds.

3. Fluorescence Spectrometry

Fluorescence measurements were performed using a 2500 W xenon lamp as a source which was powered by a SRH-333D(S) Miller power

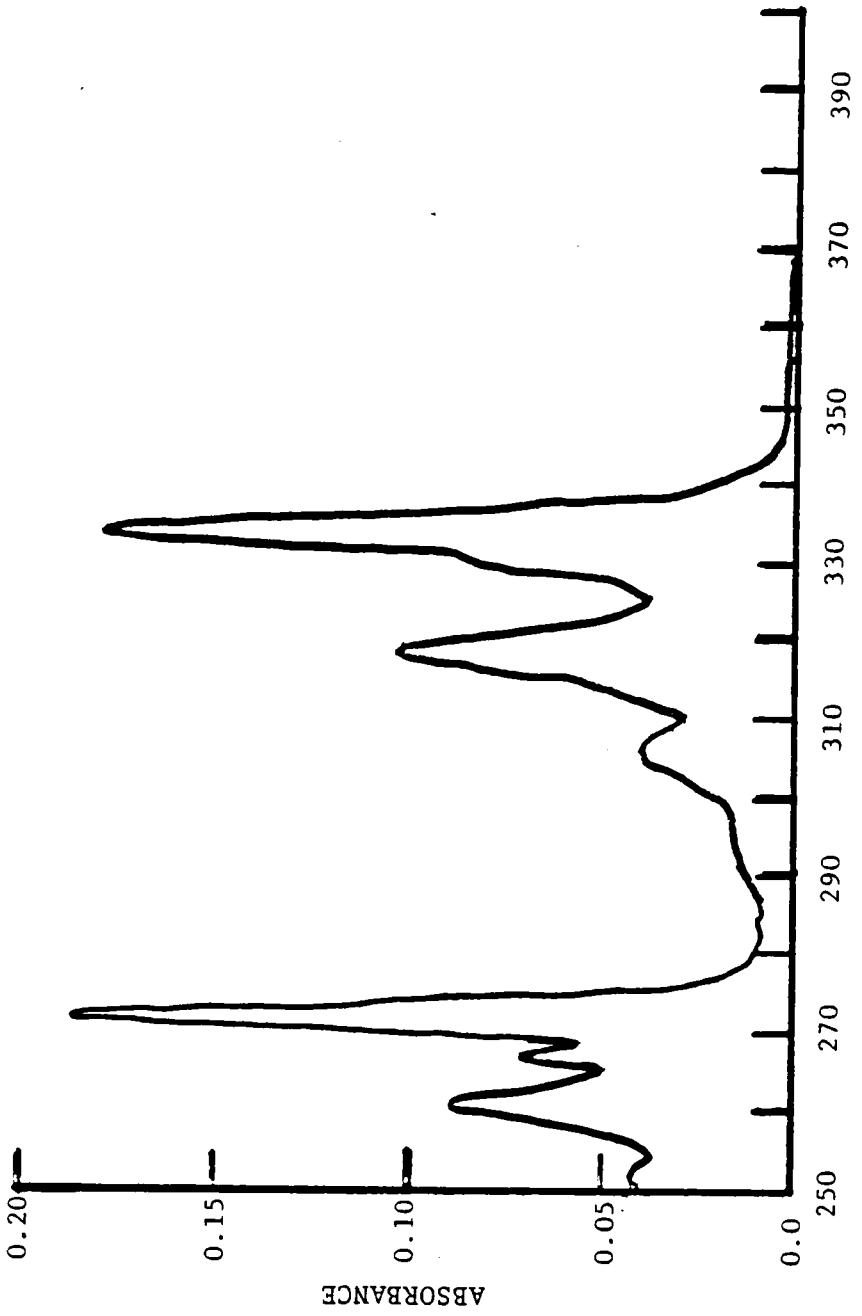



Figure 14. Absorption Spectrum for Pyrene (0.65 ppm) Dissolved in Methanol.

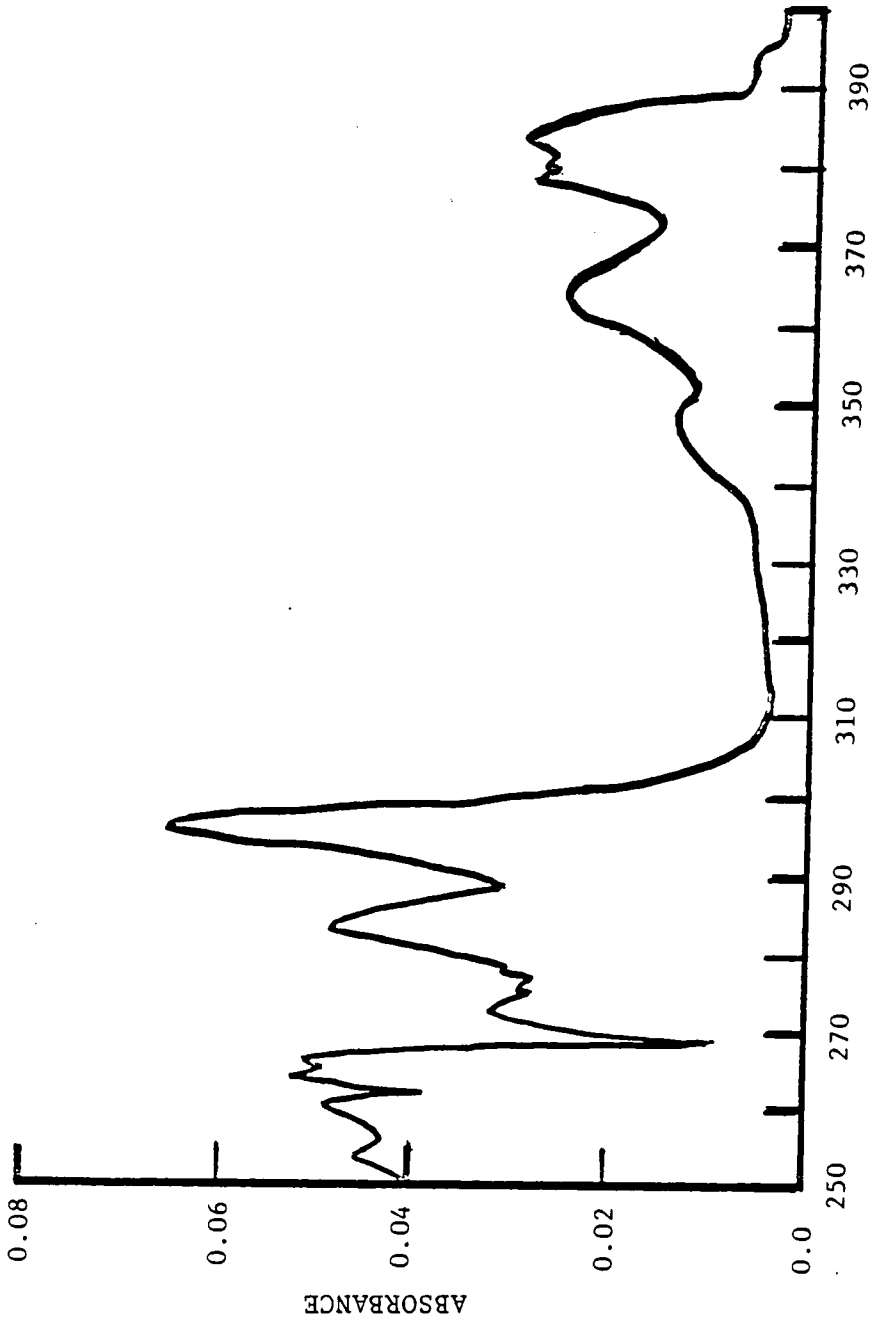



Figure 15. Absorption Spectrum for Benzo(a)pyrene (0.48 ppm) Dissolved in Methanol.

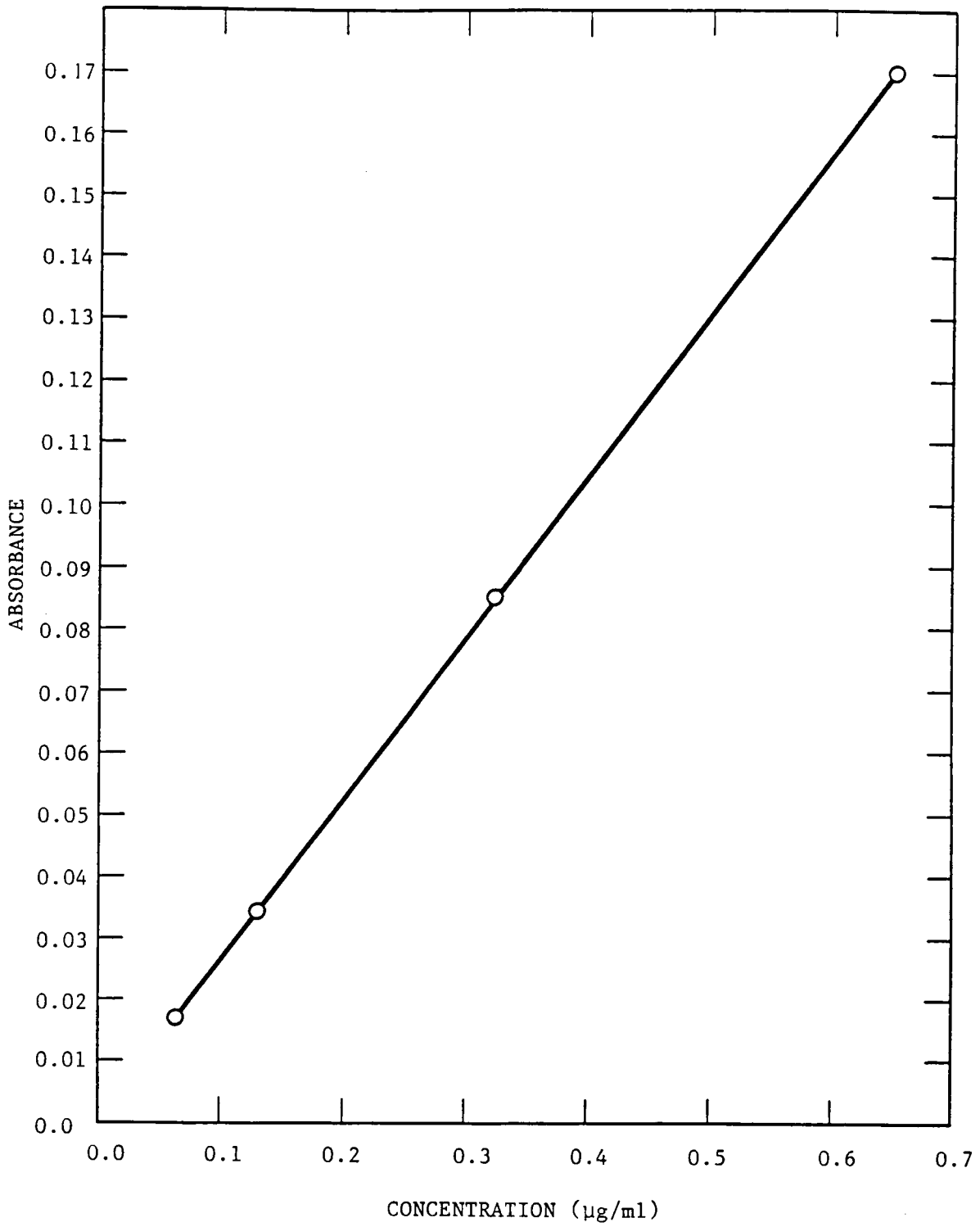



Figure 16. Beer's Law Plot for Pyrene Dissolved in Methanol (334 nm).

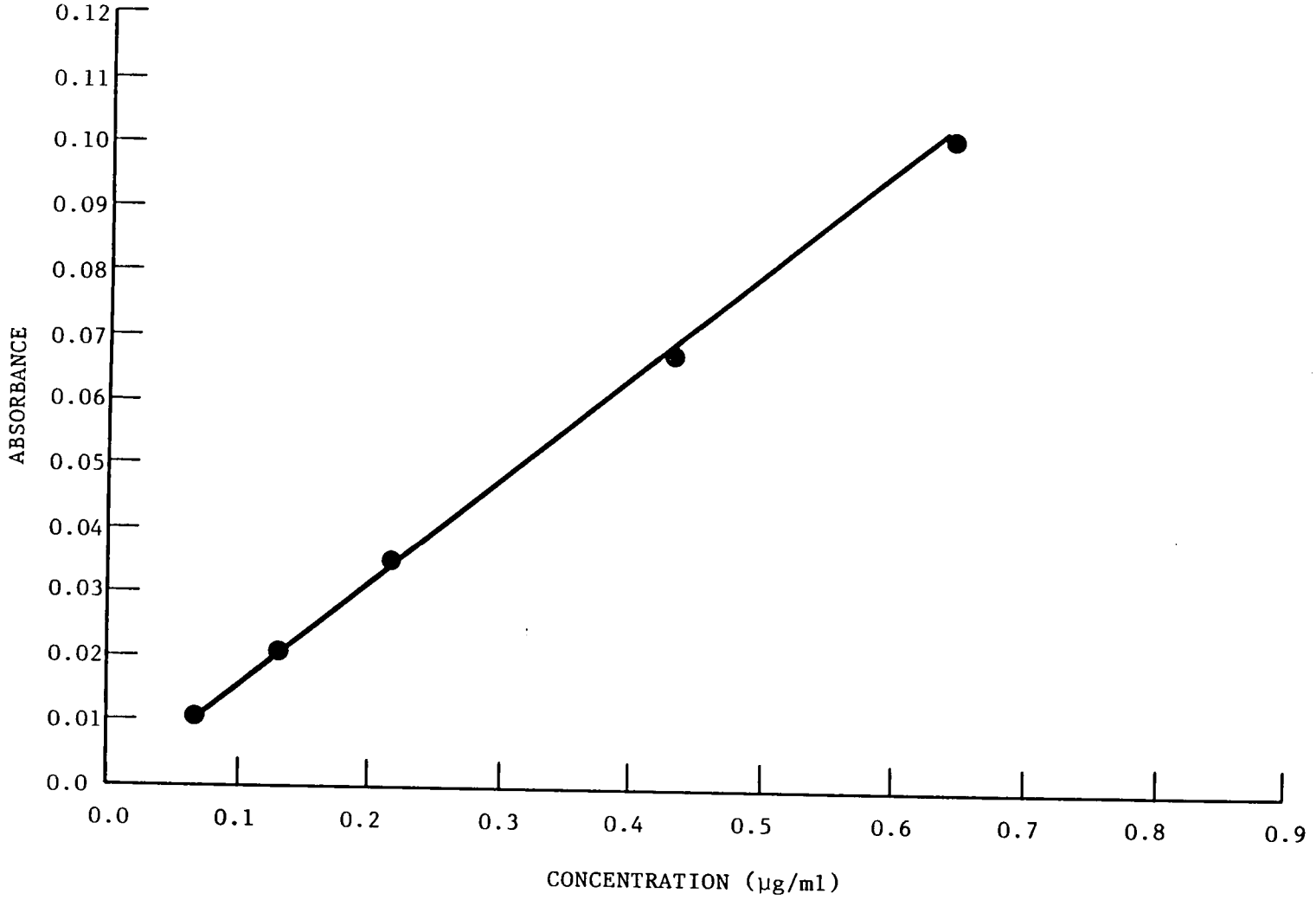



Figure 17. Beer's Law Plot for Benzo(a)pyrene Dissolved in Methanol (298 nm).

supply. A Spex 1702 Czerny-Turner scanning spectrometer (1200 groves/millimeter grating) was used for scanning the emission spectrum. The emitted radiation was collected by an RCA 8850 photomultiplier tube and photon counting was performed by an ORTEC model 9315 photon counter. Analyses of both samples and standards were performed on the same day.

Samples were quantitated in a similar fashion to the samples analyzed by ultraviolet absorption spectroscopy. A series of standards of varying concentration was analyzed along with the samples of interest and the peak heights were measured. A linear regression analysis of peak height versus concentration was performed. Figure 18 shows a fluorescence emission spectrum of pyrene dissolved in toluene. The most intense peak shown in Figure 18 was used for quantitation.

4. Direct-Probe Mass Spectrometry

The instrument used for this work was a Hewlett-Packard 5980 A mass spectrometer. All spectra recorded were the result of 70 electron-volt electron impact (EI), quadrupole mass analysis, and Be-Cu electron multiplier detection.

Samples were presented to the ion source of the mass spectrometer by the direct-probe technique, which consisted of placing a few milligrams of solid sample into a small capillary attached to the end of a stainless steel probe. The probe was then inserted through a vacuum lock and heated from ambient to 393°C in about four to five minutes. A mass spectrum was obtained every 2 to 3 s during the heating period and stored in a Hewlett-Packard model 5934A data system until needed for further study. The total ion current (TIC) was monitored to ascertain

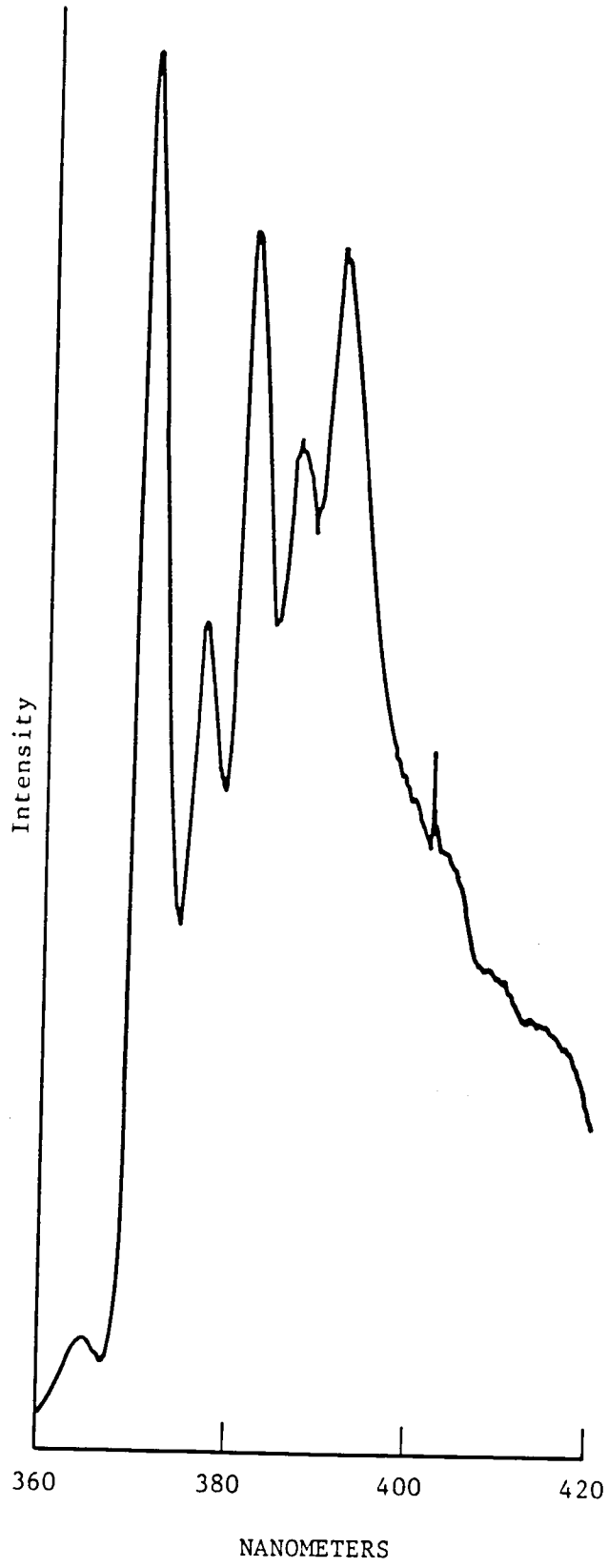



Figure 18. Fluorescence Spectrum of Pyrene Dissolved in Toluene.

if species were desorbed from the solid substrate during the course of the experiment.

Pure standards were also presented to the ion source in the same fashion so that qualitative comparisons could be made. These mass spectra were useful only for qualitative analyses, since one could not control the amount of PAHs and/or derivatives desorbed from the surface of the substrate under study.

## G. pH Measurements

The aqueous pH of each substrate was determined by weighing 1 gram of the sieved substrate ($\leq$ 45 micrometer) into a 50 ml beaker. Then 30 ml of distilled water was added and the suspension was stirred for 1 min using a teflon-covered stir bar and a Corning PC-353 stirrer. At the end of 1 min, the suspension was allowed to settle for 15 s and then a glass pH electrode (Fisher Scientific Company) and an SCE reference electrode, connected to a Fisher Accumet model 230A pH meter, were inserted and the pH was read from the pH scale.

The pH meter was standardized by using pH 6.86 and 4.01 buffer solutions. The pH of the distilled water used in these experimentrs was also measured to help determine if apparent pH changes were "real" or were artifacts of the water used in the experiment.

## H. Total % Carbon

The total % carbon content of each substrate was determined by Galbraith Laboratories, Knoxville, Tennessee. The method used was that typically used for % carbon analyses and involved complete combustion of the substrate and measurement of the $CO_2$ produced.

## I. Porosity and Surface Area Measurements

Porosity and surface area measurements were performed at Oak Ridge National Laboratory (ORNL) using the Brunauer-Emmett-Teller (BET) gas adsorption method. This method depended on the measurement of the amount of gas leaving the gas phase (i.e., a gas volumetric method) as opposed to methods which measure the uptake of the gas as determined by an increase in mass (gravimetric methods). The instrumentation used for these measurements was designed and built at ORNL. A description of how this experiment was performed may be found in Appendix 1.

## J. Diffuse Reflectance Measurements

Diffuse reflectance (DR) spectra were obtained on several substrates by using a Cary 14L spectrophotometer having a DR attachment of the reflecting type. This instrument utilized a double monochromator with an echelette grating (600 lines/mm) in series with a fused silica prism. The sources were a tungsten-halogen lamp for the visible and a hydrogen-deuterium lamp for the ultraviolet regions of the spectrum. The lamps were changed at 350 nanometers and detection for both sources was via a photomultiplier tube.

The Cary 14 model L spectrophotometer was located at the Transuranium Research Laboratory at ORNL, Oak Ridge, Tennessee.

## K. Techniques for Pollutant Gas Studies

The pollutant gas used in this study was $NO_2$ diluted in $N_2$ (typically about 100 parts per million). The concentration of the $NO_2$ in

the gas cylinder was measured by chemiluminescence and certified by the Linde Gas Company, Birmingham, Alabama.

A block diagram of this experiment is shown in Figure 19. A simple T-connection allowed one to pass either pure $N_2$ and/or $NO_2/N_2$ through the photoreactor; the flow rate was controlled by a Matheson 150 millimeter flowmeter (flowmeter tube #604).

Nylon filters (Membrana, Inc.) were placed in the stainless steel filter holders to adsorb $HNO_3$ that might be present in the $NO_2/N_2$ gas cylinder. The $HNO_3$, adsorbed by the nylon filters, was analyzed by a slightly modified version of the method of Mullin and Riley.[98] This technique essentially consisted of placing the nylon filters in a 125 ml Erlenmeyer flask containing 35 ml of distilled water, followed by an ultrasonic extraction for 1 hr. This extract was then transferred to a 50 ml volumetric flask (using an additional 5 ml of distilled water for rinsing). Then 2 ml of phenol-sodium phenolate buffer (described below) and 1 ml of hydrazine-copper solution (described below) were added. This solution was mixed and set aside in the dark.

After 24 hr, 2 ml of acetone was added. The reaction was allowed to proceed for at least 2 min and then 2 ml of sulfanilic acid (described below) reagent was added and the solution was thoroughly mixed. After not less than 5 min, 1 ml of N-(1-naphthyl)-ethylenediamine dihydrochloride reagent (described below) was added, the flask was shaken, and then 2 ml of 2 M sodium acetate was added. This solution was then diluted to 50 ml and thoroughly mixed. After 15 min the absorbance of the solution was measured at 530 nm by the use of a Model 20 Bausch and Lomb spectrometer.

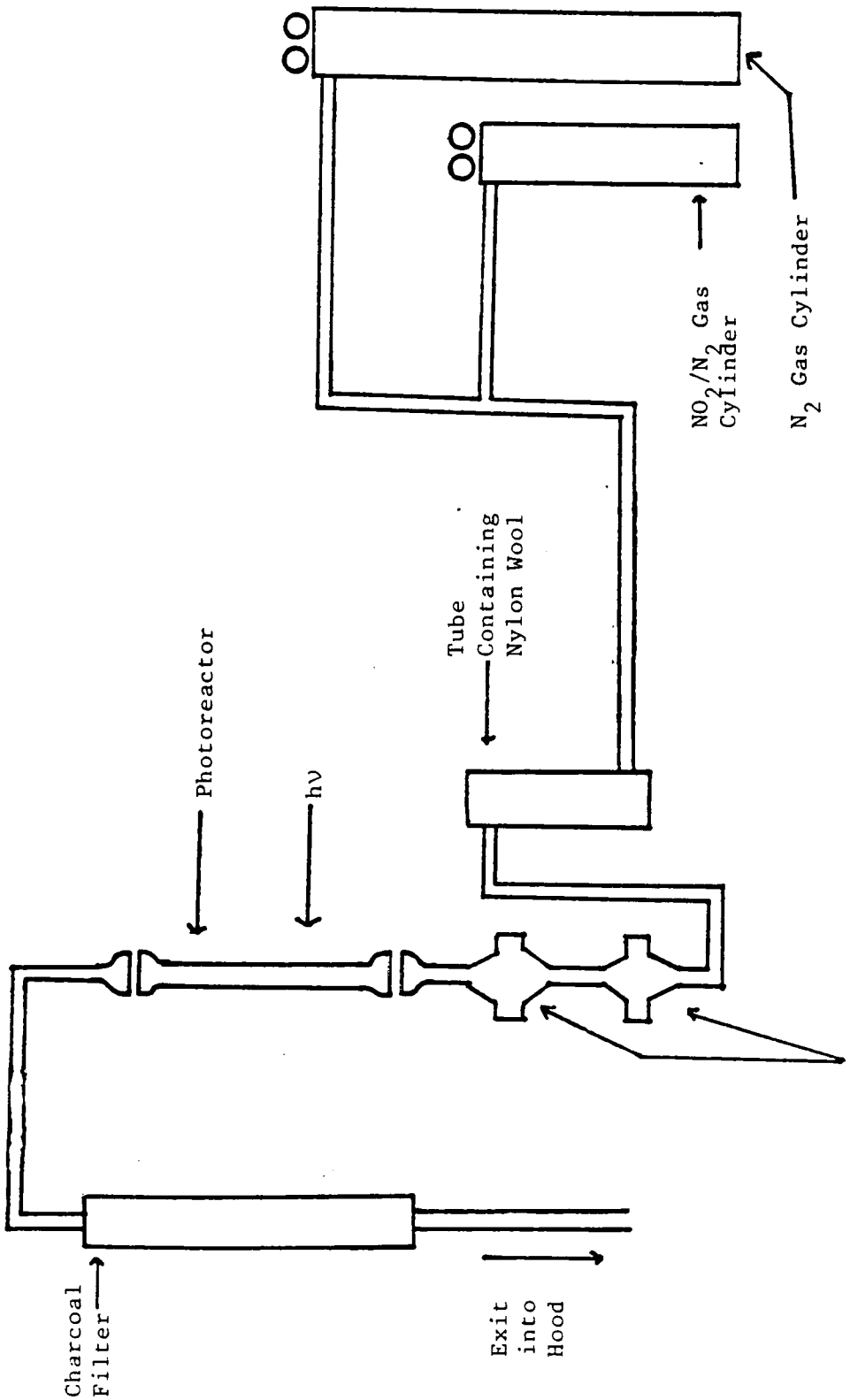



Figure 19. Block Diagram of Pollutant Gas Experiments Using the Photoreactor.

A calibration curve was constructed by treating standards (aqueous solutions of $KNO_3$) in the same fashion as were the extracts. A blank was prepared simply by using 40 ml of distilled water instead of the nylon filter extracts.

The various reagents used in this procedure were prepared as follows:

1. Phenol-sodium phenolate buffer. Vacuum sublimed phenol (9.4 g) was dissolved in 250 ml of distilled water. An aliquot of this solution (50 ml) was pipetted into a 100 ml volumetric flask and then 16 ml of 1.00 N sodium hydroxide was added. This solution was then diluted to the mark and was stored in a dark bottle and discarded when it became colored.

2. Copper sulfate catalyst. Copper sulfate pentahydrate (0.0393 g) was weighed into a 100 ml volumetric flask and diluted to the mark with distilled water.

3. Hydrazine sulfate solution. Hydrazine sulfate (1.2 g) was weighed into a 250 ml volumetric flask and then diluted to the mark with distilled water.

4. Hydrazine-copper reducing agent. An aliquot of the hydrazine sulfate solution (25 ml) was mixed with 5 ml of the copper sulfate catalyst solution in a 50 ml volumetric flask and diluted to the mark with distilled water. This reagent was prepared daily.

5. N-(1-Naphthyl)ethylenediamine dihydrochloride. N-(1-Naphthyl)ethylenediamine dihydrochloride (0.60 g) was transferred to about 80 ml of distilled water containing 1 ml of concentrated HCl. This solution was then diluted to 100 ml.

6. Sulfanilic acid. Sulfanilic acid (0.30 g) was transferred to a 100 ml volumetric flask. Then 80 ml of distilled water and 12.9 ml of concentrated HCl was added and the resulting solution was diluted to the mark.

Nylon wool (Atlas Electric Devices Company, Chicago, Illinois) was boiled in distilled deionized water for one hr and dried in an oven (95°C) for 48 hr before packing it into the tube described in the photoreactor experiments, Section II-E. This procedure was a slight modification of the procedure used by Sanhueza, et al.[99]

An aliquot of the nylon wool was also ultrasonically extracted and analyzed using the same technique as described for the nylon filters.

To insure that $NO_2$ was passing through the photoreactor (since a large quantity of nylon wool was being used), the output from the photoreactor, before and after addition of the nylon wool, was passed through a fritted glass tube into 10 ml of an absorbing reagent containing sulfanilic acid, N-(1-naphthyl)ethylenediamine dihydrochloride, and acetic acid (the absorbing reagent to be described below). The solution turned from colorless to pink when $NO_2$ was present in the gas stream. The detection limit of this technique was reported to be 5 parts per billion or 10 $\mu g/m^3$.[100]

The reagents used in this procedure were prepared as follows:

1. Absorbing reagent. Sulfanilic acid (5 g) was dissolved in almost 1 l of distilled deionized water containing 140 ml of glacial acetic acid. The solution was gently heated to speed up the dissolution and then allowed to cool. Then 20 ml of aqueous 0.1%

N-(1-naphthyl)ethylenediamine dihydrochloride was added and the resulting solution was diluted to 1 l.

2. N-(1-naphthyl)ethylenediamine dihydrochloride, stock reagent. The reagent (0.1 g) was dissolved in 100 ml of distilled deionized water.

## L. Selected Wavelength Irradiation Experiments

Benzo(a)pyrene was vapor- and solution-deposited onto ground cobalt glass plates (45 μm), some of which had been etched for 30 min with 5% HF. These samples were ground by first using a hammer to break up the cobalt glass plates and then rotating the smaller broken pieces in a ball mill for 48 hr. The $\leq$ 45 μm fraction was etched (with 5% HF for 30 min) in an attempt to increase the surface of the glass particles. Aliquot samples of these "benzo(a)pyrene-coated" samples were irradiated with the 2500 W xenon lamp, as described in Section II-F-3, using the excitation monochromator at 365 and 284 nm in different experiments. The 365 nm illumination was in a region in which the cobalt glass plates transmitted and the 284 nm illumination was in a region in which the cobalt glass plates absorbed. Aliquot samples, before and after illumination, were subjected to micro-soxhlet extractions.

# CHAPTER III

## RESULTS AND DISCUSSION OF PHOTOCHEMICAL AND NON-PHOTOCHEMICAL TRANSFORMATIONS

### A. Initial Vapor-Adsorption Experiments

Experiments were performed to determine if the diffusion cell in the generator oven (Figure 7, p 39) could deliver a constant vapor-phase pyrene concentration, using $N_2$ as the carrier gas. This was done, after temperature equilibration (144 ± 1°C in the generator oven and 154 ± 1°C in the expanded bed reactor oven), by passing the gas stream from the expanded bed reactor (which did not contain an adsorbent) in the second oven through a fritted glass tube into a collection vessel containing 20 ml of toluene. The vapor was bubbled through the solvent for 5 min at a flow rate of 200 ml/min. This procedure was repeated every 5 min. After passage through the collection vessel, the gas stream was allowed to exit into a well-vented hood. These toluene solutions were then transferred to 50 ml volumetric flasks and analyzed by fluorescence spectroscopy. The efficiency of the collection process for pyrene was determined to be 100% by connecting a second collection vessel in series with the first collection vessel and analyzing the toluene extract; the result for analysis of the extract from the second collection vessel was below the detection limit of the method used for quantification.

Table 9 shows the results of these measurements. From these data one can see that the vapor phase pyrene concentration was nearly constant over the time period of the experiment (1.5 hr). A

TABLE 9

CONCENTRATION OF PYRENE SOLUTIONS OBTAINED BY BUBBLING DIFFUSION CELL EFFLUENT THROUGH TOLUENE

| Solution Number | Pyrene Concentration |
|---|---|
| 1. | 0.52 ppm |
| 2. | 0.58 ppm |
| 3. | 0.44 ppm |
| 4. | 0.59 ppm |
| 5. | 0.44 ppm |
| 6. | 0.69 ppm |
| 7. | 0.52 ppm |
| 8. | 0.52 ppm |
| 9. | 0.52 ppm |

statistical analysis of these data was performed; the mean and the 95% confidence interval were calculated to be 0.54 ± 0.06 ppm for the solution concentration.

An experiment was performed to try to determine the pyrene adsorption capacity of East Tennessee bituminous coal fly ash. About 1 g of unsieved fly ash was placed in the expanded bed reactor and then degassed for 1 hr. The degassing procedure essentially involved passage of only $N_2$ through the fly ash in the expanded bed reactor after the expanded bed reactor oven had reached temperature equilibration (154 ± 1°C). After the generator oven was close to temperature equilibration (144 ± 1°C), the output from the expanded bed reactor was passed through a collection vessel containing toluene, as in the experiment described in the preceding paragraphs. The first three sample solutions were collected when the 4-port 2-way valve (Figure 8, p 41) was in the by-pass position (so that vapor was not passing through the fly ash in the expanded bed reactor). The next thirteen sample solutions were collected while vapor-phase pyrene was passing through the fly ash. Then, the valve was turned back to the by-pass position and three more sample solutions were collected. These solutions were quantified by fluorescence spectrometry.

Table 10 shows the results of this experiment. From these data it can been seen that the vapor-phase pyrene concentration exiting the expanded bed reactor oven decreased considerably when the vapor stream was passed through the fly ash bed, indicating adsorption of pyrene by the fly ash. As adsorption continued, the vapor-phase pyrene concentration gradually increased until, after about 354 min, it approached

TABLE 10

RESULTS OF PYRENE ADSORPTION CAPACITY OF
EAST TENNESSEE COAL FLY ASH EXPERIMENT

| Sample Number | Pyrene Concentration (ppm) | Time (minutes) | Valve Position | |
|---|---|---|---|---|
| 1 | 0.25 | 19 | by-pass | (a) |
| 2 | 0.35 | 27 | " | |
| 3 | 0.45 | 37 | " | |
| 4 | 0.09 | 5 | adsorbent bed | (b) |
| 5 | 0.13 | 14 | " | |
| 6 | 0.16 | 22 | " | |
| 7 | 0.24 | 34 | " | |
| 8 | 0.29 | 74 | " | |
| 9 | 0.33 | 99 | " | |
| 10 | 0.36 | 149 | " | |
| 11 | 0.41 | 179 | " | |
| 12 | 0.43 | 209 | " | |
| 13 | 0.43 | 234 | " | |
| 14 | 0.43 | 294 | " | |
| 15 | 0.42 | 342 | " | |
| 16 | 0.44 | 354 | " | |
| 17 | 0.45 | 5 | by-pass | (c) |
| 18 | 0.42 | 20 | " | |
| 19 | 0.46 | 30 | " | |

(a) Zero time was when diffusion cell was placed in first box. The 19 minutes represents 14 minutes from zero time plus a 5 minute collection period.

(b) Valve was turned to adsorbent bed position and a 5 minute sample collection was started at the same time.

(c) Valve was returned to by-pass position and a 5 minute sample collection started immediately.

the original concentration, presumably indicating that the adsorption of pyrene by the fly ash had virtually ceased.

Figure 20 is a plot of pyrene solution concentration versus time. These data indicate that, within the 99% confidence interval calculated for the original vapor-phase pyrene concentration, the East Tennessee bituminous coal fly ash was saturated with pyrene in about three hours. If one assumes the 0.45 ppm level shown in Figure 20 to be constant throughout the 354 min "coating" time period, one can estimate the concentration of the pyrene adsorbed on the fly ash. This is done by calculating the amount of pyrene that passed through the expanded bed reactor over the 354 min time period. By knowing the flow rate through the vapor-adsorption apparatus (182 ml/min), the toluene solution volume and concentration (50 ml and 0.45 μg/ml, respectively), the weight of the fly ash in the expanded bed reactor, and that each solution represents 5 min of "coating" time, one only needs to compare the area above the curve to the total area in the plot shown in Figure 20 to obtain the pyrene concentration adsorbed on the fly ash. The results of such a calculation indicated that the fly ash contained about 300 μg pyrene per g of fly ash at saturation.

Another calculation was also performed, since the amount of pyrene vaporized from the diffusion cell was measured by weighing the amount of pyrene in the diffusion cell, before and after the experiment. This calculation showed the pyrene concentration on the fly ash to be 283 μg per g of fly ash. This "weighing" method, however, was probably not as accurate as the method previously mentioned because of the large uncertainties involved in weighing. In this experiment the

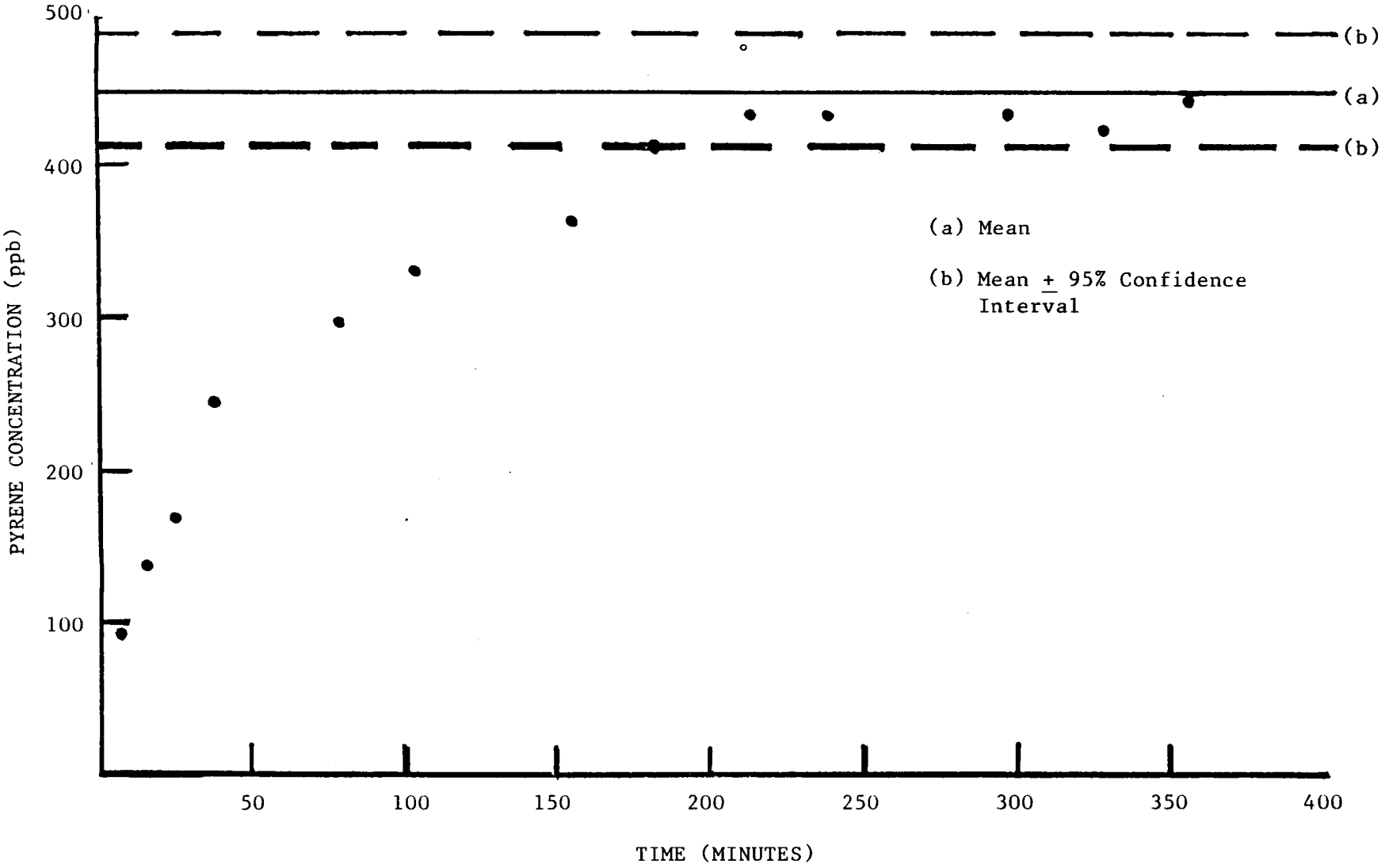



Figure 20. Plot of Pyrene Extract Concentration versus Time.

diffusion tube and pyrene weighed only 6.5580 g before and 6.5565 g after the pyrene had been vaporized. This indicates that only 1500 μg of vapor-phase pyrene was generated during the experiment. These calculated "loading" levels would probably be higher if the fly ash had been sieved to $\leq$ 45 micrometer size particles before the experiment, since the specific surface area of the fly ash would have been increased by restricting the experiment to small fly ash particles.

The vapor-adsorption apparatus parameters for almost all subsequent experiments of this type were very similar to those specified above. The only significant differences in "coating" procedures were the equilibration temperatures used for pyrene (144 ± 1°C for the generator oven and 154 ± 1°C for the expanded bed reactor oven) and benzo(a)pyrene (171 ± 1°C for the generator oven and 186 ± 1°C for the expanded bed reactor oven), and the "coating" and degassing times. Later sample preparation involved degassing times of 24 hr (to drive off water and/or organics and to "standardize" the degassing time for all the substrates). The "coating" time varied from 3 to 48 hr. The longer the "coating" time, the higher the PAH concentration on the substrate. Some substrates were more difficult to "coat" than other substrates to achieve reasonable PAH concentration levels. Table 11 is a list of various substrates and the level of difficulty to "coat" a substrate with about 100 μg/g of pyrene and benzo(a)pyrene. Of course, the real difficulty may be the extraction efficiency for extracting the PAHs from the substrates by the micro-soxhlet extraction technique.

The data in Table 11 appear to indicate that, for many adsorbents, pyrene is much less difficult to "coat" or extract than

TABLE 11

SEMI-QUANTITATIVE LEVEL OF DIFFICULTY FOR "COATING" VARIOUS SUBSTRATES AT THE 100 µg/g LEVEL

| Substrate | Pyrene | Benzo(a)pyrene |
|---|---|---|
| Silica Gel | 0 | 0 |
| Alumina | 0 | 0 |
| Commercial Fly Ash (lot no. 720-1) | 0 | + |
| Commercial Fly Ash (lot no. 720-2) | 0 | + |
| Controlled Porosity Glass | 0 | 0 |
| Glass, Brown Bottle | 0 | + |
| Glass, Cobalt Plates | | ++ |
| Crawford Fly Ash | 0 | |
| Texas Lignite Coal Fly Ash | 0 | + |
| Flaked Graphite | 0 | 0 |
| East Tennessee Bituminous Coal Fly Ash | 0 | ++ |
| Western Kentucky Bituminous Coal Fly Ash | + | ++ |
| Illinois Bituminous Coal Fly Ash | + | ++ |
| New Mexico Subbituminous Coal Fly Ash | 0 | + |
| Kaneb Coal Fly Ash | 0 | + |
| Eastern Appalachian Coal Fly Ash | 0 | 0 |

0 = Easy to "Coat" or Extract at the 100 µg level after a 12 hr "coating-time."

+ = Moderately Difficult to "Coat" or Extract at the 100 µg level after a 12 hr "coating-time."

++ = Highly Difficult to "Coat" or Extract at the 100 µg level after a 12 hr "coating-time."

benzo(a)pyrene. It was necessary to prepare several samples of "benzo-(a)pyrene-coated" substrate for the East Tennessee bituminous, Western Kentucky bituminous, and Illinois bituminous coal fly ashes, as well as the cobalt plate glass, before benzo(a)pyrene could be detected in the extracts. For this work, limits of detection for benzo(a)pyrene using ultraviolet absorption and fluorescence spectroscopy were, typically, about 5 μg/g and 3 μg/g, respectively.

### B. Comparisons of Different Extraction Techniques

After vapor-depositing PAHs onto the surfaces of various adsorbents, it was necessary to determine how much PAH was present. The method used in this work was micro-soxhlet extraction. Although the micro-soxhlet extraction technique did not achieve quantitative recoveries of adsorbates, it was sufficiently reproducible to be used to detect any treatment of the adsorbent (e.g., irradiation) that significantly altered the concentration of the PAH (by reextracting the adsorbent and analyzing the corresponding extracts).

Comparisons between the micro-soxhlet extraction and two other extraction techniques were performed to determine which extraction technique was more efficient. The use of hydrofluoric acid (HF), to try to dissolve the adsorbent surface and thereby release the adsorbed PAH,[101] was attempted, and the other extraction technique studied was sonication (use of high frequency sound waves).

Studies were performed to determine the concentration of HF that was most efficient for the extraction of pyrene from East Tennessee bituminous coal fly ash. These studies were performed with

solution-deposited samples so that the concentration of pyrene on the fly ash surface was known with reasonable accuracy. Figure 21 shows the effect of increasing the HF concentration on extraction efficiency. These extractions were performed by weighing 100 to 300 mg of solution-deposited fly ash into a polyethylene bottle (covered with aluminum foil) containing 40 ml HF and 40 ml toluene. The HF concentration was varied from bottle to bottle. The samples were gently stirred for 48 hr and then the organic phase was transferred to a 50 ml volumetric flask and analyzed by ultraviolet absorption spectroscopy. One can see from Figure 21 that, as the HF concentration decreases, the extraction efficiency increases.

The HF extraction technique (using 1% HF) was also attempted by weighing 100 to 300 mg of sample into a 100 ml teflon separatory funnel containing 40 ml 1% HF and 40 ml toluene. This was shaken vigorously for 3 min and then the organic layer was transferred to a 50 ml volumetric flask and analyzed by ultraviolet absorption spectroscopy. The results of the 1% HF (3 min) extraction were within the confidence intervals calculated for the 1% HF (48 hr) extraction. It would appear, therefore, that many more samples could be extracted by the 3 min technique, without sacrificing extraction efficiency, as compared with the 48 hr technique.

A comparison between these two HF extraction techniques and the micro-soxhlet extraction was performed. In this experiment, pyrene was vapor-deposited on East Tennessee bituminous coal fly ash. Table 12 shows the results of extracting the adsorbent by the three techniques. One can see from these data that the micro-soxhlet extraction technique

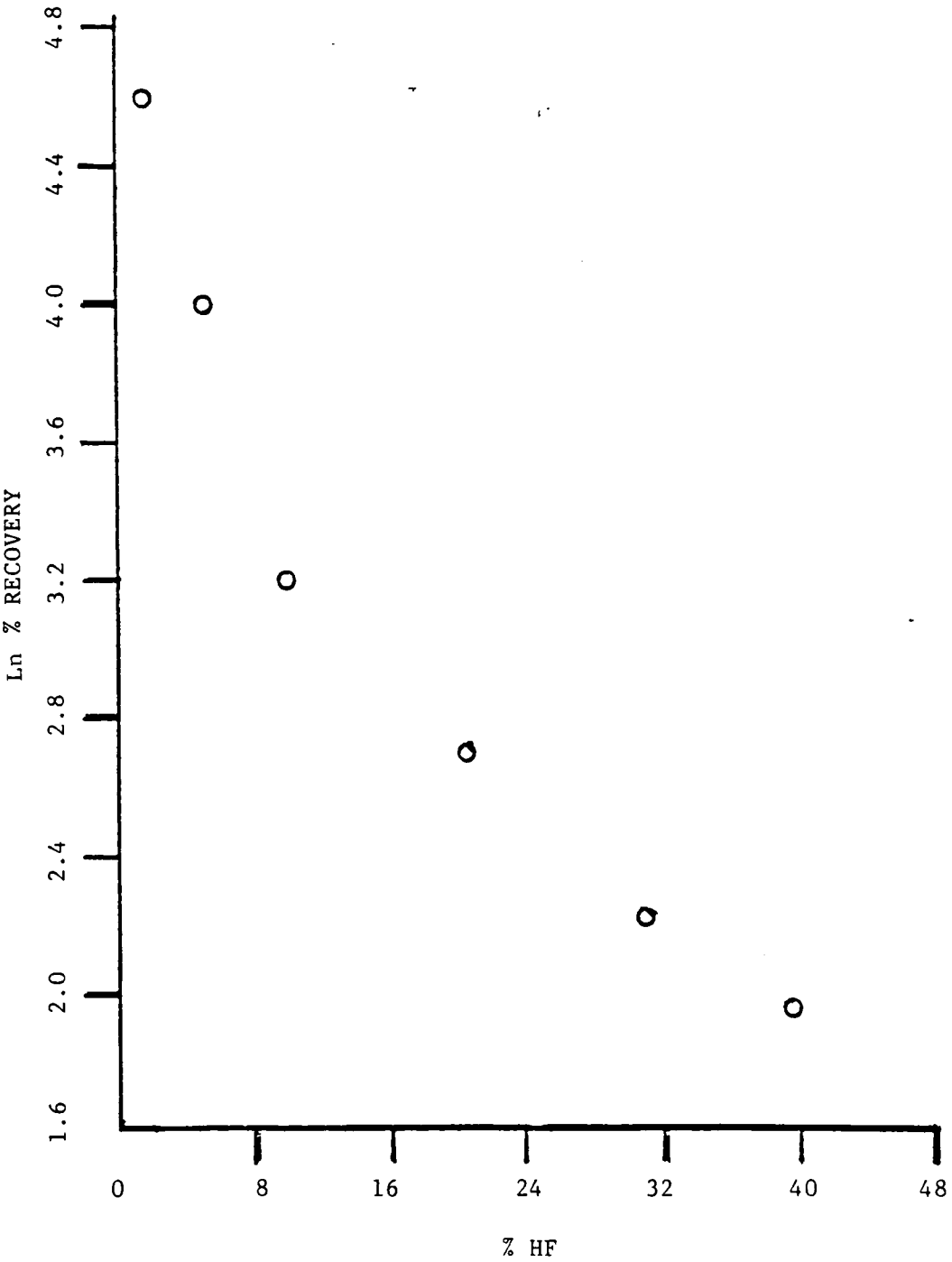



Figure 21. Plot of Logarithim of Percentage Recovery versus Percentage of HF.

TABLE 12

EXTRACTION EFFICIENCY OF THREE TECHNIQUES

| Micro-soxhlet (24 hour) | | 1% HF (48 hour) | 1% HF (3 minute) |
|---|---|---|---|
| Extraction 1 | 87 µg/g | 83 | 61 |
| Extraction 2 | 89 | 71 | 60 |
| Extraction 3 | 97 | 73 | 65 |
| Extraction 4 | 85 | 76 | |
| Mean ± 95% Confidence Interval | 90 ± 12 | 76 ± 12 | 62 ± 11 |
| RSD | 6% | 7% | 4% |

was more efficient than either of the two HF methods. Although the precise pyrene/fly ash concentration was not known, the data indicate that the micro-soxhlet technique did recover more pyrene from the fly ash than the HF extraction procedures.

The micro-soxhlet extraction technique was also compared with a sonication extraction technique. Vapor-deposited and solution-deposited samples (pyrene adsorbed on East Tennessee bituminous coal fly ash) weighing about 100 mg were weighed directly into 30 ml fine fritted glass funnels. After the addition of 25 ml toluene, a Brabson sonicator was adjusted to a setting of 3 (about 60% power) and was lowered into the solution for 3 min. Then toluene was vacuum filtered through the frit and transferred to a 100 ml volumetric flask. Two more 25 ml extractions were performed and added to the 100 ml flask. The micro-soxhlet extractions were performed as described earlier.

Table 13 shows the results of the two extraction techniques.[102] One can see from these data that the micro-soxhlet and sonication techniques appear to be very similar in extraction efficiency.

As a result of these studies, the micro-soxhlet extraction was chosen for this work because of its higher extraction efficiency when compared to the HF extraction techniques and because it was not as expensive as the sonication technique. When using the sonication technique, one could only use a fritted funnel for one extraction because fly ash particles embedded themselves into a frit. A "memory" effect occurred if the funnel was used for another extraction. The sonication technique also required twice as much solvent as the micro-soxhlet extraction method. Both extraction techniques required about

TABLE 13

COMPARISON OF MICRO-SOXHLET AND SONICATION EXTRACTION EFFICIENCY[102]

| | Method | Concentration | 95% Conf. Int. |
|---|---|---|---|
| Vapor-Deposited Samples | | | |
| Extraction 1 | MS | 110 µg/g | |
| Extraction 2 | MS | 111 | |
| | | | 110 ± 2 |
| Extraction 3 | MS | 110 | |
| Extraction 4 | MS | 108 | |
| Extraction 1 | S | 111 | |
| Extraction 2 | S | 109 | |
| | | | 110 ± 2 |
| Extraction 3 | S | 109 | |
| Extraction 4 | S | 111 | |
| Solution-Deposited Samples | | | |
| Extraction 1 | MS | 93 | |
| | | | 89 ± 12 |
| Extraction 2 | MS | 95 | |
| Extraction 3 | MS | 89 | |
| Extraction 4 | MS | 78 | |
| Extraction 1 | S | 84 | |
| Extraction 2 | S | 99 | |
| | | | 97 ± 23 |
| Extraction 3 | S | 117 | |
| Extraction 4 | S | 89 | |

MS = Micro-soxhlet.

S = Sonication.

one hour of actual working time (although the micro-soxhlet procedure then required an additional 24 hr for extraction). Therefore, the most significant advantage of the sonication technique was that more samples could be extracted per day.

It is stressed again that none of the extraction techniques was presumed to exhibit 100% recovery of pyrene or benzo(a)pyrene. Therefore, only differences in extraction recoveries (e.g., between illuminated samples and those stored in the dark) were significant and then only if the differences significantly exceeded the confidence intervals for the respective recoveries. The data in Tables 12 (p 75) and 13 (p 77) indicate the precision that can be achieved by micro-soxhlet extraction with sufficiently careful technique.

### C. Non-Photochemical Transformation

Samples of various substrates which had been "coated" with a particular PAH were stored in aluminum foil-covered screw cap vials in the presence of air in the dark for varying periods of time after an aliquot portion of that sample had been extracted. Extraction of the substrate several weeks or months later allowed one to compare the apparent concentration of the PAH adsorbed on the substrate after storage to the initial PAH concentration. These data provided information regarding the non-photochemical behavior of PAHs adsorbed on the surface of the substrates under study. If the confidence intervals of the two extractions (initial extraction after sample preparation and an extraction at some later date) overlapped, then one could not conclude that a non-photochemical transformation had occurred. If the

confidence intervals did not overlap, however, one could conclude that a non-photochemical transformation had occurred. In addition to providing information regarding transformation of adsorbed PAHs in the dark, these studies also were necessary to ensure that PAH transformations reported as "photochemical" actually resulted from illumination of samples rather than from thermal degradation of absorbates.

Table 14 shows the results of storing several "pyrene coated" substrates for various periods of time and then reextracting aliquots of the sample at the end of the storage period. The commercial fly ash (lot no. 720-1) and brown glass are the only substrates which appear to be associated with non-photochemical reactions of pyrene. The data listed in Table 14 for the other substrates are not as conclusive. Pyrene adsorbed on alumina, for example, appears to undergo "dark" reaction over a long period of time, but the calculated confidence intervals for some of the extractions are larger than desirable.

Table 15 lists the other substrates that had been "coated" with pyrene and later reextracted. It appears from these data that a slow non-photochemical reaction takes place in some cases; for most of the substrates listed in Table 15, a period of about 100 days is required before any significant change in pyrene concentration occurs. Pyrene adsorbed on East Tennessee bituminous coal fly ash did not exhibit any significant change until after 600 days of storage in the dark. The Western Kentucky bituminous, Illinois bituminous, Texas lignite, Kaneb, and Eastern Appalachian coal fly ashes do not appear to be associated

TABLE 14

NON-PHOTOCHEMICAL BEHAVIOR OF PYRENE ADSORBED ON VARIOUS SUBSTRATES

| Substrate | Extractable Pyrene (days between preparation and analysis) |
|---|---|
| Silica Gel | 317 ± 41 (0), 318 ± 8 (7), 315 ± 72 (41), 319 ± 35 (599)<br>140 ± 6 (3), 132 ± 30 (121)<br>180 ± 3 (6), 156 ± 4 (130) |
| Alumina | 2482 ± 9 (4), 2384 ± 22 (9), 2243 ± 78 (271),<br>185 ± 12 (85), 186 ± 1 (122),<br>814 ± 44 (12), 720 ± 31 (64) |
| Commercial Fly Ash (lot no. 720-1) | 186 ± 19 (0), 75 ± 4 (88) |
| Commercial Fly Ash (lot no. 720-2) | 155 ± 6 (22), 141 ± 3 (121) |
| Controlled Porosity Glass | 317 ± 13 (0), 318 ± 10 (63), 290 ± 26 (157), |
| Brown Bottle Glass | 106 ± 6 (7), 87 ± 1 (30) |
| Crawford Fly Ash | 302 ± 14 (2), 292 ± 25 (41), 285 ± 37 (72) |
| Flaked Graphite | 1032 ± 38 (0), 1033 ± 28 (36) |

*μg Pyrene/g Substrate.

TABLE 15

NON-PHOTOCHEMICAL BEHAVIOR OF PYRENE ADSORBED ON COAL FLY ASHES

| Substrate | Extractable Pyrene (days between preparation and analysis) |
|---|---|
| East Tennessee Bituminous Coal Fly Ash | 45 ± 1 (0), 43 ± 9 (120), 124 ± 7 (6), 123 ± 3 (132), 74 ± 2 (32), 75 ± 3 (38), 45 ± 9 (606), 152 ± 3 (3), 136 ± 5 (614), 134 ± 6 (627), 134 ± (653), 61 ± 13 (10), 49 ± 3 (28), 42 ± 6 (427), 41 ± 4 (551) |
| Western Kentucky Bituminous Coal Fly Ash | 30 ± 2 (7), 30 ± 8 (22) |
| Illinois Bituminous Coal Fly Ash | 53 ± 13 (53), 59 ± 6 (48), 50 ± 8 (192), 39 ± 3 (219) |
| New Mexico Subbituminous Coal Fly Ash | 185 ± 11 (13), 191 ± 15 (19), 176 ± 11 (37), 917 ± 8 (2), 834 ± 10 (84), 786 ± 12 (97), 800 ± 3 (140), 782 ± 3 (157) |
| Texas Lignite Coal Fly Ash | 390 ± 5 (3), 380 ± 5 (9), 375 ± 2 (30), 299 ± 17 (276), 474 ± 10 (24), 464 ± 10 (157), 523 ± 4 (2), 472 ± 9 (78) |
| Kaneb Coal Fly Ash | 1074 ± 40 (6), 1044 ± 34 (69) |
| Eastern Appalachian Coal Fly Ash | 222 ± 10 (13), 216 ± 24 (47), 212 ± 17 (144), 204 ± 4 (227) |

*µg Pyrene/g Substrate.

with non-photochemical reactions of pyrene. Pyrene adsorbed on New Mexico subbituminous coal fly ash appears to undergo a slight non-photochemical change after about 84 days. It should be stressed that these "dark" reactions appear to be sufficiently slow that they should not materially affect the data for photochemical transformation (Tables 19 through 23).

The data listed in Table 16 are the results of extracting "benzo-(a)pyrene-coated" substrates that have been stored in the dark for varying periods of time. These data appear to indicate that no non-photochemical transformations occurred. The data listed for benzo(a)-pyrene adsorbed on alumina are most unusual since the benzo(a)pyrene concentration appears to increase. There were no observed experimental errors which warranted rejection of these data although the possibility of error still exists. Other workers[103-105] have observed translational motion (molecules moving from one site to another on the surface) of pyrene adsorbed on such substrates as alumina, silica gel, and calcium fluoride, in which this translational motion strengthened the pyrene-substrate interaction. The pyrene-substrate interaction could be weakened, however, by competition for adsorption sites by some gaseous species (e.g., $H_2O$). These workers did not study benzo(a)-pyrene, but if a similar site competition between gaseous species and benzo(a)pyrene occurred, it could be a possible explanation for the increased benzo(a)pyrene concentration extracted from alumina after storage. If, over a period of time, the average benzo(a)pyrene-alumina interaction weakened, then the micro-soxhlet extraction efficiency could increase.

TABLE 16

NON-PHOTOCHEMICAL BEHAVIOR OF BENZO(a)PYRENE ADSORBED ON VARIOUS SUBSTRATES

| Substrate | Extractable Benzo(a)pyrene (days between preparation and analysis) |
|---|---|
| Silica Gel | 85 ± 12 (32), 70 ± 5 (133), 73 ± 12 (183) |
| Alumina | 394 ± 16 (21), 468 ± 27 (138), 664 ± 19 (252) |
| Commercial Fly Ash (lot no. 720-1) | 163 ± 15 (3), 165 ± 5 (47), 143 ± 17 (60)<br>56 ± 1 (21), 57 ± 7 (55) |
| Controlled Porosity Glass | 227 ± 4 (4), 230 ± 6 (11), 212 ± 7 (52) |
| Cobalt Plate Glass | 24 ± 10 (0), ND (9) |

*μg Benzo(a)pyrene/g Substrate.

ND = Not Detected.

Table 17 lists the extraction results for benzo(a)pyrene adsorbed on other substrates. It appears that none of the coal fly ash substrates is associated with non-photochemical transformations except the Kaneb coal fly ash and the commercial fly ash (720-1) (Table 14, p 80). On Kaneb coal fly ash, after 288 days the benzo(a)pyrene concentration had decreased from about 40 μg/g to about 5 μg/g. On the commercial fly ash (720-1) the pyrene concentration had decreased by about 60% after 88 days.

A qualitative summary of non-photochemical transformations is shown in Table 18. The Kaneb coal fly ash that had been "coated" with benzo(a)pyrene is listed as a + even though a time interval somewhere between 21 and 288 days was required for this transformation to occur to a reasonable extent. No extractions were performed in the interim between the 21st and 288th day so no conclusions can be drawn about the behavior during this time period. However, the validity of the photochemical studies of benzo(a)pyrene adsorbed on this fly ash should not be affected adversely by this slow dark reaction. Furthermore, the validity of the photochemical studies of pyrene adsorbed on the commercial fly ash should not be affected by the slow dark reaction observed on that substrate.

Precautions to prevent simple PAH evaporation from the substrates were not taken during this study. Presumably, the interactions between PAHs and the various substrates are quite strong as evidenced by the long storage times for which no significant change in PAH concentration occurred. The possibility still exists, however, that benzo(a)pyrene

TABLE 17

NON-PHOTOCHEMICAL BEHAVIOR OF BENZO(a)PYRENE ADSORBED ON COAL FLY ASHES

| Substrate | Extractable Benzo(a)pyrene (days between preparation and analysis) |
|---|---|
| East Tennessee Bituminous Coal Fly Ash | 25 ± 2 (10), 24 ± 3 (67), 27 ± 5 (117) |
| Western Kentucky Bituminous Coal Fly Ash | 25 ± 2 (21), 24 ± 3 (120), 39 ± 10 (349) |
| Illinois Bituminous Coal Fly Ash | 31 ± 6 (5) 33 ± 6 (44), 28 ± 2 (79), 33 (96)** |
| New Mexico Subbituminous Coal Fly Ash | 43 ± 2 (7), 52 ± 15 (233), 38 ± 9 (463)<br>282 ± 85 (7), 391 ± 29 (339), 256 ± 12 (396) |
| Texas Lignite Coal Fly Ash | 53 ± 3 (30), 48 ± 3 (80), 51 ± 22 (247) |
| Kaneb Coal Fly Ash | 42 ± 3 (3), 40 ± 2 (21), 9 ± 5 (288), 5 ± 1 (292) |
| Eastern Appalachian Coal Fly Ash | 118 ± 8 (55), 109 ± 11 (63), 119 ± 8 (106) |

*µg Benzo(a)pyrene/g Substrate.

**Only one sample was analyzed because the other three extractions had gone to dryness.

TABLE 18

QUALITATIVE SUMMARY OF NON-PHOTOCHEMICAL EXPERIMENTS

| Substrate | Pyrene | Benzo(a)pyrene |
|---|---|---|
| Silica Gel | 0 | 0 |
| Alumina | 0 | 0 |
| Commercial Fly Ash (lot no. 720-1) | ++ | 0 |
| Commercial Fly Ash (lot no. 720-2) | 0 | |
| Controlled Porosity Glass | 0 | 0 |
| Glass, Brown Bottle | ++ | ++ |
| Glass, Cobalt Plates | | ++ |
| Crawford Fly Ash | 0 | |
| Texas Lignite Coal Fly Ash | 0 | 0 |
| Flaked Graphite | 0 | |
| East Tennessee Bituminous Coal Fly Ash | 0 | 0 |
| Western Kentucky Bituminous Coal Fly Ash | 0 | 0 |
| Illinois Bituminous Coal Fly Ash | 0 | 0 |
| New Mexico Subbituminous Coal Fly Ash | 0 | 0 |
| Kaneb Coal Fly Ash | 0 | + |
| Eastern Appalachian Coal Fly Ash | 0 | 0 |

0 = Little or non-photochemical transformation.

+ = Moderate non-photochemical transformation.

++ = High non-photochemical transformation.

adsorbed on Kaneb coal fly ash simply evaporated during its long storage rather than undergoing a non-photochemical transformation.

### D. Irradiation Experiments with "PAH-coated" Substrates

As described in Section I-D, various adsorbents that had been vapor-deposited with a particular PAH were illuminated in a quartz irradiation cell (Figure 11, p 44). Table 19 lists the results of micro-soxhlet extractions of various adsorbents that had been "coated" with pyrene, before and after irradiation. It can be seen from the data in Table 19 that photochemical changes were observed for pyrene on many of these adsorbents. When the calculated confidence intervals for each set of extractions (before and after irradiation) did not overlap, one could conclude that a photochemical change had occurred. If the confidence intervals overlapped, then one could not conclude that a significant photochemical change had occurred. The data in Table 19 suggest that the irradiation of pyrene, adsorbed on the surface of various adsorbents, led to a photochemical change when the adsorbents were silica gel, alumina, commercially available fly ash, controlled porosity glass, or Crawford fly ash. The extraction results for flaked graphite, however, indicate that no photochemical transformation took place.

To be sure that the procedure used for the irradiation experiments did not cause PAH concentration decreases, other than those caused by photochemical processes, it was necessary to treat aliquot portions of each sample in exactly the same fashion as one treated samples during the irradiation experiments, except for lack of

TABLE 19

PHOTOCHEMICAL BEHAVIOR OF PYRENE ADSORBED ON VARIOUS SUBSTRATES

| Substrate | *Results (hours of illumination) |
|---|---|
| Silica Gel | 317 ± 41 (0), 68 ± 6 (24) |
| Alumina | 2482 ± 9 (0), 1527 ± 18 (24); 186 ± 1 (0), ND (24) |
| Commercial Fly Ash (lot no. 720-1) | 186 ± 19 (0), 64 ± 10 (24) |
| Commercial Fly Ash (lot no. 720-2) | 155 ± 6 (0), 140 ± 6 (24); 141 ± 3 (0), 120 ± 3 (24) |
| Controlled Porosity Glass | 318 ± 10 (0), 45 ± 3 (24) |
| Glass, Brown Bottle | 30 ± 1 (0), ND (24)<br>106 ± (0), ND (24) |
| Crawford Fly Ash | 302 ± 14 (0), 252 ± 18 (24) |
| Flaked Graphite | 1032 ± 38 (0), 1048 ± 38 (24); 583 ± 5 (0), 580 ± 12 (24) |

ND = Not Detected (detection limit of 3 μg/g).

*μg Pyrene/g Substrate.

illumination. These experiments indicated whether or not rotation of the sample and/or vacuum had any effects upon the PAH concentration. Table 20 shows the results of several such experiments. From these data one could conclude that no significant change in PAH concentration occurred due to the way the sample was treated in the absence of light. Therefore, when a significant PAH concentration decrease occurred, it could be attributed to photochemical transformations.

The extraction of other adsorbents, before and after irradiation, that had been "coated" with pyrene are listed in Table 21 (see also Table 20). This table lists seven well-characterized fly ash samples. Photochemical transformations were not observed on any of these substrates except Texas lignite coal fly ash.

Table 22 lists the results of extracting adsorbents that had been "coated" with benzo(a)pyrene, before and after irradiation. Photochemical changes were observed on all of the substrates listed except flaked graphite. Table 23 lists the results obtained on seven well-characterized fly ash samples. Only on the Texas lignite coal fly ash sample can one conclude that a photochemical change had occurred.

The observed results of irradiating various substrates that had been "coated" with pyrene and benzo(a)pyrene were very similar. When a photochemical change was observed on one substrate for pyrene, a photochemical change was also observed for benzo(a)pyrene on the same substrate. These results are summarized in Table 24. One can see from this table that silica gel, alumina, controlled porosity glass, glass (brown bottle), and Texas lignite coal fly ash were substrates on which high photochemical reactivity was observed for both adsorbates.

TABLE 20

QUANTIFICATION (IN μg PAH/g SUBSTRATE) OF EXTRACTS BEFORE AND AFTER ROTATION UNDER VACUUM OF "PAH-COATED" SUBSTRATES IN THE DARK AS COMPARED TO THEIR PHOTOCHEMICAL BEHAVIOR

| PAH/Substrate | Original PAH Concentration | PAH Concentration After Rotation Under Vacuum (24 hr) | PAH Concentration After Illumination (24 hr) |
|---|---|---|---|
| Pyrene/East Tennessee Bituminous Coal Fly Ash | 94 ± 2 μg/g | 84 ± 25 μg/g | * 70 ± 8 μg/g |
| Pyrene/East Tennessee Bituminous Coal Fly Ash | 74 ± 2 | 75 ± 3 | * 43 ± 3 |
| Pyrene/Texas Lignite Coal Fly Ash | 388 ± 20 | 401 ± 65 | 299 ± 34 |
| Pyrene/Texas Lignite Coal Fly Ash | 390 ± 5 | 380 ± 5 | 288 ± 12 |
| Pyrene/Western Kentucky Bituminous Coal Fly Ash | 48 ± 2 | 50 ± 9 | 35 ± 12; 84 ± 40 |
| Pyrene/Illinois Bituminous Coal Fly Ash | 54 ± 9 | 53 ± 13; 50 ± 8 | 46 ± 18 |
| Pyrene/Silica Gel | 317 ± 41 | 318 ± 8 | 68 ± 6 |
| BaP/Western Kentucky Bituminous Coal Fly Ash | 25 ± 2 | 24 ± 3 | 22 ± 5 |
| BaP/Kaneb Coal Fly Ash | 42 ± 3 | 40 ± 2 | 35 ± 4 |
| BaP/New Mexico Sub-bituminous Coal Fly Ash | 282 ± 85 | **307 | 305 ± 36 |
| BaP/Texas Lignite Coal Fly Ash | 48 ± 3 | 44 ± 5 | 25 ± 3 |
| BaP/Alumina | 394 ± 6 | 320 ± 47 | 158 ± 12 |

BaP = Benzo(a)pyrene.

*These irradiations were inadvertently performed using a cell, containing water, in which the ends were made of glass instead of quartz.

**Only one sample was analyzed; therefore, no confidence interval was calculated.

TABLE 21

PHOTOCHEMICAL BEHAVIOR OF PYRENE ADSORBED ON COAL FLY ASHES

| Substrate | *Results (hours of illumination) |
|---|---|
| East Tennessee Bituminous Coal Fly Ash | 44 ± 2 (0), 42 ± 9 (24); 124 ± 7 (0), 107 ± 10 (24), 104 ± 8 (48) |
| Western Kentucky Bituminous Coal Fly Ash | 30 ± 8 (0), 29 ± 10 (24); 48 ± 2 (0), 47 ± 36 (24) |
| Illinois Bituminous Coal Fly Ash | 54 ± 9 (0), 46 ± 18 (24) |
| New Mexico Subbituminous Coal Fly Ash | 176 ± 11 (0), 180 ± 17 (24)<br>834 ± 10 (0), 793 ± 14 (24)<br>917 ± 8 (0), 824 ± 83 (24) |
| Texas Lignite | 375 ± 2 (0), 244 ± 8 (24)<br>474 ± 10 (0), 223 ± 5 (24) |
| Kaneb Coal Fly Ash | 96 ± 5 (0), 89 ± 3 (24) |
| Eastern Appalachian Coal Fly Ash | 212 ± 17 (0), 241 ± 24 (24) |

*µg Pyrene/g substrate.

TABLE 22

PHOTOCHEMICAL BEHAVIOR OF BENZO(a)PYRENE ADSORBED ON VARIOUS SUBSTRATES

| Substrate | *Results (hours of Illumination) |
|---|---|
| Silica Gel | 85 ± 12 (0), 6 ± 2 (24) |
| Alumina | 394 ± 6 (0), 158 ± 12 (24) |
| Commercial Fly Ash (lot no. 720-1) | 56 ± 1 (0), 46 ± 1 (24) |
| Controlled Porosity Glass | 227 ± 4 (0), 10 (24) |
| Glass, Brown Bottle | 14 ± 1 (0), ND (24) |
| Glass, Cobalt Plate | 13 ± 10 (0), ND (24) |
| Flaked Graphite | 29 ± 11 (0), 33 ± 9 (24) |

ND = Not Detected (detection limit of 3 μg/g).

*μg Benzo(a)pyrene/g Substrate.

TABLE 23

PHOTOCHEMICAL BEHAVIOR OF BENZO(a)PYRENE ADSORBED ON COAL FLY ASHES

| Substrate | *Results (hours of illumination) |
|---|---|
| East Tennessee Bituminous Coal Fly Ash | 25 ± 2 (0), 26 ± 3 (24) |
| Western Kentucky Bituminous Coal Fly Ash | 25 ± 2 (0), 22 ± 5 (24) |
| Illinois Bituminous Coal Fly Ash | 31 ± 6 (0), 27 ± 1 (24) |
| New Mexico Subbituminous Coal Fly Ash | 43 ± 2 (0), 40 ± 9 (24) |
| Texas Lignite Coal Fly Ash | 53 ± 3 (0), 16 ± 2 (24), 25 ± 3 (24) |
| Kaneb Coal Fly Ash | 42 ± 3 (0), 35 ± 4 (24) |
| Eastern Appalachian Coal Fly Ash | 118 ± 8 (0), 108 ± 4 (24) |

*μg Benzo(a)pyrene/g Substrate.

TABLE 24

QUALITATIVE SUMMARY OF PHOTOCHEMICAL EXPERIMENTS

| Substrate | Pyrene | Benzo(a)pyrene |
|---|---|---|
| Silica Gel | ++ | ++ |
| Alumina | ++ | ++ |
| Commercial Fly Ash (lot no. 720-1) | ++ | + |
| Commercial Fly Ash (lot no. 720-2) | + | |
| Controlled Porosity Glass | ++ | ++ |
| Glass, Brown Bottle | ++ | ++ |
| Glass, Cobalt Plate | | ++ |
| Crawford Fly Ash | + | |
| Texas Lignite Coal Fly Ash | ++ | ++ |
| Flaked Graphite | 0 | 0 |
| East Tennessee Bituminous Coal Fly Ash | 0 | 0 |
| Western Kentucky Bituminous Coal Fly Ash | 0 | 0 |
| Illinois Bituminous Coal Fly Ash | 0 | 0 |
| New Mexico Subbituminous Coal Fly Ash | 0 | 0 |
| Kaneb Coal Fly Ash | 0 | 0 |
| Eastern Appalachian Coal Fly Ash | 0 | 0 |

0 = Little or no photochemical reactivity (confidence intervals overlap or just meet).

+ = Moderate photochemical reactivity (confidence intervals do not overlap; 10 to 50% change in original PAH concentration).

++ = High photochemical reactivity (confidence intervals do not overlap; >50% change in original PAH concentration).

Moderate photochemical reactivity was observed on the two commercial fly ashes and the Crawford fly ash, except in the case of "pyrene-coated" commercial fly ash (lot no. 720-1), which exhibited high photochemical reactivity.

### E. Attempted Identification of Photochemical Products

Almost all of the "PAH-coated" substrates which exhibited a PAH concentration decrease either in the presence or absence of illumination, as determined by micro-soxhlet extraction, were subjected to direct-probe mass spectrometry (DP-MS). These analyses were an attempt to determine if PAH photochemical products were present on the surface of the various substrates. Attempts were made to identify photochemical products.

Table 25 shows the mass and relative abundance of each ion obtained from the mass spectrum of an "uncoated" sample of Texas lignite coal fly ash. The only treatment applied to this sample was sieving to $\leq$ 45 μm. As can be seen from this table, the only peaks producted by the Texas lignite coal fly ash were $H_2O$ (mass 18), $N_2$ and/or CO (mass 28), and a mass 32 peak which could be $O_2$. The only other detected peak was at mass 128 and its identity was not determined. The mass 128 peak occasionally appeared in the mass spectra of several samples (but not always) and was assumed not to be significant.

Table 26 shows the mass and relative abundance of each peak obtained from the mass spectrum of uncoated, degassed Texas lignite coal fly ash. The sample was degassed using the vapor-adsorption apparatus as described in Section II-C. These data appear to indicate

TABLE 25

MASS AND RELATIVE ABUNDANCE OF EACH ION OBTAINED FROM THE MASS SPECTRUM OF TEXAS LIGNITE COAL FLY ASH (SIEVED TO $\leq$ 45 μm)

| MASS | ABUND |
|---|---|
| 18 | 67.7 |
| 28 | 100 |
| 32 | 25.8 |
| 128 | 45.2 |

TABLE 26

MASS AND RELATIVE ABUNDANCE OF EACH ION OBTAINED FROM THE MASS SPECTRUM OF DEGASSED (24 HR) TEXAS LIGNITE COAL FLY ASH

| MASS | ABUND | MASS | ABUND | MASS | ABUND |
|---|---|---|---|---|---|
| 17 | 5.3 | 91 | 1.8 | 168 | 1.9 |
| 18 | 40.2 | 95 | 12.3 | | |
| | | 96 | 4.7 | 227 | 1.9 |
| 28 | 100.0 | 97 | 21.8 | | |
| 32 | 23.8 | 98 | 2.3 | | |
| | | 99 | 5.3 | | |
| 40 | 1.6 | | | | |
| 41 | 1.8 | 105 | 1.9 | | |
| 43 | 13.5 | 109 | 7.4 | | |
| 44 | 30.2 | 110 | 2.3 | | |
| | | 111 | 12.9 | | |
| 55 | 7.8 | 113 | 3.1 | | |
| 56 | 1.9 | 115 | 2.9 | | |
| 57 | 22.4 | | | | |
| 58 | 1.6 | 119 | 1.8 | | |
| | | 123 | 4.5 | | |
| 67 | 3.3 | 125 | 4.5 | | |
| 69 | 13.8 | 127 | 1.9 | | |
| 70 | 3.1 | | | | |
| 71 | 20.1 | 137 | 2.7 | | |
| | | 139 | 3.7 | | |
| 81 | 10.3 | 141 | 2.7 | | |
| 82 | 5.3 | | | | |
| 83 | 15.6 | 147 | 1.6 | | |
| 84 | 2.1 | 149 | 1.9 | | |
| 85 | 17.0 | 151 | 1.9 | | |

that the degassing procedure, to some extent, resulted in the adsorption of gaseous species from the $N_2$ carrier gas onto the surface of the coal fly ash since several new masses were detected that were not detected in the mass spectrum of the undegassed sample mentioned in the previous paragraph. Mass spectra obtained for many samples (many adsorbents other than the Texas lignite coal fly ash) showed the mass 227 peak as seen in Table 26, as well as peaks as masses 168, 111, and 97. Direct-probe mass spectrometric experiments were also performed on blanks (i.e., no sample was present in the probe) and these also revealed the mass 227 and several other peaks. Peaks that appeared under these circumstances were disregarded and attempts to identify them were not made.

Tables 27 and 28 show the mass and relative abundance of each mass obtained from the mass spectra of "pyrene-coated" Texas lignite coal fly ash and irradiated "pyrene-coated" Texas lignite coal fly ash, respectively. These samples were degassed and "coated" as described in Section II-C. These mass spectra are quite similar, even though the micro-soxhlet extraction revealed a 42% decrease in pyrene concentration caused by illumination. No assignment of photochemical products formed in the illumination experiment is possible from these data. Furthermore, experimental evidence for the photochemical oxidation of pyrene to pyrenequinone, in solution, has not been obtained,[20] although pyrene had been observed to undergo photochemical transformation.

If a photochemical oxidation product of pyrene (mass 202) was present then a compound of molecular mass greater than 202 should have been present in the illuminated sample. The mass spectrum of

TABLE 27

MASS AND RELATIVE ABUNDANCE OF EACH ION OBTAINED FROM THE MASS SPECTRUM OF "PYRENE-COATED" TEXAS LIGNITE COAL FLY ASH

| MASS | ABUND | MASS | ABUND | MASS | ABUND |
|---|---|---|---|---|---|
| 17 | 3.4 | 88 | 5.7 | 169 | .4 |
| 18 | 17.5 | | | 173 | .4 |
| | | 95 | 1.6 | | |
| 28 | 4.1 | 96 | .7 | 174 | 2.2 |
| 32 | 1.2 | 97 | 3.1 | 175 | 1.2 |
| | | 98 | .8 | 176 | .4 |
| 43 | 1.5 | 100 | 14.8 | | |
| 44 | 6.6 | 101 | 18.1 | 197 | .4 |
| | | | | 198 | 3.4 |
| 51 | .6 | 109 | .9 | 199 | 5.2 |
| 55 | 1.3 | 110 | .5 | 200 | 23.4 |
| 56 | .3 | 111 | 2.0 | 201 | 21.2 |
| 57 | 4.1 | 113 | .5 | | |
| | | | | 202 | 100.0 |
| 67 | .6 | 119 | .4 | 203 | 16.7 |
| 69 | 3.5 | 122 | .3 | 204 | .8 |
| 70 | .6 | 123 | .9 | 208 | .7 |
| 71 | 3.3 | 125 | 1.0 | | |
| 74 | .6 | 131 | .4 | | |
| 75 | 1.1 | | | | |
| | | 137 | .5 | | |
| 81 | 1.6 | 139 | .3 | | |
| 82 | .6 | | | | |
| 83 | 2.8 | 149 | .7 | | |
| 84 | .3 | 150 | 1.3 | | |
| 85 | 2.7 | 151 | 1.2 | | |
| 87 | 2.8 | | | | |

TABLE 28

MASS AND RELATIVE ABUNDANCE OF EACH ION OBTAINED FROM THE MASS SPECTRUM OF IRRADIATED "PYRENE-COATED" TEXAS LIGNITE COAL FLY ASH

| MASS | ABUND | MASS | ABUND | MASS | ABUND |
|---|---|---|---|---|---|
| 17 | 2.8 | 88 | 5.0 | 197 | .4 |
| 18 | 11.7 | | | 198 | 3.3 |
| | | 95 | 1.1 | 199 | 4.7 |
| 28 | 4.4 | 96 | .5 | 200 | 24.7 |
| 32 | 1.2 | 97 | 2.3 | 201 | 20.4 |
| | | 98 | .7 | | |
| 43 | 1.3 | 99 | 3.7 | 202 | 100.0 |
| 44 | 6.9 | 101 | 19.5 | 203 | 16.8 |
| | | | | 204 | 1.1 |
| 51 | .3 | 109 | .7 | 208 | .5 |
| 55 | 1.0 | 110 | .5 | | |
| 56 | .4 | 111 | 1.9 | | |
| 57 | 3.0 | | | | |
| | | 122 | .3 | | |
| 67 | .5 | 123 | .7 | | |
| 69 | 2.3 | 125 | .8 | | |
| 70 | .4 | | | | |
| 71 | 2.6 | 137 | .3 | | |
| 74 | .6 | | | | |
| 75 | 1.1 | 149 | .5 | | |
| | | 150 | 1.4 | | |
| 81 | 1.0 | 151 | .8 | | |
| 82 | .5 | | | | |
| 83 | 2.0 | 174 | 2.5 | | |
| 84 | .3 | 175 | 1.1 | | |
| 85 | 1.9 | 176 | .5 | | |
| 87 | 2.8 | | | | |

pyrenequinone, for example, should exhibit a parent ion in the spectrum of mass 232. If such photochemical products were not desorbed from the surface of the substrate during the DP-MS analysis, however, then the products would not be detected. Intuitively, one would suspect that compounds such as pyrenequinone would desorb from the surface of the substrates during a DP-MS experiment (in which the desorption temperature reached a maximum of 393°C). However, the control experiment, in which an authentic sample of pyrenequinone was vapor-deposited onto the surface of a substrate and then subjected to DP-MS, was not attempted primarily due to the difficulty in locating a standard sample of pyrenequinone.

Tables 29 and 30 show the mass and relative abundance of each mass obtained from the mass spectra of "pyrene-coated" alumina and irradiated "pyrene-coated" alumina, respectively. These spectra are also very similar to each other, even though micro-soxhlet extraction revealed a 39% decrease in pyrene concentration caused by illumination. The mass 208 and 219 peaks were peaks that often appeared in the mass spectra even when uncoated samples were subjected to DP-MS. Furthermore, when even a small leak was present in the vacuum system of the mass spectrometer, anomalous peaks (such as 208 and 219) sometimes appeared. No attempts were made to identify these peaks.

Since the mass spectra of the irradiated "pyrene-coated" substrates were ineffective in providing possible photochemical product information, micro-soxhlet extracts of, for example, the irradiated "pyrene-coated" alumina, were concentrated (from 50 ml to about 5 ml) by gently passing $N_2$ gas over the extract while the flask was immersed

TABLE 29

MASS AND RELATIVE ABUNDANCE OF EACH ION OBTAINED FROM THE MASS SPECTRUM OF "PYRENE-COATED" ALUMINA

| MASS | ABUND | MASS | ABUND | MASS | ABUND |
|---|---|---|---|---|---|
| 17 | 3.4 | 95 | 4.6 | 201 | 20.9 |
| 18 | 18.8 | 96 | 1.7 | | |
| | | 97 | 9.2 | 202 | 100.0 |
| 28 | 10.8 | 98 | 1.0 | 203 | 17.3 |
| 32 | 2.1 | 99 | 5.0 | 208 | 1.2 |
| | | 100 | 15.4 | | |
| 43 | 4.4 | 101 | 17.1 | | |
| 44 | 12.9 | | | | |
| | | 109 | 2.3 | | |
| 51 | 1.0 | 110 | 1.3 | | |
| 55 | 3.5 | 111 | 5.7 | | |
| 56 | 1.4 | 113 | 1.5 | | |
| 57 | 11.0 | | | | |
| | | 123 | 2.0 | | |
| 67 | 1.9 | 125 | 2.3 | | |
| 69 | 8.0 | 131 | 1.0 | | |
| 70 | 1.5 | | | | |
| 71 | 10.8 | 149 | .9 | | |
| | | 150 | 1.1 | | |
| 81 | 4.4 | 151 | 1.6 | | |
| 82 | 2.1 | | | | |
| 83 | 7.4 | 174 | 2.1 | | |
| 84 | 1.2 | 175 | 1.0 | | |
| 85 | 7.2 | | | | |
| 87 | 2.4 | 198 | 2.2 | | |
| 88 | 4.9 | 199 | 4.3 | | |
| | | 200 | 23.1 | | |

TABLE 30

MASS AND RELATIVE ABUNDANCE OF EACH ION OBTAINED FROM THE MASS SPECTRUM OF IRRADIATED "PYRENE-COATED" ALUMINA

| MASS | ABUND | MASS | ABUND | MASS | ABUND | MASS | ABUND |
|---|---|---|---|---|---|---|---|
| 17 | 2.8 | 77 | .2 | 113 | .7 | 163 | .3 |
| 18 | 13.9 | 81 | 1.9 | | | 165 | .3 |
| | | 82 | .9 | 119 | .5 | 167 | .2 |
| 28 | 6.8 | 83 | 3.2 | 121 | .3 | 169 | .6 |
| 29 | .3 | 84 | .6 | 122 | .4 | 173 | .5 |
| 32 | 2.1 | 85 | 2.9 | 123 | 1.1 | | |
| | | 86 | .5 | 124 | .4 | 174 | 2.1 |
| 40 | .2 | 87 | 2.5 | 125 | 1.2 | 175 | 1.3 |
| 41 | .6 | 88 | 4.4 | 126 | .3 | 176 | .8 |
| 43 | 1.9 | | | 127 | .4 | 178 | .3 |
| 44 | 8.4 | 91 | .2 | 131 | .5 | 179 | .2 |
| 45 | .2 | 93 | .3 | | | 181 | .3 |
| | | 94 | .2 | 133 | .2 | 183 | .2 |
| 51 | .5 | 95 | 2.3 | 135 | .4 | | |
| 55 | 1.5 | 96 | .8 | 137 | .5 | 197 | .4 |
| 56 | .6 | 97 | 3.8 | 138 | .2 | 198 | 3.3 |
| 57 | 4.4 | 98 | 1.1 | 139 | .5 | 199 | 5.1 |
| 58 | .3 | 99 | 3.6 | 141 | .3 | 200 | 23.4 |
| 60 | .2 | 101 | 15.4 | 145 | .2 | 201 | 20.2 |
| 67 | .9 | 105 | .3 | 149 | .8 | 202 | 100.0 |
| 68 | .2 | 107 | .2 | 150 | 1.5 | 203 | 16.3 |
| 69 | 3.0 | 108 | .2 | 151 | 1.2 | 204 | .7 |
| 70 | .8 | 109 | 1.3 | 152 | .3 | 208 | .3 |
| 71 | 3.9 | 110 | .9 | 153 | .3 | | |
| 74 | .6 | 111 | 2.5 | 155 | .2 | 219 | .4 |
| 75 | .9 | 112 | .3 | | | | |

in a 35°C water bath. This concentrated extract was then analyzed by ultraviolet absorption spectroscopy. This procedure was also ineffective as far as providing clues to the identity of photochemical products, if they were indeed present in the micro-soxhlet extracts. There were no new features in the ultraviolet absorption spectra of the extracts of the illuminated samples that were not present in the ultraviolet absorption spectrum of pure pyrene.

Attempts were made to separate and detect possible photochemical products by gas chromatography (GC). A glass gas chromatography column, 1/8 inch in diameter and 6 feet long, was packed with 100/120 mesh Chromosorb W that had been coated with 5% SE-30 and the instrument used was a Perkin-Elmer model Sigma 3 GC equipped with a flame ionization detector (FID). The noise level obtained with this detector was considerable even though precautions were taken to ensure flame stability such as filtering the $N_2$ carrier and the air and $H_2$ combustion gases. All gases were carefully regulated with respect to flow rate. Injection of 10 µl aliquots of concentrated micro-soxhlet extracts of the "PAH-coated" substrates did not show any peaks other than a small peak for the particular PAH that had been coated on the extracted substrate. In most cases the detected peak was only slightly greater than the signal to noise ratio (S/N) which for these experiments was assigned a value of 2. The detection limits, therefore, were not sufficiently low for detecting photochemical products (if present) that were probably at concentrations lower than the initial PAH that had been coated on the substrate. Substrates that were associated with high (++) photochemical reactivity were also extracted and then

concentrated before 10 µl aliquots were injected onto the GC. No peaks were observed other than the PAH peak. Again it must be emphasized that the detection limits were probably not adequate for detection of possible photochemical products.

An attempt was also made to identify possible photochemical products by liquid chromatography (LC). The LC utilized Altex Model 110A reciprocating piston pumps and a 20 µl injection loop. The column was an Alltech C-18 reverse phase, 25 cm by 4.6 mm i.d., of 10 µm particle size. The solvent system was methanol/water (70/30 by volume) at a flow rate of 1.0 ml/min. Two detection systems were employed. The first detector employed was an LDC model 1203 fixed-wavelength (254 nm) ultraviolet-visible absorption detector. However, the detection limits obtained with this detector were not low enough to be of analytical utility for this work. The detection limit obtained (based on S/N = 2) by injecting pyrene standards was only 2 ng/µl. This figure (2ng/µl) also considers that 20 µl of sample was injected (i.e., the detection limit was 40 ng/20 µl).

The relatively high detection limit obtained by using ultraviolet (254 nm) detection initiated the idea to explore laser-induced fluorescence as a possible detection method for possible photochemical products. This study was performed using a National Research Group (5202/B) $N_2$ laser. An excitation wavelength of 337 nm and an emission wavelength of 374 nm was used for concentrated extracts of "pyrene-coated" substrates. A 40 ml micro-soxhlet extract was concentrated to about 1 ml and then this solution was used to fill the 20 µl injector loop, and injected onto the column. The detection limit obtained in

this manner (0.2 ng/μl) was much better than that for the fixed wavelength detector at a S/N = 2. This method was not considered further, however, since the possible photochemical products obtained by illuminating pyrene and/or benzo(a)pyrene would most likely be non-fluorescing compounds and would not be detected by laser-induced fluorescence. Instability of the baseline and non-reproducibility of injection did not allow quantitation of the micro-soxhlet extracts.

The possibility that the use of a more "polar" solvent (than methanol) in the micro-soxhlet extraction procedure might extract polar photochemical products was investigated. The solvent chosen for this experiment was acetonitrile. Figures 22 and 23 show the ultraviolet absorption spectra of acetonitrile extracts of "pyrene-coated" alumina and Texas lignite coal fly ash, respectively, before and after irradiation (24 hr). These extracts were also concentrated (from 50 ml to about 5 ml) by immersing the flask containing the extract in a water bath (30°C) while gently passing a stream of dry $N_2$ over the extract. One can see from these figures that the only new feature in the spectra of extracts from the irradiated sample was a weak broad band extending from 470 to 420 nm for the alumina sample, and a small peak at about 385 nm for the Texas lignite coal fly ash sample. The sharp rise at about 350 nm shown in Figures 22 and 23 was due to pyrene in each sample (the pyrene spectrum is shown in Figure 14, p 51), since the sensitivity of the measurement was made quite high to help distinguish possible new spectral features. This evidence was also very inconclusive.

Direct-probe mass spectra were also obtained of several of the "PAH-coated" substrates that showed no apparent change in PAH




Figure 22. Ultraviolet-Visible Absorption Spectra of the Concentrated Micro-Soxhlet Extracts (in Acetonitrile) of "Pyrene-Coated" Alumina (a) After and (b) Before Irradiation.

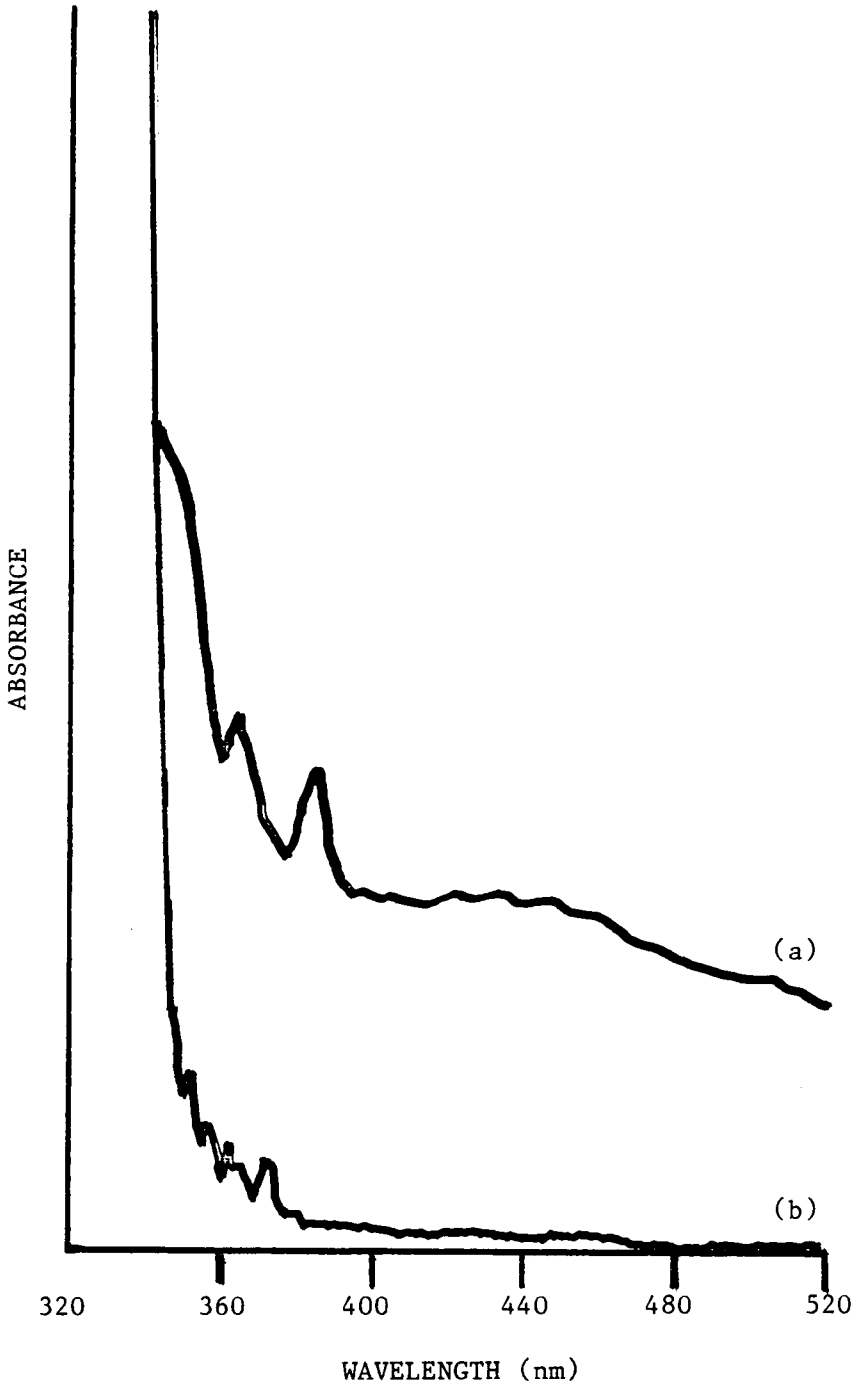



Figure 23. Ultraviolet-Visible Absorption Spectra of the Concentrated Micro-Soxhlet Extracts (in Acetonitrile) of "Pyrene-Coated" Texas Lignite Coal Fly Ash (a) After and (b) Before Irradiation.

concentration after irradiation, as determined by micro-soxhlet extraction. Tables 31 and 32 show the mass and relative abundance of each mass obtained from the mass spectra of "benzo(a)pyrene-coated" New Mexico subbituminous coal fly ash and irradiated "benzo(a)pyrene-coated" New Mexico subbituminous coal fly ash, respectively. From these data one can see that there was essentially no difference between the mass spectra obtained for the two samples. This result was expected, since the micro-soxhlet extraction did not indicate any change in benzo(a)pyrene concentration caused by illumination.

"Benzo(a)pyrene-coated" alumina and Texas lignite coal fly ash, on which photochemical transformations had been observed to occur, as determined by micro-soxhlet extraction, were also subjected to DP-MS. In these spectra, shown in Tables 33, 34, 35, and 36, no peaks of mass greater than that of benzo(a)pyrene were observed. The mass 258 peak was anomalous and was detected occasionally in DP-MS experiments. The mass 258 peak was observed in an unirradiated "benzo(a)pyrene-coated" alumina sample (Table 33) and in an irradiated "benzo(a)pyrene-coated" Texas lignite coal fly ash sample (Table 36). This peak was also occasionally observed in blank DP-MS experiments (no substrate in the probe).

The isotopic abundance ratio for masses 252 and 253 was within the acceptable range (±10%) when compared to calculated isotopic contribution tables for the A + 1 peak for all of the data shown in Tables 33 through 36. The spectra for the "benzo(a)pyrene-coated" alumina samples, before and after illumination, were very similar. The spectra for the "benzo(a)pyrene-coated" Texas lignite coal fly ash

TABLE 31

MASS AND RELATIVE ABUNDANCE OF EACH ION OBTAINED FROM THE MASS SPECTRUM OF "BENZO(a)PYRENE-COATED" NEW MEXICO SUBBITUMINOUS COAL FLY ASH

| MASS | ABUND |
|---|---|
| 28 | 47.3 |
| 32 | 11.4 |
| 44 | 16.8 |
| 57 | 7.1 |
| 69 | 4.3 |
| 71 | 7.1 |
| 83 | 6.0 |
| 85 | 4.9 |
| 97 | 9.8 |
| 111 | 6.5 |
| 112 | 4.3 |
| 113 | 9.2 |
| 125 | 11.4 |
| 126 | 12.0 |
| 248 | 6.5 |
| 250 | 25.5 |
| 251 | 8.2 |
| 252 | 100.0 |
| 253 | 20.7 |

TABLE 32

MASS AND RELATIVE ABUNDANCE OF EACH ION OBTAINED FROM THE MASS SPECTRUM OF IRRADIATED "BENZO(a)PYRENE-COATED" NEW MEXICO SUBBITUMINOUS COAL FLY ASH

| MASS | ABUND | MASS | ABUND |
|---|---|---|---|
| 28 | 9.1 | 249 | 4.3 |
| 32 | 2.1 | 250 | 28.6 |
| | | 251 | 10.4 |
| 44 | 2.7 | 252 | 100.0 |
| | | 253 | 21.0 |
| 57 | 1.6 | 254 | 2.1 |
| 71 | 1.9 | | |
| 83 | 1.6 | | |
| 85 | 1.8 | | |
| 97 | 2.2 | | |
| 111 | 2.7 | | |
| 112 | 5.1 | | |
| 113 | 8.8 | | |
| 125 | 10.6 | | |
| 126 | 10.7 | | |
| 223 | 1.4 | | |
| 224 | 4.0 | | |
| 225 | 2.4 | | |
| 226 | 2.4 | | |
| 248 | 6.1 | | |

TABLE 33

MASS AND RELATIVE ABUNDANCE OF EACH ION OBTAINED FROM THE MASS SPECTRUM OF "BENZO(a)PYRENE-COATED" ALUMINA

| MASS | ABUND | MASS | ABUND |
|---|---|---|---|
| 17 | 7.9 | 112 | 7.6 |
| 18 | 33.9 | 113 | 13.9 |
| 28 | 5.0 | 124 | 7.7 |
| 32 | .9 | 126 | 18.9 |
| 41 | .5 | 200 | .8 |
| 43 | .9 | | |
| 44 | 4.9 | 222 | 1.5 |
| | | 223 | 1.3 |
| 55 | .9 | 224 | 4.9 |
| 57 | 2.3 | 225 | 2.5 |
| | | 226 | 2.7 |
| 59 | 1.3 | | |
| 71 | 1.7 | 247 | 1.0 |
| | | 248 | 6.9 |
| 81 | .7 | 249 | 5.2 |
| 83 | 1.3 | 250 | 28.9 |
| 85 | 1.1 | 251 | 10.6 |
| | | 252 | 100.0 |
| 95 | .7 | 253 | 22.7 |
| 97 | 1.6 | 254 | 1.9 |
| 99 | 1.4 | | |
| 100 | 1.3 | 258 | 1.1 |
| 109 | .5 | | |
| 111 | 3.0 | | |

TABLE 34

MASS AND RELATIVE ABUNDANCE OF EACH ION OBTAINED FROM THE MASS SPECTRUM OF IRRADIATED "BENZO(a)PYRENE-COATED" ALUMINA

| MASS | ABUND | MASS | ABUND |
|---|---|---|---|
| 17 | 3.5 | 109 | 2.3 |
| 18 | 17.3 | 111 | 6.5 |
| | | 112 | 6.8 |
| 28 | 14.5 | 113 | 11.8 |
| 32 | 3.3 | | |
| | | 123 | 2.1 |
| 41 | 1.7 | 124 | 5.3 |
| 43 | 4.1 | 125 | 11.8 |
| 44 | 16.5 | 126 | 11.7 |
| 55 | 4.2 | 224 | 3.6 |
| 56 | 1.8 | 225 | 1.8 |
| 57 | 9.5 | 226 | 2.4 |
| 69 | 5.8 | 248 | 6.5 |
| 71 | 8.2 | 250 | 27.6 |
| | | 251 | 11.8 |
| 81 | 3.5 | 252 | 100.0 |
| 82 | 1.4 | 253 | 20.6 |
| 83 | 7.9 | 254 | 1.4 |
| 84 | 1.4 | | |
| 85 | 5.0 | | |
| 95 | 3.8 | | |
| 96 | 1.8 | | |
| 97 | 8.0 | | |
| 99 | 2.7 | | |

TABLE 35

MASS AND RELATIVE ABUNDANCE OF EACH ION OBTAINED FROM THE MASS SPECTRUM OF "BENZO(a)PYRENE-COATED" TEXAS LIGNITE COAL FLY ASH

| MASS | ABUND | MASS | ABUND | MASS | ABUND |
|---|---|---|---|---|---|
| 17 | 23.6 | 82 | 7.1 | 129 | 2.5 |
| 18 | 83.1 | 83 | 20.9 | 131 | 6.7 |
| | | 84 | 6.1 | | |
| 28 | 38.0 | 85 | 20.2 | 135 | 3.1 |
| 32 | 9.5 | | | 137 | 4.3 |
| | | 91 | 4.9 | 139 | 3.4 |
| 41 | 7.4 | 93 | 3.1 | | |
| 42 | 3.4 | 94 | 4.0 | 151 | 4.9 |
| 43 | 17.2 | 95 | 17.5 | | |
| 44 | 100.0 | 96 | 7.7 | 169 | 3.7 |
| 45 | 4.0 | 97 | 25.2 | | |
| | | 98 | 5.2 | 248 | 2.8 |
| 51 | 4.0 | 99 | 6.4 | 249 | 2.5 |
| 55 | 13.8 | | | 250 | 11.0 |
| 56 | 7.1 | 105 | 4.9 | 251 | 4.0 |
| 57 | 31.3 | 109 | 10.7 | 252 | 36.5 |
| 60 | 3.4 | 110 | 4.0 | 253 | 8.3 |
| | | 111 | 14.1 | | |
| 64 | 6.7 | 112 | 4.6 | | |
| 67 | 6.7 | 113 | 8.3 | | |
| 68 | 3.4 | | | | |
| 69 | 23.6 | 119 | 5.5 | | |
| 70 | 7.1 | 123 | 8.0 | | |
| 71 | 26.7 | 124 | 5.5 | | |
| 73 | 3.4 | 125 | 12.3 | | |
| | | 126 | 6.1 | | |
| 81 | 12.9 | 127 | 3.1 | | |

TABLE 36

MASS AND RELATIVE ABUNDANCE OF EACH ION OBTAINED FROM THE MASS SPECTRUM OF IRRADIATED "BENZO(a)PYRENE-COATED" TEXAS LIGNITE COAL FLY OIL

| MASS | ABUND | MASS | ABUND | MASS | ABUND | MASS | ABUND |
|---|---|---|---|---|---|---|---|
| 16 | 3.0 | 60 | 2.4 | 96 | 6.8 | 131 | 6.8 |
| 17 | 21.7 | | | 97 | 19.9 | | |
| 18 | 98.2 | 64 | 18.1 | 98 | 5.4 | 133 | 2.6 |
| | | 65 | 2.6 | 99 | 4.4 | 138 | 2.6 |
| 27 | 4.0 | 66 | 2.2 | 101 | 2.2 | 140 | 2.0 |
| 28 | 37.1 | 67 | 8.2 | | | 142 | 2.2 |
| 29 | 5.4 | 68 | 4.2 | 104 | 4.4 | | |
| 32 | 7.0 | 69 | 22.9 | 105 | 5.2 | 146 | 2.4 |
| | | 70 | 7.8 | 106 | 2.2 | 151 | 4.2 |
| 36 | 5.2 | 71 | 16.1 | 107 | 3.0 | 154 | 1.8 |
| 38 | 1.6 | | | 109 | 6.8 | | |
| 39 | 4.4 | 77 | 5.0 | 110 | 2.6 | 169 | 3.4 |
| 40 | 1.8 | 78 | 2.8 | 111 | 10.6 | | |
| 41 | 12.2 | 79 | 4.6 | 112 | 4.8 | 180 | 1.6 |
| 42 | 5.2 | 80 | 3.4 | 113 | 7.8 | 182 | 2.8 |
| 43 | 19.7 | 81 | 12.7 | 115 | 2.2 | | |
| 44 | 100.0 | 82 | 7.8 | 117 | 3.6 | 194 | 1.8 |
| 45 | 3.2 | 83 | 17.1 | | | | |
| | | 84 | 6.0 | 118 | 1.8 | 220 | 3.4 |
| 48 | 5.8 | 85 | 12.0 | 119 | 4.6 | | |
| 51 | 7.0 | 86 | 1.8 | 121 | 3.0 | 248 | 2.6 |
| 53 | 2.2 | | | 123 | 5.0 | 249 | 2.4 |
| 54 | 2.6 | 91 | 10.6 | 124 | 3.8 | 250 | 11.6 |
| 55 | 14.5 | 92 | 2.2 | 125 | 9.6 | 251 | 6.0 |
| 56 | 8.0 | 93 | 3.6 | 126 | 8.0 | 252 | 48.0 |
| 57 | 22.7 | 94 | 2.6 | 127 | 2.6 | 253 | 11.0 |
| 58 | 1.8 | 95 | 11.0 | 128 | 3.0 | 258 | 2.2 |

samples, before and after illumination, were also very similar except for the appearance of more peaks at 1, 2, or 3 mass units higher than some of the more abundant ions (e.g., masses 57 and 58 in Table 36). This was due primarily to a higher gain setting on the detector (electron multiplier) since the irradiated samples were expected to have a lower benzo(a)pyrene concentration on the surface of the substrate than the unirradiated samples (as demonstrated by analyses of micro-soxhlet extracts).

The only DP-MS experiment that provided some evidence for the presence of a photochemical product was performed using "benzo(a)-pyrene-coated" commercial fly ash (lot no. 720-1). Tables 37 and 38 show the results of these experiments, before and after irradiation. It can be seen in Table 38 that a mass 282 peak appeared in the spectrum of the illuminated sample. This mass was consistent with the presence of a benzo(a)pyrenequinone (mass 282). The abundance relative to the base peak was extremely small (0.9), however, and calculation of isotopic abundances was not possible (since the mass 283 peak was not detected). Thus, this evidence is not very conclusive. The irradiation of benzo(a)pyrene, dissolved in benzene in the presence of $O_2$, led to the photochemical products 6,12-; 1,6-; and 3,6-benzo(a)pyrene-quinones, when illuminated with ultraviolet light of wavelength greater than 280 nm.[56]

The ultraviolet absorption spectrum of the micro-soxhlet extract of the irradiated sample discussed in the previous paragraph did not exhibit any spectroscopic features not also present in spectra of pure benzo(a)pyrene. Further investigation was attempted by analyzing

TABLE 37

MASS AND RELATIVE ABUNDANCE OF EACH ION OBTAINED FROM THE MASS SPECTRUM OF "BENZO(a)PYRENE-COATED" COMMERCIAL FLY ASH (LOT NO. 720-1)

| MASS | ABUND | MASS | ABUND |
|---|---|---|---|
| 17 | .8 | 248 | 6.1 |
| 18 | 4.4 | 249 | 4.2 |
| | | 250 | 25.6 |
| 28 | 18.1 | 251 | 7.8 |
| 32 | 4.3 | 252 | 100.0 |
| | | 253 | 20.9 |
| 43 | 1.4 | 254 | 1.5 |
| 44 | 3.8 | | |
| | | 258 | 1.3 |
| 69 | 2.4 | | |
| 100 | 1.1 | | |
| 112 | 4.2 | | |
| 113 | 7.6 | | |
| 124 | 4.4 | | |
| 125 | 10.5 | | |
| 126 | 12.4 | | |
| 131 | .9 | | |
| 219 | 1.8 | | |
| 222 | .7 | | |
| 223 | 1.0 | | |
| 224 | 2.8 | | |
| 225 | 1.6 | | |
| 226 | 1.5 | | |

TABLE 38

MASS AND RELATIVE ABUNDANCE OF EACH ION OBTAINED FROM THE MASS SPECTRUM OF IRRADIATED "BENZO(a)PYRENE-COATED" COMMERCIAL FLY ASH (LOT NO. 720-1)

| MASS | ABUND | MASS | ABUND |
|---|---|---|---|
| 17 | 2.0 | 91 | 1.1 |
| 18 | 9.5 | 95 | 2.3 |
| | | 96 | 1.4 |
| 28 | 100.0 | 97 | 3.0 |
| 29 | 2.2 | 98 | 1.4 |
| 32 | 26.1 | | |
| | | 111 | 1.6 |
| 40 | 1.9 | 113 | 3.6 |
| 41 | 1.4 | | |
| 42 | .9 | 119 | 1.4 |
| 43 | 2.3 | 124 | 1.4 |
| 44 | 9.3 | 125 | 3.7 |
| | | 126 | 3.7 |
| 55 | 2.6 | 131 | 3.9 |
| 56 | 1.2 | | |
| 57 | 3.6 | 219 | 5.1 |
| 60 | 1.1 | 225 | 1.2 |
| 64 | .9 | 248 | 1.6 |
| 69 | 7.6 | 249 | 1.2 |
| 71 | 3.0 | 250 | 7.3 |
| | | 251 | 2.8 |
| 81 | 1.6 | 252 | 32.8 |
| 83 | 3.0 | 253 | 6.1 |
| 84 | 1.2 | | |
| 85 | 1.7 | 282 | .9 |

micro-soxhlet extracts by ultraviolet absorption spectroscopy of "benzo(a)pyrene-coated" controlled porosity glass, before and after illumination. This substrate was chosen because the benzo(a)pyrene concentration, as determined by micro-soxhlet extraction, decreased by almost 96% after illumination. Figures 24(a,b, and c) show the results of these analyses. One can see from these data that no distinct features were present in the spectrum of the illuminated sample. While this observation is consistent with the extraction results (i.e., substantial decomposition of benzo(a)pyrene was induced by illumination), it furnishes no assistance in identifying products of the photoreaction.

Some of the concentrated micro-soxhlet extracts were concentrated further by passing dry $N_2$ gas over the extract while the flask, containing the extract, was immersed in a water bath, held at 35°C. As the extracts just reached dryness the flasks were removed and 1 ml of carbon disulfide was added. The $CS_2$ extracts were then transferred to a small infrared cell which had AgCl windows and analyzed by Fourier transform infrared spectroscopy (FTIR). If photochemical products were present in these extracts they could not be detected by this method since there were no observed features in the spectra. Even the PAH that had been "coated" on the substrates could not be detected. The detection limits of FTIR were not sufficient for this work even though the extracts had been concentrated (initial concentrations of about 0.1 ppm) and many scans (500) had been made.

An attempt was also made to identify possible photochemical products by subjecting concentrated micro-soxhlet extracts to gas

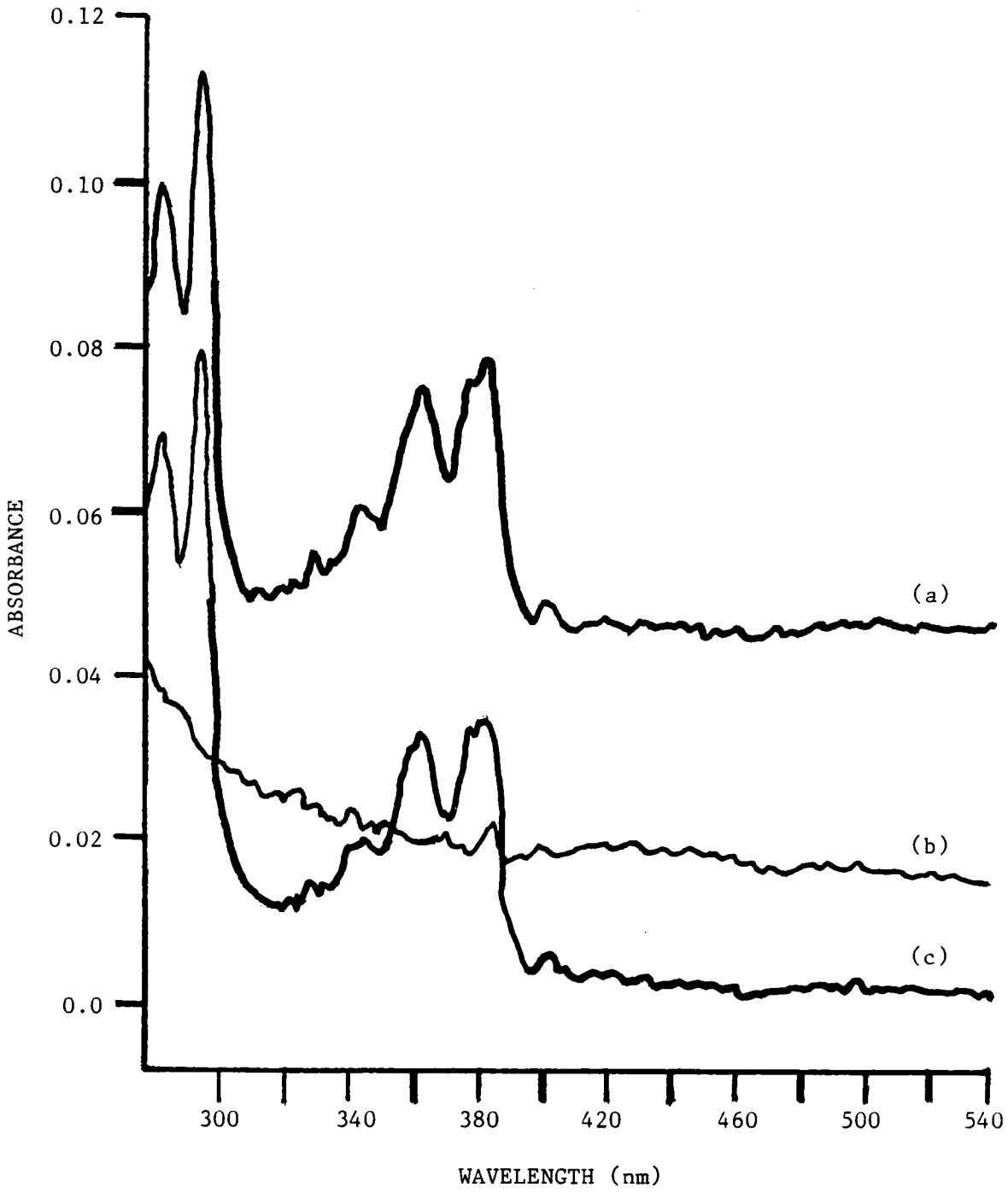



Figure 24. Absorption Spectra of (a) Benzo(a)pyrene, (b) Irradiated (24 hr) "Benzo(a)pyrene-Coated" Controlled Porosity Glass, and (c) Unirradiated "Benzo(a)pyrene-Coated" Controlled Porosity Glass.

chromatography-mass spectrometry (GC-MS). The membrane separator which interfaced the GC with the MS, used in this work, was very inefficient which resulted in detection limits that were too high to be of analytical utility.

The use of proton nuclear magnetic resonance spectroscopy (NMR) for product identification was not attempted due to the relative insensitivity of the technique even for Fourier transform NMR.

It appears from the data presented in this section that pyrene and benzo(a)pyrene adsorbed on the surface of controlled porosity glass, alumina, silica gel, brown glass bottle, and cobalt glass plates, as well as Texas lignite, Crawford, and the two commercial coal fly ashes, undergo photochemical transformations upon illumination. Attempts to identify possible photochemical products have been largely unsuccessful. Some evidence has been presented for the presence of a benzo(a)pyrenequinone on the surface of the commercial fly ash (lot no. 720-1); however, this evidence is certainly not conclusive.

Numerous photochemical products have been identified by other researchers after illuminating pyrene, solution-deposited onto silica gel chromatographic plates. Two of these compounds were 1,6 and 1,8-pyrenediones.[60] Benzo(a)pyrene, solution-deposited onto glass fiber filters, was reported to undergo photochemical transformations,[61] but the products were not identified.

It may be possible that the photochemical products (if present) were not extracted by either toluene, methanol, or acetonitrile. The new features observed in the ultraviolet absorption spectra of some of the micro-soxhlet extracts were too broad and/or weak to be useful in

determining the identity of the products. It may also be possible that the photochemical products were not being desorbed from the surface of the substrates during the DP-MS experiments. Despite strenuous efforts, no evidence can be presented to determine the identity of the photochemical products, but evidence is presented that shows that pyrene and benzo(a)pyrene undergo photochemical transformations on some of the substrates used in this study. That evidence is based solely on analysis of extracted reactant PAH before and after illumination.

F. Chemical and Physical Characteristics of Various Substrates

Table 39 lists some chemical and physical characteristics of the various substrates used in this study. The pH of extracts of the substrates was measured as discussed in Section II-G. The total % carbon analyses were obtained as discussed in Section II-H and the colors of the various substrates were the apparent colors as perceived by several members of the Fly Ash Research Group.

The pH results shown in Table 39 do not appear to correlate clearly with the observed photochemical results. In other words, substrates on which PAH photochemical transformation had been observed to occur included acidic, neutral, and basic substrates. It appears from these data, however, that the acidic substrates of pH <5 (e.g., Illinois bituminous coal fly ash) are those which were associated with no photochemical transformations.

It appears, from the data listed in Table 39, that there may be some correlation between photochemical reactivity and total % carbon, although there are exceptions. All substrates associated with

TABLE 39

CHEMICAL AND PHYSICAL CHARACTERISTICS OF VARIOUS SUBSTRATES

| Substrate | Extract pH | Color | % Carbon |
|---|---|---|---|
| Silica Gel | 6.4 | White | |
| Alumina | 7.2 | White | |
| Commercial Fly Ash (lot no. 720-1) | 11.4 | Beige | 0.23 |
| Commercial Fly Ash (lot no. 720-2) | 11.4 | Beige | 0.28 |
| Controlled Porosity Glass | 7.9 | White | |
| Glass, Brown Bottle | | Light Brown | 1.37 |
| Glass, Cobalt Plate | | Light Purple | 0.063 |
| Crawford Fly Ash | | Beige | 0.67 |
| Texas Lignite Coal Fly Ash | 10.8 | Beige | 0.46 |
| Flaked Graphite | | Black | |
| East Tennessee Bituminous Coal Fly Ash | 4.7 | Grey | 0.51 |
| Western Kentucky Bituminous Coal Fly Ash | 4.4 | Dark Brown | 3.6 |
| Illinois Bituminous Coal Fly Ash | 3.3 | Reddish Brown | 0.31 |
| New Mexico Subbituminous Coal Fly Ash | 11.9 | Grey | 1.04 |
| Kaneb Coal Fly Ash | 6.4 | Greyish-Brown | 2.81 |
| Eastern Appalachian Coal Fly Ash | 8.2 | Grey | 1.81 |

photochemical transformations are low in % carbon except the glass (brown bottle) which was 1.37% carbon. All of the substrates associated with the absence of photochemical transformations are high in total % carbon except the East Tennessee and Illinois bituminous coal fly ashes.

The color of the substrate appears to be correlated with the observed photochemical rectivity. In other words, all of the substrates associated with photochemical reactivity are light beige or white in color except the glass (brown bottle) which is light brown. All of the substrates which are associated with the absence of photochemical transformations range from grey to black in color.

Figure 25 shows the diffuse reflectance (DR) spectrum of silica gel. The instrument used for this work (Cary 14 L) had only two absorbance ranges; a 0 to 1 absorbance range and a 1 to 2 absorbance range. Therefore, when a substrate absorbed above 0.8 absorbance units (the instrument was zeroed at the 0.2 absorbance mark on the chart paper so that the white filter paper used as a reference could be zeroed over the entire 650 to 250 nm range), the absorbance range was switched from the 0 to 1 to the 1 to 2 absorbance range. This resulted in a sharp downward slide of the recorder pen. The spectrum shown in Figure 25 for silica gel did not reach an absorbance higher than about 0.55 absorbance units so the absorbance range switch was not changed. The negative absorbance obtained for the silica gel indicates that this substrate was less absorptive than the reference material (white filter paper).

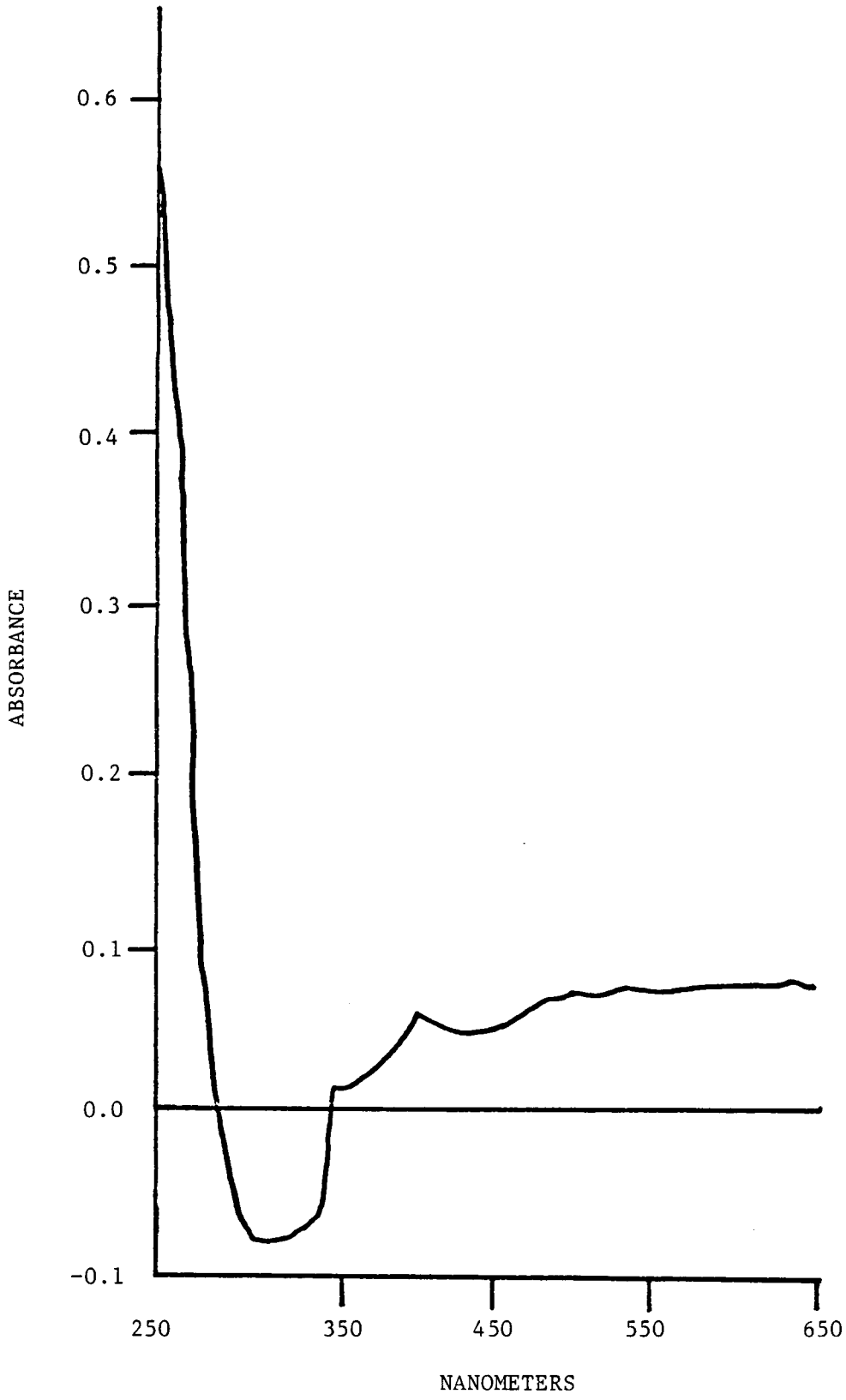



Figure 25. Diffuse Reflectance Spectrum of Silica Gel.

Diffuse reflectance spectra were obtained for all of the substrates used in this study. By compiling absorbance versus wavelength data from these DR spectra, one could obtain the data as represented in Table 40. These data indicate the absorbance of each substrate in 5 nm increments over the range of 400 to 250 nm. Also shown in Table 40 are "relative absorbance" values (as determined below) for pyrene and benzo(a)pyrene dissolved in methanol in 5 nm increments over the range of 400 to 250 nm. The relative absorbance values were calculated by assigning the most intense peak in each spectrum the value of 1.0 and then assigning all of the other peaks as decimal fractions of the most intense peak of that spectrum.

Figure 26 shows graphically some of the data from Table 40. It can more easily be seen in this figure how the DR spectra of the various substrates vary from very low absorbance to very high absorbance in the 400 to 250 nm region. Comparison of the absorption spectra for pyrene (Figure 14, p 51) and benzo(a)pyrene (Figure 15, p 52) with the data in Table 40, as well as with Figure 26, showed that for these two PAHs the wavelength range of 400 to 250 nm was the most important region of the spectrum.

By comparing the data in Table 40 with the qualitative summary of photochemical experiments (Table 24, p 94) of pyrene and benzo(a)pyrene adsorbed on various substrates, one can see that the controlled porosity glass, silica gel, brown glass bottle, cobalt glass plates, and alumina were substrates that were associated with photochemical transformations and were also substrates of very low absorbance over the 400 to 250 nm region as determined by DR spectra. Furthermore, the

TABLE 40

ABSORBANCE OF VARIOUS SUBSTRATES LISTED IN 5 nm INCREMENTS OVER THE 400 TO 250 nm RANGE AS DETERMINED BY DIFFUSE REFLECTANCE SPECTROSCOPY

| Substrate | 400 | 395 | 390 | 385 | 380 | 375 | 370 | 365 | 360 | 355 | 350 | 345 | 340 | 335 | 330 |
|---|---|---|---|---|---|---|---|---|---|---|---|---|---|---|---|
| CP | .01 | .005 | 0 | 0 | -.01 | 0.01 | -.015 | -.02 | -.02 | -.02 | -.03 | -.03 | -.1 | -.1 | -.05 |
| SG | .05 | .04 | .035 | .03 | .025 | .02 | .015 | .015 | .015 | .01 | 0 | -.07 | -.075 | -.075 | -.08 |
| BG | .08 | .08 | .08 | .08 | .08 | .08 | .08 | .08 | .08 | .08 | .08 | .08 | .04 | .04 | .04 |
| PG | -.02 | -.03 | -.03 | -.035 | -.04 | -.045 | -.045 | -.05 | -.05 | -.095 | -.095 | -.095 | -.095 | -.095 | -.09 |
| AO | -.2 | -.21 | -.22 | -.22 | -.22 | -.22 | -.22 | -.21 | -.2 | -.19 | -.18 | -.2 | -.2 | -.19 | -.17 |
| TX | .35 | .37 | .39 | .41 | .43 | .46 | .48 | .51 | .55 | .54 | .56 | .6 | .62 | .65 | .67 |
| AA | .51 | .53 | .55 | .58 | .6 | .63 | .66 | .69 | .73 | .73 | .75 | .79 | .82 | .85 | .93 |
| AB | .6 | .62 | .64 | .66 | .68 | .71 | .74 | .78 | .81 | .84 | .87 | .88 | .91 | .95 | .98 |
| ET | .2 | .2 | .21 | .22 | .24 | .27 | .29 | .33 | .35 | .38 | .38 | .41 | .46 | .5 | .55 |
| NM | .58 | .58 | .6 | .61 | .62 | .63 | .64 | .65 | .68 | .67 | .69 | .73 | .75 | .77 | .81 |
| KA | .97 | .98 | 1.0 | 1.01 | 1.01 | 1.02 | 1.03 | 1.04 | 1.05 | 1.05 | 1.05 | 1.07 | 1.08 | 1.08 | 1.08 |
| EA | .68 | .69 | .71 | .73 | .75 | .76 | .78 | .81 | .95 | .91 | .92 | .95 | .97 | 1.01 | 1.04 |
| IL | 1.09 | 1.09 | 1.1 | 1.11 | 1.12 | 1.13 | 1.14 | 1.16 | 1.17 | 1.18 | 1.19 | 1.2 | 1.21 | 1.22 | 1.23 |
| WK | 1.16 | 1.16 | 1.17 | 1.17 | 1.18 | 1.19 | 1.2 | 1.21 | 1.22 | 1.22 | 1.23 | 1.24 | 1.25 | 1.25 | 1.26 |
| FG | .87 | .86 | .85 | .84 | .83 | .83 | .83 | .83 | .82 | .82 | .79 | .76 | .75 | .75 | 1.0 |
| Pyrene | 0 | 0 | 0 | 0 | 0 | 0 | 0 | 0 | 0 | 0 | 0 | 0 | .07 | .7 | .45 |
| BaP | .03 | .04 | .11 | .43 | .41 | .28 | .24 | .4 | .36 | .20 | .20 | .20 | .15 | .09 | .08 |

TABLE 40 (Continued)

| Substrate | 325 | 320 | 315 | 310 | 305 | 300 | 295 | 290 | 285 | 280 | 275 | 270 | 265 | 260 | 255 | 250 |
|---|---|---|---|---|---|---|---|---|---|---|---|---|---|---|---|---|
| CP | -.075 | -.075 | -.075 | -.075 | -.075 | -.09 | -.09 | -.09 | -.09 | -.09 | -.09 | -.09 | -.085 | -.08 | -.06 | 0.05 |
| SG | 0.08 | -.08 | -.08 | -.08 | -.08 | -.065 | -.05 | -.03 | 0 | .05 | .11 | .2 | .35 | .42 | .48 | .49 |
| BG | .06 | .08 | .08 | .08 | .15 | .2 | .23 | .25 | .26 | .26 | .26 | .3 | .3 | .35 | .42 | .49 |
| PG | -.08 | -.06 | -.04 | -.02 | 0 | .04 | .08 | .11 | .19 | .24 | .3 | .4 | .49 | .56 | .58 | .6 |
| AO | -.15 | -.13 | -.11 | -.1 | -.07 | -.06 | -.04 | -.03 | -.02 | -.01 | 0 | .01 | .08 | .1 | .14 | .14 |
| TX | .7 | .72 | .75 | .78 | .8 | .86 | .86 | .86 | .88 | .9 | .92 | .95 | 1.0 | 1.04 | 1.04 | 1.02 |
| AA | .93 | .97 | 1.0 | 1.03 | 1.06 | 1.08 | 1.1 | 1.12 | 1.14 | 1.16 | 1.18 | 1.22 | 1.28 | 1.3 | 1.28 | 1.26 |
| AB | 1.02 | 1.05 | 1.08 | 1.1 | 1.13 | 1.15 | 1.17 | 1.19 | 1.21 | 1.22 | 1.24 | 1.28 | 1.33 | 1.36 | 1.38 | 1.4 |
| ET | .6 | .65 | .7 | .75 | .8 | .82 | .85 | .9 | .92 | .98 | 1.05 | 1.07 | 1.11 | 1.19 | 1.22 | 1.21 |
| NM | .85 | .88 | .9 | .93 | .96 | .98 | 1.0 | 1.03 | 1.05 | 1.07 | 1.1 | 1.12 | 1.14 | 1.15 | 1.16 | 1.17 |
| KA | 1.08 | 1.08 | 1.13 | 1.14 | 1.16 | 1.17 | 1.18 | 1.18 | 1.19 | 1.2 | 1.23 | 1.28 | 1.3 | 1.3 | 1.29 | 1.26 |
| EA | 1.06 | 1.08 | 1.11 | 1.14 | 1.16 | 1.18 | 1.2 | 1.22 | 1.23 | 1.25 | 1.26 | 1.29 | 1.34 | 1.38 | 1.37 | 1.35 |
| IL | 1.24 | 1.25 | 1.26 | 1.27 | 1.27 | 1.28 | 1.29 | 1.29 | 1.3 | 1.32 | 1.32 | 1.34 | 1.37 | 1.41 | 1.44 | 1.45 |
| WK | 1.27 | 1.27 | 1.28 | 1.29 | 1.3 | 1.31 | 1.31 | 1.32 | 1.33 | 1.34 | 1.34 | 1.35 | 1.36 | 1.36 | 1.37 | 1.38 |
| FG | 1.5 | 1.72 | 1.72 | 1.71 | 1.71 | 1.7 | 1.69 | 1.68 | 1.67 | 1.66 | 1.64 | 1.63 | 1.64 | 1.66 | 1.67 | 1.65 |
| Pyrene | .2 | .45 | .32 | .17 | .23 | .13 | .08 | .07 | .05 | .05 | .20 | .6 | .28 | .45 | .19 | .20 |
| BaP | .07 | .04 | .04 | .05 | .08 | .27 | 1.0 | .51 | .67 | .57 | .45 | .55 | .91 | .84 | .77 | .67 |

Pyrene Maxima (wavelength/intensity; 333 (1.0), 318 (.57), 305 (.23), 272 (1.02), 261 (.49), 252 (.22).

BaP Maxima (wavelength/intensity); 383 (.47), 377 (.43), 363 (.41), 347 (.21), 295 (1.0), 282 (.77), 264 (.93), 253 (.79).

Intensity; The largest peak in the absorption spectrum was assigned a value of 1.00 and the other peaks are presented as decimal fractions of this peak. The pyrene 272 nm peak was slightly larger than the quantitation peak but was not used since it was in a region that was often masked by interferences when analyzing extracts.

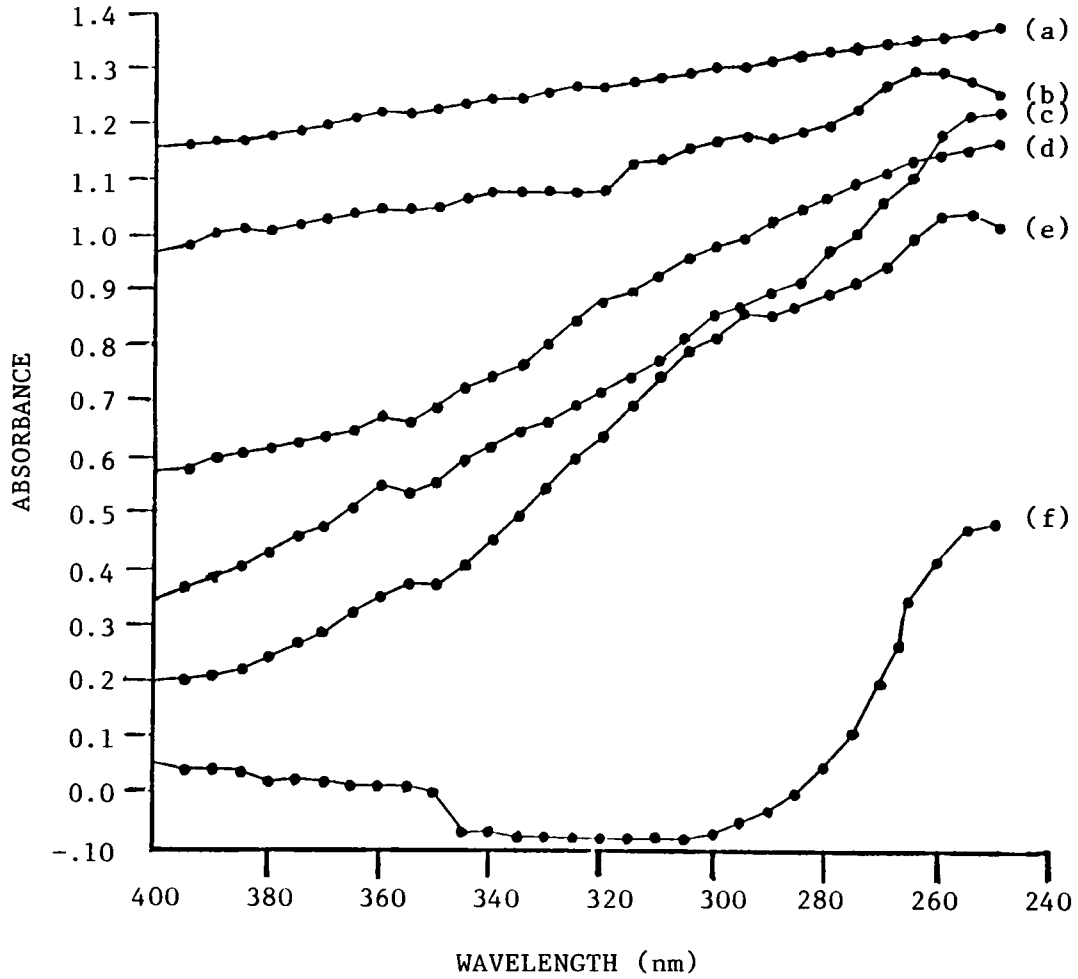



Figure 26. Graphical Representation of Data obtained from the Diffuse Reflectance Spectra of (a) Western Kentucky Bituminous, (b) Kaneb, (c), East Tennessee Bituminous, (d) New Mexico Subbituminous, and (e) Texas Lignite Coal Fly Ashes and, (f) Silica Gel.

substrates that were not associated with photochemical transformations, such as flaked graphite and the Eastern Appalachian, Illinois bituminous, Western Kentucky bituminous, and Kaneb coal fly ashes, were substrates of very high absorbance in the 400 to 250 nm region.

Some of the substrates were intermediate (0.6 to 1.2) in absorbance in the 400 to 250 nm region, including substrates such as Texas lignite and the two commercial coal fly ashes which were associated with photochemical transformations, and other substrates such as East Tennessee bituminous and New Mexico subbituminous coal fly ashes which were not associated with photochemical transformations.

These data indicated that a relationship existed between the absorbance of the substrate in the 400 to 250 nm region and the photochemical reactivity of pyrene and benzo(a)pyrene adsorbed on the surface of the substrate. However, some substrates of intermediate absorbance were associated with photochemical behavior and some were not, which implies that at least one or more other factors may have been operative.

## G. Surface Area and Porosity of Adsorbents

The Brunauer-Emmett-Teller (BET) gas adsorption method has become the most widely used procedure for the determination of the surface area of porous and finely-divided materials.[106] The method has gained widespread recognition even though the model on which the theory is based is oversimplified. The BET equation is an extention of the Langmuir equation. The Langmuir model is recognized to have three fundamental assumptions: 1) adsorption is limited to a monolayer; 2)

the adsorbent surface is composed of identical sites; and 3) adsorbed molecules do not interact with each other.[107] The BET method extends the Langmuir approach to multilayer adsorption by assuming that the Langmuir equation applies to each layer. The heat of adsorption for the first layer may have some special value (due to adsorbent-adsorbate interactions), but for all successive layers the heat of adsorption is assumed equal to the heat of vaporization of the liquid adsorbate. Furthermore, it is assumed that evaporation and condensation can occur only from or on exposed surfaces.[107]

The following derivations of the Langmuir and BET equations were obtained from the text by Gregg and Sing.[108] Let $\Theta_1$ = the fraction of occupied sites and $\Theta_0$ = the fraction of unoccupied surface sites so that $\Theta_0 + \Theta_1 = 1$. The rate of condensation per unit area of surface is given by

$$a_1 K P \Theta_0 \qquad (1)$$

where P = pressure of the gaseous adsorbate, K is a constant given by the kinetic theory of gases ($K = 1/2\ L/[MRT]^{1/2}$), $a_1$ is the condensation coefficient (defined as the fraction of available adsorbate molecules which actually condense on a surface), M is the molar mass, and L is Avogadro's number. The rate of evaporation from unit area of surface is given by

$$z_m \Theta_1 v_1 \exp(-Q_1/RT) \qquad (2)$$

where $z_m$ is the number of sites per unit area (therefore, $z_m \Theta_1$ is the corresponding number of adsorbed molecules), $Q_1$ is the isosteric

heat of adsorption, and $v_1$ is the frequency of oscillation of the molecule in a direction normal to the surface. At equilibrium

$$a_1 K P \theta_0 = z_m \theta_1 v_1 \exp(-Q_1/RT) \tag{3}$$

and since $\theta_0 = 1 - \theta_1$, then

$$\theta_1 = \frac{a_1 K P}{a_1 K P + z_m v_1 \exp(-Q_1/RT)} \tag{4}$$

If n (in moles) is the amount of adsorbate on 1 g of adsorbent and $n_m$ is the monolayer capacity, then

$$\theta_1 = n/n_m \tag{5}$$

and insertion of Equation (5) into Equation (4) gives

$$n/n_m = \frac{B P}{1 + BP} \tag{6}$$

Here $n/n_m$ is equivalent to the fraction of occupied surface sites, and B is given by

$$B = \frac{a_1 K}{z_m v_1} \exp(Q_1/RT) \tag{7}$$

Equation (6) is the Langmuir equation for the case when adsorption is limited to a monolayer. B is an empirical constant and cannot be evaluated from Equation (7). The multilayer treatment, as derived by Brunauer, Emmett, and Teller, requires that the rate of condensation of molecules from the gas phase to an already existing monolayer be equal to the rate of evaporation from the second layer. Therefore,

$$a_2 K P \Theta_1 = z_m \Theta_2 v_2 \exp(-Q_2/RT) \quad (8)$$

and for the $i^{th}$ layer

$$a_i K P \Theta_{i-1} = z_m \Theta_i v_i \exp(-Q_1/RT) \quad (9)$$

where $a_2$ is the condensation coefficient (defined as the fraction of available adsorbate molecules which actually condense on surface-adsorbed adsorbate molecules, i.e., the next layer on top of the initial monolayer).

At any pressure below the saturation vapor pressure, the fraction of the surface covered with 1, 2, . . . i molecules of adsorbate will be $\Theta_1$, $\Theta_2$, . . . $\Theta_i$, so the thickness of the adsorbed layer will not be constant throughout. The total number of molecules (z) adsorbed on the specific surface area (A) of the adsorbent is given by

$$z = A z_m (\Theta_1 + 2\Theta_2 + . . . + i\Theta_i) \quad (10)$$

The amount of adsorbate (in moles) adsorbed (n) is given by

$$n = \frac{A z_m}{N_0} \sum_1^i (i\Theta_i) \quad (11)$$

where $N_0$ is Avogadro's Number (substituting $N_0$ for L). Each layer has its own values of a, Q, and v, and the summation of Equation (11) cannot be carried out because of the various values of these quantities. The BET treatment makes three simplifying assumptions:

1) In all layers except the first layer, the heat of adsorption of the adsorbate is equal to its molar heat of condensation.

2) In all layers except the first layer, the evaporation-condensation conditions are identical, so that

$$v_2 = v_3 = \ldots v_i \text{ and } a_2 = a_3 = \ldots = a_i \tag{12}$$

3) When $P = P^0$ ($P^0$ = saturation vapor pressure), the number of layers becomes infinite and the adsorbate condenses to a bulk liquid on the surface of the solid. These assumptions allow the summation of Equation (11) and they lead to what is often called the BET equation.

$$\frac{P}{n\,(P^0 - P)} = \frac{1}{n_m\,c} + \frac{c - 1}{n_m\,c} \cdot \frac{P}{P^0} \tag{13}$$

Rearrangement of (13) gives

$$\frac{P/P^0}{n(1 - P/P^0)} = \frac{1}{n_m\,c} + \frac{c - 1}{n_m\,c} \cdot \frac{P}{P^0} \tag{14}$$

Strictly, c in Equations (13) and (14) is given by

$$c = \frac{a_1 v_2}{a_2 v_1} \exp\,(Q_1 - Q_L)/RT \tag{15}$$

In practice, however, it is assumed that $a_1 v_2 / a_2 v_1 \simeq 1$, in which case

$$c = \exp\,(Q_1 - Q_L)/RT \tag{16}$$

or

$$Q_1 - Q_L = RT \ln c \tag{17}$$

where $(Q_1 - Q_L)$ is the net heat of adsorption, and $Q_L$ is the molar heat of condensation.

Equation (13) gives a plot of $n/n_m$ versus $P/P^0$ having the shape as shown in Figure 27. As can be seen in Figure 27, the larger the value of c, the sharper the "knee" in the curve. The inflection point in the "knee" of the curve has been termed, by Brunauer, Emmett, and Teller, as "Point B." This point indicates the completion of a monolayer. A high value of c (~100) is associated with a sharp "knee" but small values of c (<20) make it difficult to identify "Point B" as a single point on the isotherm. Unfortunately, "Point B" is not itself amenable to any precise mathematical description.

The BET plot requires a linear relationship between $n/n_m$ and $P/P^0$ over a $P/P^0$ range of 0.05 to 0.30, although this is not always achieved. This helps insure that the "Point B" (on the "knee") will be distinguishable.

To obtain the total area (A) and the specific surface area (a) of the adsorbent (specific surface area is the area per g of adsorbent) requires knowing the molecular cross-sectional area ($a_m$) occupied by a substrate molecule in the complete monolayer. For close-packed $N_2$ at 77 K, $a_m$ ($N_2$) = 0.162 $nm^2$.[108] Thus,

$$A\ (BET) = n_m\ N_o\ a_m \tag{18}$$

and

$$a\ (BET) = \frac{A\ (BET)}{m} \tag{19}$$

where m is the mass of the adsorbent in g. The units of area are $m^2/g$.

The pore size terms are generally defined as "macropores" (pores with widths greater than 500 Å), "micropores" (widths not exceeding 20 Å), and "mesopores" (20 to 500 Å).[106]

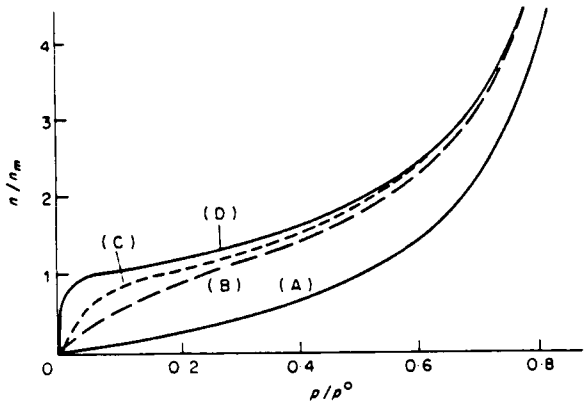



Figure 27. Adsorption Isotherm Curves of $n/n_m$ Versus $P/P^o$. (A) c=1; (B) c=11; (C) c=100; (D) c=10,000.[108]

"Hysteresis" occurs when the adsorption and desorption isotherms do not overlap. Adsorption on most porous solids exhibits hysteresis but that on a non-porous solid should not exhibit hysteresis. Hysteresis is often attributed to "capillary condensation" (condensation of adsorbate in small capillaries which occurs at adsorbate pressures below saturation of the adsorbate). The hysteresis effect can be useful to infer the shapes of adsorbent pores.

The BET model has been subjected to some criticisms. The model assumes all the adsorption sites on the surface to be energetically identical (actually, truly homogeneous surfaces are rare); also, the model restricts attention to the forces between adsorbent and the adsorbate molecules and neglects interactions between adsorbate molecules. It also is questionable to what extent it is valid to consider the molecules in all layers after the first layer as completely equivalent.[106]

Adsorption isotherms, which are the relationships, at constant temperature, between the amount of gas adsorbed and the pressure (or relative pressure) for gases on solid surfaces, may generally be grouped into six types shown in Figure 28. These six types may be generally described as follows.[106]

Type I: Usually given by microporous solids having relatively small external surfaces.

Type II: Normal form obtained with a non-porous or macroporous adsorbent representing unrestricted monolayer-multilayer adsorption in that a smooth transition is observed after the adsorbent has reached its monolayer capacity.

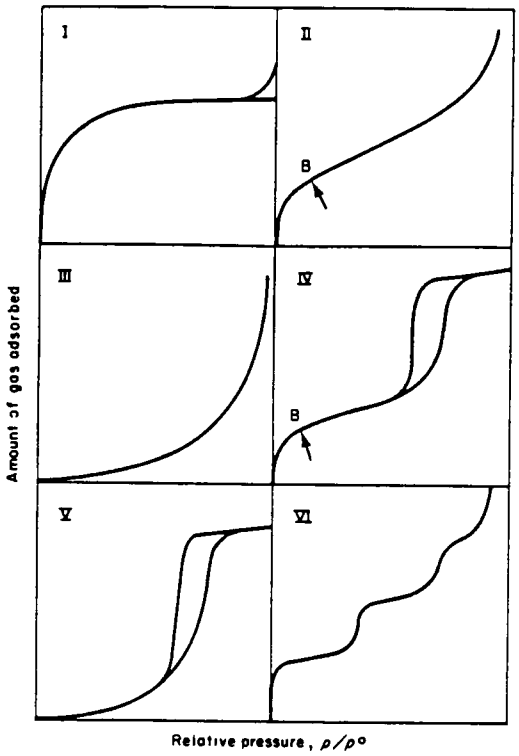



Figure 28. The Six Types of Adsorption Isotherms According to the classification of Brunauer, Deming, Deming, and Teller.[108]

Type III: Uncommon; the adsorbent-adsorbate interaction is weak as compared with the adsorbate-adsorbate interaction.

Type IV: Characterized by hysteresis loop which is associated with capillary condensation taking place in mesopores. The definition of "capillary," as by Gregg and Sing,[108] includes $r_m$ values of 10 to 250 Å, where $r_m$ is the mean radius of curvature of the pore (equal to the radius of the pore less the thickness of the adsorbed film on the walls of the pore). The upper value of 250 Å is a practical limit since the Kelvin equation ($P/P^0 = \exp[-2V\gamma/rRT]$, discussed on p 141) is limited (by experimental difficulty in measuring the very small changes of pressure) at this pore size.

Type V. Uncommon and related to Type III in that the adsorbent-adsorbate interaction is weak. This type of isotherm is usually obtained from mesoporous or microporous solids.

Type VI. Represents stepwise multilayer adsorption on a uniform non-porous surface. The step height represents the monolayer capacity for each adsorbed layer and, in the simplest case, remains nearly constant for two or three adsorbed layers.

The shapes of hysteresis loops have often been identified with specific pore structures. Figure 29 shows four general types of such loops.[106] Other types of adsorption isotherms may also exhibit hysteresis loops. They are usually interpreted as follows:

Type H1: This type is often associated with porous materials, known, from other evidence, to consist of agglomerates or compacts of approximately uniform spheres in fairly regular array, and hence to have narrow distributions of pore size.

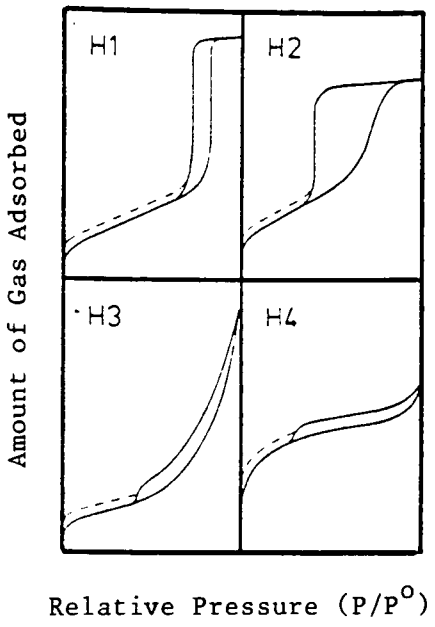



Figure 29. Types of Hysteresis Loops.[106]

Type H2: Especially difficult to interpret. The distribution of pore size and shape is not well defined. Silica gels often provide such hysteresis loops.

Type H3: This type, which does not exhibit any limiting adsorption at high $P/P^0$ (continues to adsorb adsorbate molecules when the relative pressure nears unity), is observed with aggregates of plate-like particles giving rise to slit-shaped pores.

Type H4: This type is also associated with slit-shaped pores but is usually indicative of microporosity due to the Type I isotherm character.

Low-pressure hysteresis (indicated by dashed lines in Figure 29) is thought to be associated with the swelling of a non-rigid porous structure or with irreversible uptake of molecules in pores (or through pore entrances) of about the same width as that of the adsorbate molecule.

The shapes of the isotherms may be used to calculate the pore volume and surface area distribution with respect to pore size. This technique is embodied in the Kelvin relationship:

$$P/P^0 = \exp\ (-\ 2\ V\gamma/r\ R\ T) \qquad (20)$$

where $P^0$ = saturation vapor pressure, V = molar volume of the condensed condensed liquid of temperature T and surface tension $\gamma$, and r = radius of a cylindrical pore.

The phenomenon whereby the vapor pressure of a liquid contained in a capillary is lower than that over a plane surface of the liquid at the same temperature is described by the Kelvin equation.

To detect deviations from a conventional isotherm, one compares the shape of the isotherm under study to the isotherm of a standard adsorbent. For a given gas, such as $N_2$, adsorbed on a series of substrates which have different specific surface areas but otherwise are not too dissimilar, one can expect the variation in isotherm shape to vary mainly by the amount of $N_2$ adsorbed (due to the difference in surface areas between the two adsorbents). The "t-plot" of Lippens and de Boer[108,109] is a convenient means of testing the "superimposability" of a standard isotherm with an isotherm under study. The "t-plot" is a curve of the amount (or volume) of $N_2$ adsorbed versus the thickness of a monolayer. The value of t is actually an average thickness and is obtained by

$$t = (n/n_m)\,\sigma \tag{21}$$

where n and $n_m$ are as defined previously and $\sigma$ is the thickness of a single molecular layer. For $N_2$ at 77 K, $\sigma$ = 3.54 Å (assuming that the arrangement of molecules in the film is hexagonal close-packed). The change of independent variable from $P/P^0$ to t is effected by reference to the standard t-curve (a plot of the standard adsorbent isotherm using t rather than $n/n_m$). The "t-plot" must be a straight line passing through the origin (slope = $n_m/\sigma = b_t$). From Equation (18),

$$A = n_m N_o a_m \tag{18}$$

and A (total surface area) is related to the slope ($b_t$) by the expression

$$A = a_m \sigma N_0 b_t \quad (22)$$

For $N_2$ at 77 K, and $a_m = 16.2 \times 10^{-20}$ $m^2$/molecule, $\sigma = 3.54$ Å, and t expressed in Å, then

$$A = 3.45 \times 10^5 b_t \quad (23)$$

Therefore, the surface area is calculable from the "t-plot" and the mass (m) of the adsorbent. This approach is sometimes more convenient than use of the BET plot.[108]

At higher t values, upward deviations from a straight line in a t-plot indicate capillary condensation in the pores while a downward deviation is observed when micropores or slit-shaped pores are present in the adsorbent solid.[110]

As mentioned in Section II-J, the experimental details of the surface area measurements can be found in Appendix 1.

Table 41 lists the specific surface areas measured by the BET method for some of the substrates listed in Section II-B. The c constant, as described on p 136, must be > 20 for the BET method to obtain reasonably accurate surface area measurements (± 10%). Furthermore, the c constant, as has been shown in practice,[108] should not exceed about 150 since the BET analysis does not take into account the possibility of micropore filling or penetration of adsorbate molecules into cavities of molecular size, and can thus falsify the BET surface area measurements.

Examination of Table 41 reveals that all of the c constants, as determined by the BET method, are between 20 and 150 except those for

TABLE 41

THE SPECIFIC SURFACE AREA AND c CONSTANT AS DETERMINED BY THE BET GAS ADSORPTION METHOD

| Substrate | Specific Surface Area ($m^2/g$) | "c Constant" |
|---|---|---|
| East Tennessee Bituminous Coal Fly Ash | 4.01 | 890 |
| Kaneb Coal Fly Ash | 3.15 | 432 |
| Texas Lignite Coal Fly Ash | 2.61 | 148 |
| Commercial Coal Fly Ash (720-2) | 0.84 | 30 |
| Flaked Graphite | 4.43 | 115 |
| Brown Glass Bottle | 0.48 | 31 |
| Controlled Porosity Glass | 125.0 | 126 |

East Tennessee bituminous and Kaneb coal fly ashes. Values of c between 20 and 150 indicate reasonable confidence in the validity of the surface area measurements. The high c values for these two adsorbents (on the order of hundreds) are a strong indication of the presence of microporosity, or adsorption on active sites, or even chemisorption.[108] These factors must be taken into account when calculating the surface area.

There does not appear to be any relationship between the observed c constant and the total % carbon of the various substrates subjected to the BET procedure, at least with the substrates examined in this study. There are indications that PAHs tend to associate very strongly with carbonaceous fly ash particles;[111] however, the c constant pertains to association of $N_2$, not PAHs. The flaked graphite (very high carbon content) has a c constant of only 115. The two substrates that have high c constants, East Tennessee bituminous and Kaneb coal fly ashes, differ significantly in their total carbon analyses (0.51 and 2.81 %, respectively). In the absence of data for enthalpies of adsorption for PAHs on the fly ashes, it is not possible to decide whether or not the high c constants observed for the East Tennessee bituminous and Kaneb coal fly ashes bear any possible relationship to adsorption of PAHs at unusually active surface sites for these ashes.

The very high specific surface area of the controlled porosity glass is expected since this substrate is characterized by regularly shaped spherical particles containing pores of 100 Å diameter. The very small specific surface area of the brown glass bottle is also

somewhat expected since the particles may have only been pulverized sufficiently to pass the 45 μm sieve, whereas other adsorbents probably contained particles ranging in size from 45 μm to well below the submicrometer level. The commercial coal fly ash (720-2) also has a low specific surface area when compared with the other fly ash samples.

Table 42 lists the substrates and their respective isotherm types. Figures 30 and 31 show the adsorption-desorption isotherms for the controlled porosity glass (Type IV, hysteresis type H1) and the Texas lignite coal fly ash (Type II, hysteresis type H3), respectively. The adsorption-desorption isotherm for the controlled porosity glass agrees well with what is known about this substrate since it is characterized by uniform spheres of narrow pore distribution. The Kaneb coal fly ash, flaked graphite, and brown glass bottle adsorption-desorption isotherms indicated only a slight hysteresis (the desorption isotherm came very close to retracing the adsorption isotherm).

The Texas lignite coal fly ash adsorption-desorption isotherm (Figure 31) is characterized by more hysteresis than any of the other substrates. This is suggestive of plate-like particles with slit-shaped pores (as discussed in the preceding theoretical section). This may mean that the Texas lignite coal fly ash has a slightly higher percentage of pores that could be described as slit-shaped. This may or may not have some bearing on the fraction of PAH molecules that adsorb inside of pores or are adsorbed more closely to or on the surface (not inside a pore).

TABLE 42

THE VARIOUS TYPES OF ADSORPTION-DESORPTION ISOTHERMS FOR VARIOUS SUBSTRATES AS DETERMINED BY THE BET GAS ADSORPTION METHOD

| Substrate | Class of Adsorption-Desorption Desorption Isotherm | Hysteresis Type |
|---|---|---|
| East Tennessee Bituminous Coal Fly Ash | II | H3 |
| Kaneb Coal Fly Ash | II | H3 |
| Texas Lignite Coal Fly Ash | II | H3 |
| Commercial Coal Fly Ash (720-2) | II | H3 |
| Flaked Graphite | II | H3 |
| Brown Glass Bottle | II | H3 |
| Controlled Porosity Glass | IV | H1 |

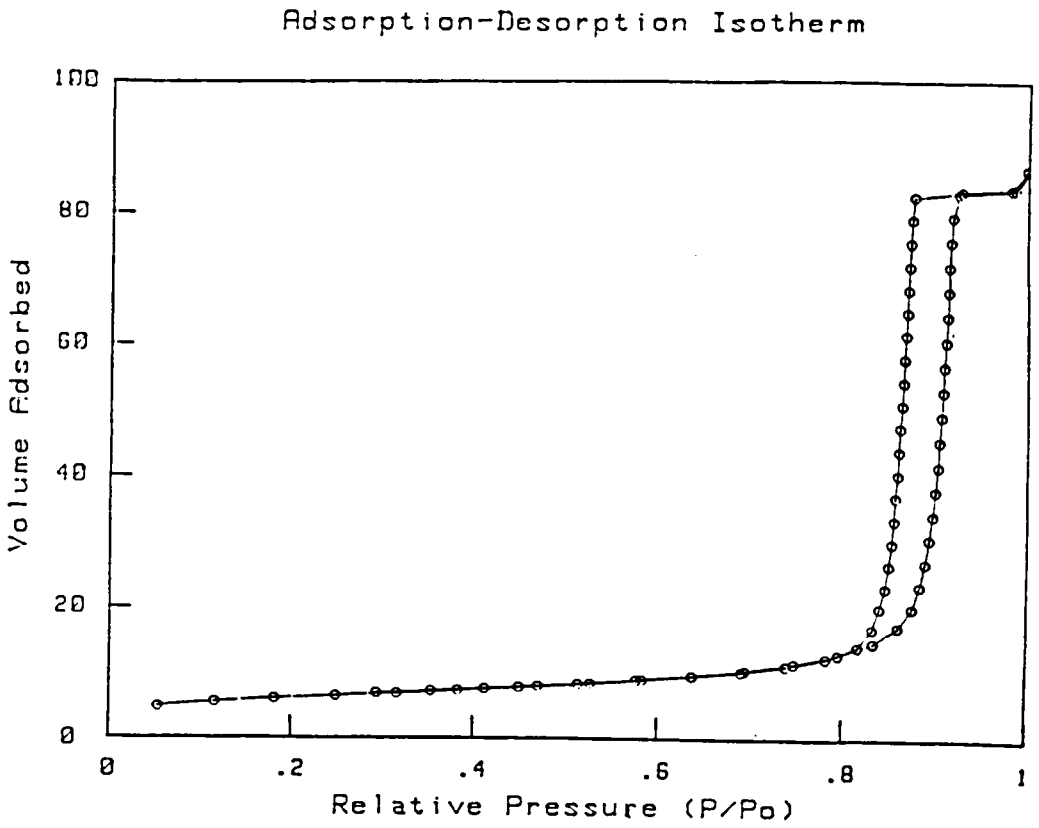



Figure 30. The Adsorption-Desorption Isotherm for Controlled Porosity Glass Obtained by Plotting Data Collected by the BET Method.

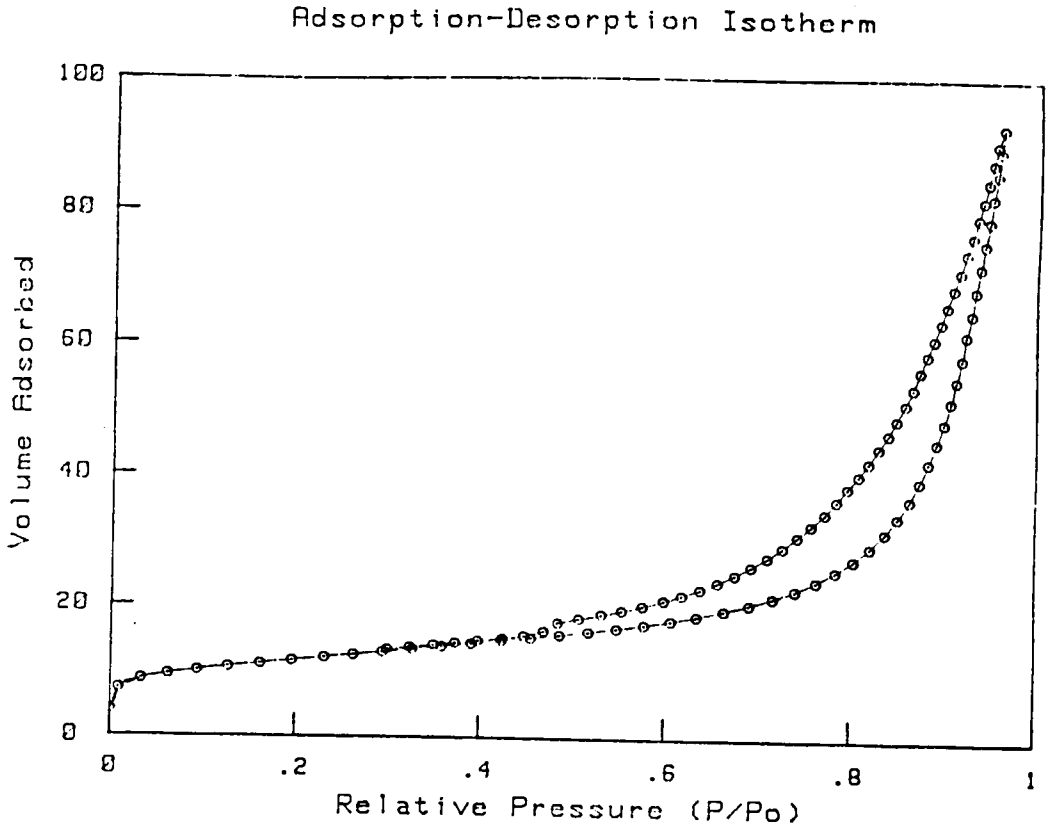



Figure 31. The Adsorption-Desorption Isotherm for Texas Lignite Coal Fly Ash Obtained by Plotting Data Collected by BET Method.

The East Tennessee bituminous and commercial (720-2) coal fly ashes were the only substrates subjected to the BET procedure that showed low-pressure hysteresis (i.e., the desorption isotherm never quite overlapped the adsorption isotherm in the low pressure region). Low-pressure hysteresis is thought to be associated with swelling of a non-rigid porous structure or with the irreversible uptake of adsorbate molecules in pores (or through pore entrances) of about the same width as that of the adsorbate molecule.

The "t-plots" for East Tennessee bituminous and Texas lignite coal fly ashes are shown in Figure 32 (a and b, respectively). The East Tennessee bituminous coal fly ash t-plot is also typical of the t-plots obtained for the commercial fly ash (720-2) and Kaneb coal fly ash in that a slight upward deviation is observed. These data suggest capillary condensation in the pores. The Texas lignite coal fly ash t-plot is also typical of the t-plot for flaked graphite (Figure 32) in that a definite upward deviation is observed, which suggests a strong tendency for capillary condensation in the pores. The t-plot for the controlled porosity glass (Figure 33 (a)), increases over most of the y-axis, suggests that capillary condensation is extremely prevalent on this substrate; this is the result that would be expected for this adsorbent.

Figure 33 (b) shows the t-plot for the only substrate that is characterized by a slight downward deviation (brown glass bottle). A downward deviation tends to be observed when micropores or slit-shaped pores are present in the solid (see p 151).

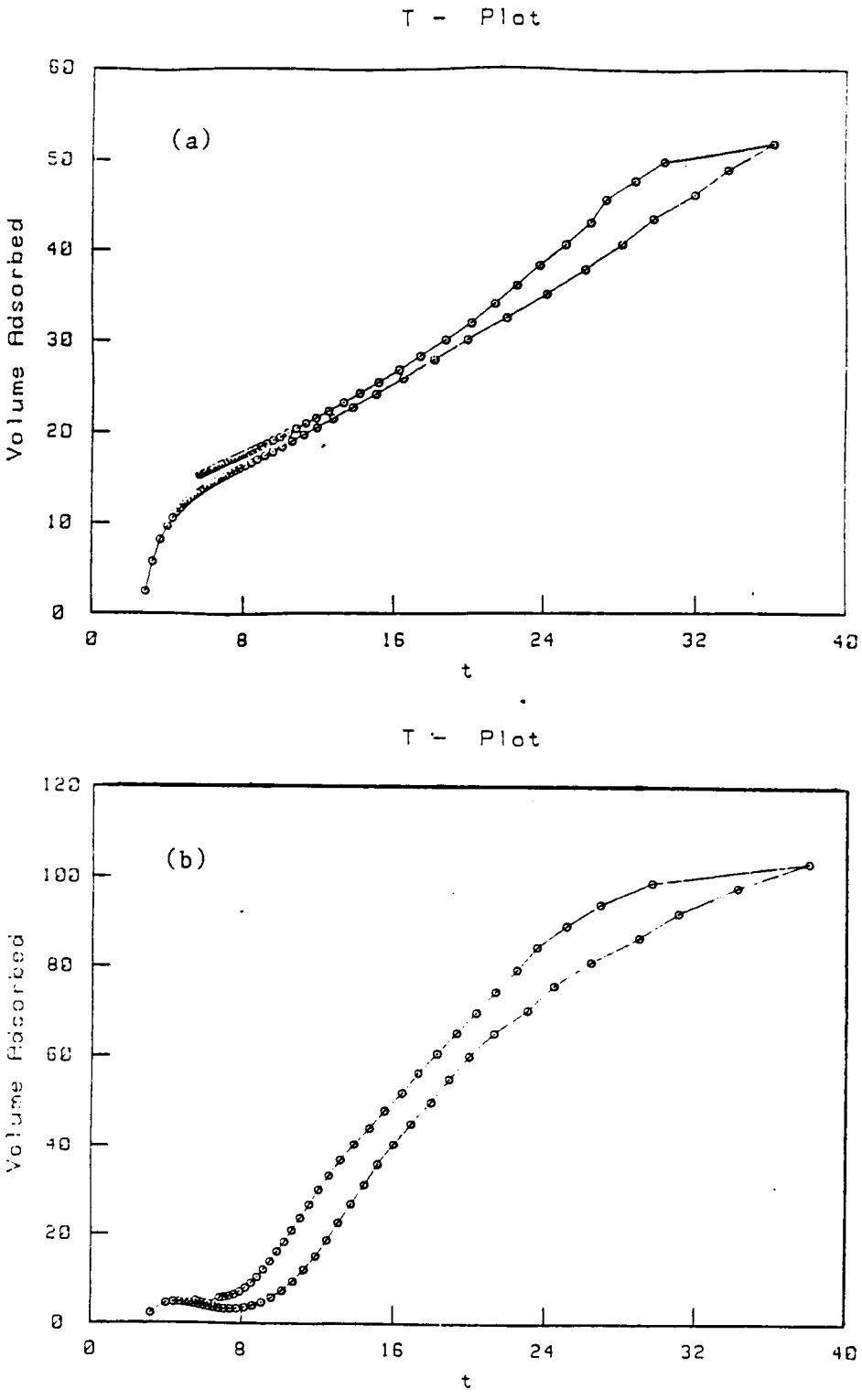



Figure 32. "T-Plots" for (a) East Tennessee Bituminous and (b) Texas Lignite Coal Fly Ashes, Obtained by Plotting Data Collected by the BET Method.

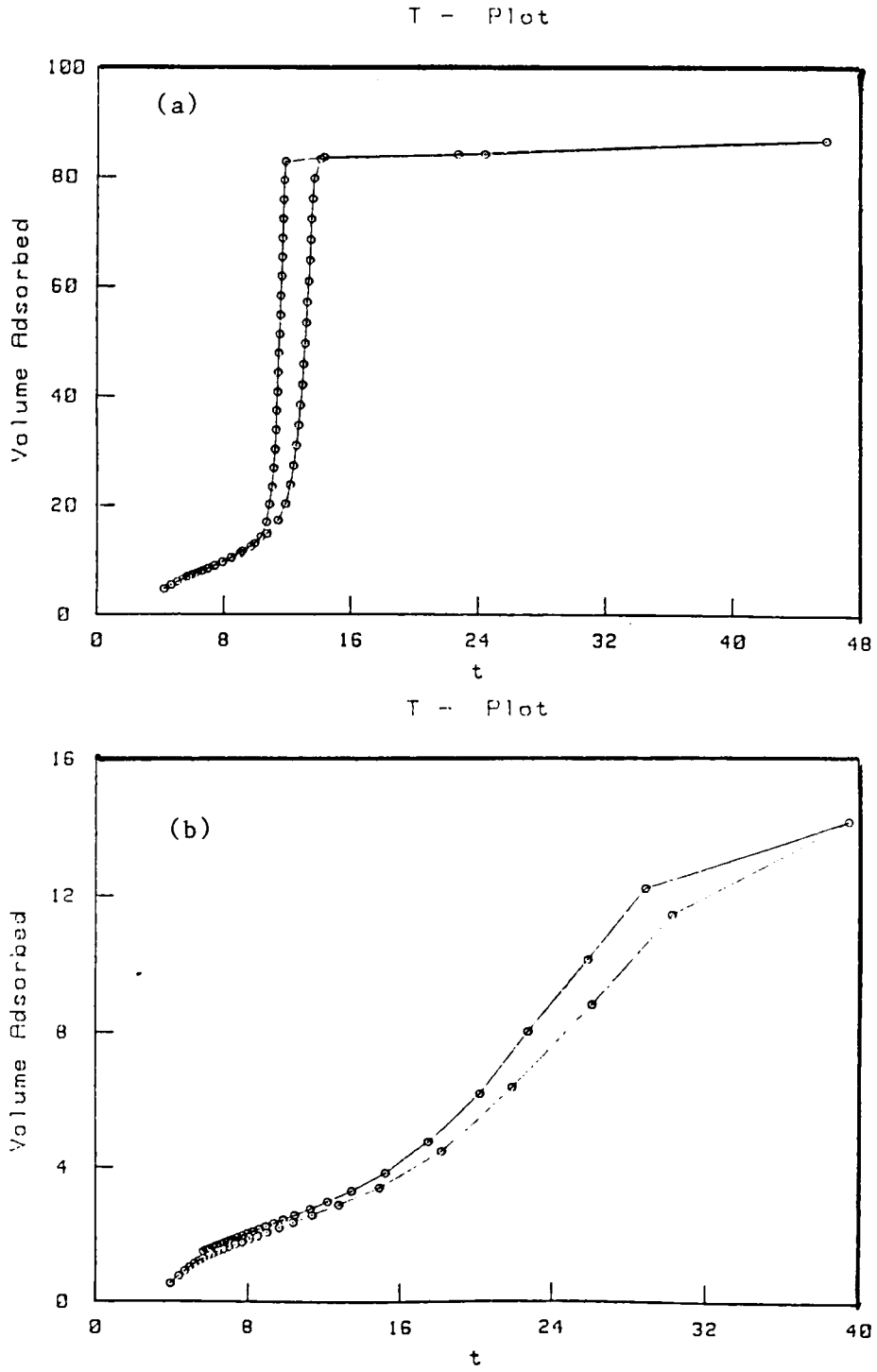



Figure 33. "T-Plots" for (a) Controlled Porosity Glass and (b) Brown Glass Bottle Obtained by Plotting Data Collected by the BET Method.

For any adsorbent, the "pore size distribution" is the distribution of pore volume as a function of pore size. Pore volume is defined as the amount of vapor adsorbed at a relative pressure close to unity by assuming that the pores are then filled with liquid adsorbate. The computation of pore size distribution involves a number of assumptions which include pore shape, mechanism of pore filling, and the validity of the Kelvin equation. The pores are assumed to be cylindrical or slit-shaped. As can be seen in Figure 34(a), the adsorption pore volume distribution for the controlled porosity glass is as expected. Most of the pore volume is centered around the 100 Å point on the plot. The pore radius shown in these figures is the "mean hydraulic pore radius"[106] (the ratio of the pore volume to the area of the pore walls) which is equal to the pore diameter. The pore volume in ml as shown on the Y-axis is the volume of gaseous $N_2$ at STP per g of adsorbent. The pore volume must be converted to the volume of liquid $N_2$ at 77 K (multiply by correction factor of 0.001558).

Figure 34(b) shows the adsorption pore volume distribution for Texas lignite coal fly ash. It must be noted that, in these types of plots, the last one or two data points usually are quite inaccurate due to the increasingly difficult problem of measuring a small difference between two (near atmospheric) pressures. Table 43 lists the adsorption pore volume distribution and maximum pore volumes for all other substrates that were subjected to the BET method.

The data listed in Table 43 show that, for all of the substrates except the controlled porosity glass, most of the pore volume is attributable to pores in the 100 to 1000 Å diameter range. It must be

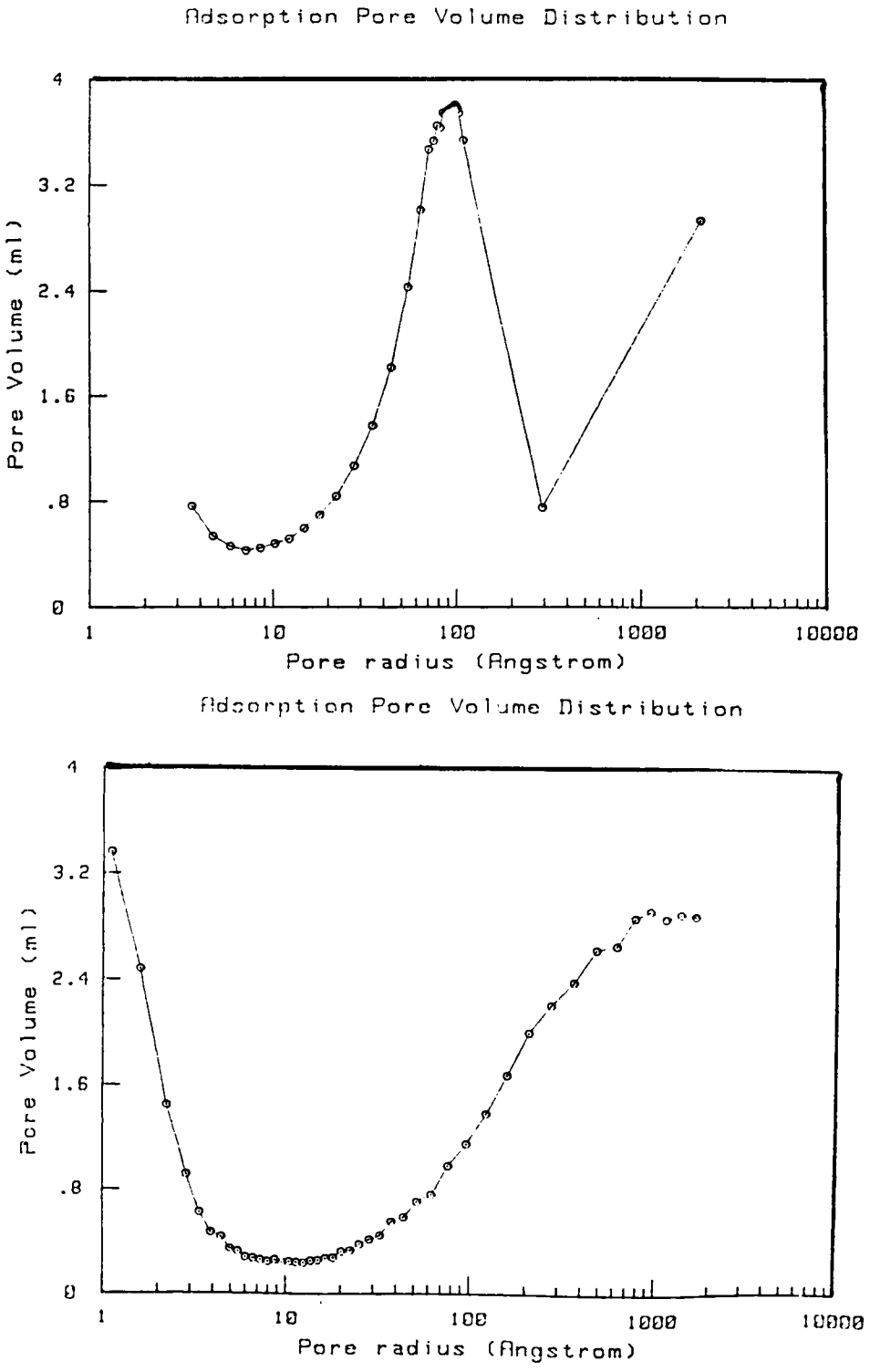



Figure 34. The Adsorption Pore Volume Distribution of (a) Controlled Porosity Glass and (b) Texas Lignite Coal Fly Ash, Obtained by Plotting Data Collected by the BET Method.

TABLE 43

ADSORPTION PORE VOLUME DISTRIBUTION AND PORE VOLUME MAXIMA OF VARIOUS SUBSTRATES SUBJECTED TO THE BET GAS ADSORPTION METHOD

| Substrate | Pore Size Range (Å) | Pore Volume (ml) |
|---|---|---|
| East Tennessee Bituminous Coal Fly Ash | 100 to 1000 | 3.0 |
| Kaneb Coal Fly Ash | 100 to 1000 | 3.8 |
| Texas Lignite Coal Fly Ash | 100 to 1000 | 5.0 |
| Commercial Coal Fly Ash (720-2) | 100 to 1000 | 1.8 |
| Flaked Graphite | 100 to 1000 | 7.0 |
| Brown Glass Bottle | 100 to 1000 | 2.6 |
| Controlled Porosity Glass | 100 | 3.8 |

noted that the BET method does not provide accurate pore volume information for pores of size less than about 20 Å. As can be seen in Table 43, the flaked graphite has the largest pore volume (7.0 ml) which is not unexpected since carbonaceous materials tend to be quite porous. The Texas lignite coal fly ash has the second largest pore volume (5.0 ml) of the substrates studied. The controlled porosity glass and brown glass bottle, and the East Tennessee bituminous and Kaneb coal fly ashes, all have pore volumes of 2.6 to 3.8 ml. The commercial fly ash (720-2) has the smallest pore volume (1.8 ml).

Table 44 lists some of the indicated characteristics of each substrate based on the observed experimental evidence. Examination of Tables 43 and 44 show that all of the coal fly ashes studied have macroporous structures (pores are present having pore sizes greater than 500 Å). The flaked graphite and brown glass bottle also have macroporous structures. Only the controlled porosity glass has a mesoporous structure (pore diameters of 20 to 500 Å), which accurately fits the manufacture's description of this adsorbent. Furthermore, it appears that slit-shaped pores may be present on all of the adsorbents except the controlled porosity glass (based on the isotherm type of the controlled porosity glass). The number of slit-shaped pores on each substrate, as opposed to more spherical or uniformly shaped uniform pores, may contribute to the adsorbent's overall pore volume.

If one compares the data listed in Tables 43 and 44 with the qualitative summary of photochemical experiments shown in Table 24 (p 94), one can see that there does not appear to be any obvious relationship between porosity and the photochemical behavior of pyrene and

TABLE 44

SURFACE CHARACTERISTICS OF VARIOUS SUBSTRATES AS EVALUATED FROM THE OBSERVED EXPERIMENTAL DATA

| Substrate | Pore Size[1] | Pore Shape[2] | Swelling or Irreversible Adsorption[3] | Capillary Condensation[4] |
|---|---|---|---|---|
| East Tennessee Bituminous Coal Fly Ash | macro | slit-shaped | medium | slight |
| Kaneb Coal Fly Ash | macro | slit-shaped | slight | very slight |
| Texas Lignite Coal Fly Ash | macro | slit-shaped | high | medium |
| Commercial Coal Fly Ash | macro | slit-shaped | medium | very slight |
| Flaked Graphite | macro | slit-shaped | slight | high |
| Brown Glass Bottle | macro | slit-shaped | slight | (negative deviation) |
| Controlled Porosity Glass | meso | uniform spheres | none | extremely high |

[1]Determined by evaluation of adsorption-desorption isotherm type.

[2]Determined by evaluation of hysteresis of adsorption-desorption isotherms.

[3]Determined by evaluation of low pressure hysteresis on adsorption-desorption isotherms.

[4]Determined by an upward deviation from a straight line as shown in t-plots.

benzo(a)pyrene adsorbed on the surfaces of these various substrates. That is, the porosity characteristics of the various fly ashes appear to be rather similar, whereas the efficiency of photochemical decomposition of a PAH is quite sensitive to the identity of the substrate. This question is pertinent to the possible relevance of "inner-filter effects" in the photochemistry of adsorbed PAHs; PAH molecules deposited inside pores of opaque adsorbents could be shielded effectively from the incident radiation, thus decreasing the rate of photon absorption by the PAH adsorbate.

The Texas lignite coal fly ash has a specific surface area and porosity distribution comparable to that of the Kaneb coal fly ash but photochemical decomposition for adsorbed pyrene and benzo(a)pyrene is observed on the former and not observed on the latter. Furthermore, the Texas lignite coal fly ash sample appears to have a slightly larger pore volume than the Kaneb coal fly ash, which suggests that perhaps more PAH molecules could be accommodated inside the pores of the Texas lignite coal fly ash as compared with the Kaneb coal fly ash. The most efficient photochemical transformations were observed for PAHs adsorbed on the controlled porosity glass, which certainly has pore sizes (100 Å diameter) large enough to accommodate molecules the size of pyrene and benzo(a)pyrene (molecular areas of 90.0 and 108.8 $Å^2$, respectively).[112] The controlled porosity glass, however, is really 96% crystalline $SiO_2$ (quartz). This substrate is transparent in the ultraviolet region of the spectrum so that even if PAH molecules are adsorbed inside the pores they should not be shielded from the incident radiation. This question is addressed in more detail in Section III-G.

Capillary condensation does not appear to be a significant factor in the interpretation of the surface area and porosity data. The Texas lignite coal fly ash (observed photochemical behavior of adsorbed PAHs) and flaked graphite (no observed photochemical behavior of adsorbed PAHs), both appear to exhibit medium to high capillary condensation. Capillary condensation is indicative of bundles of small capillaries (of varying radius) within the pore structure. The molecular dimensions of pyrene and benzo(a)pyrene would allow the adsorption of some of these PAH molecules within the pores but, as expressed in the preceding paragraph, this may not significantly alter the observed photochemical results.

## H. Selected Wavelength Irradiation Experiments

An experiment was designed to help determine the significance of the "inner-filter effect" regarding the photochemical behavior of pyrene and benzo(a)pyrene adsorbed on the surfaces of coal fly ash. Since it appeared that a relationship might exist between the absorbance of the substrate and the observed photochemical behavior of PAHs (Section III-F-4) adsorbed on these substrates, it seemed useful to examine the inner-filter effect in more detail. Furthermore, the surface area and porosity data (Section II-F-5) appeared to indicate that shielding of molecules from incident radiation by depositing inside of pores did not contribute to the observed photochemical behavior.

Figure 35 shows the transmission spectrum of a cobalt glass plate (about 2 mm thick) and the absorption spectrum of benzo(a)pyrene

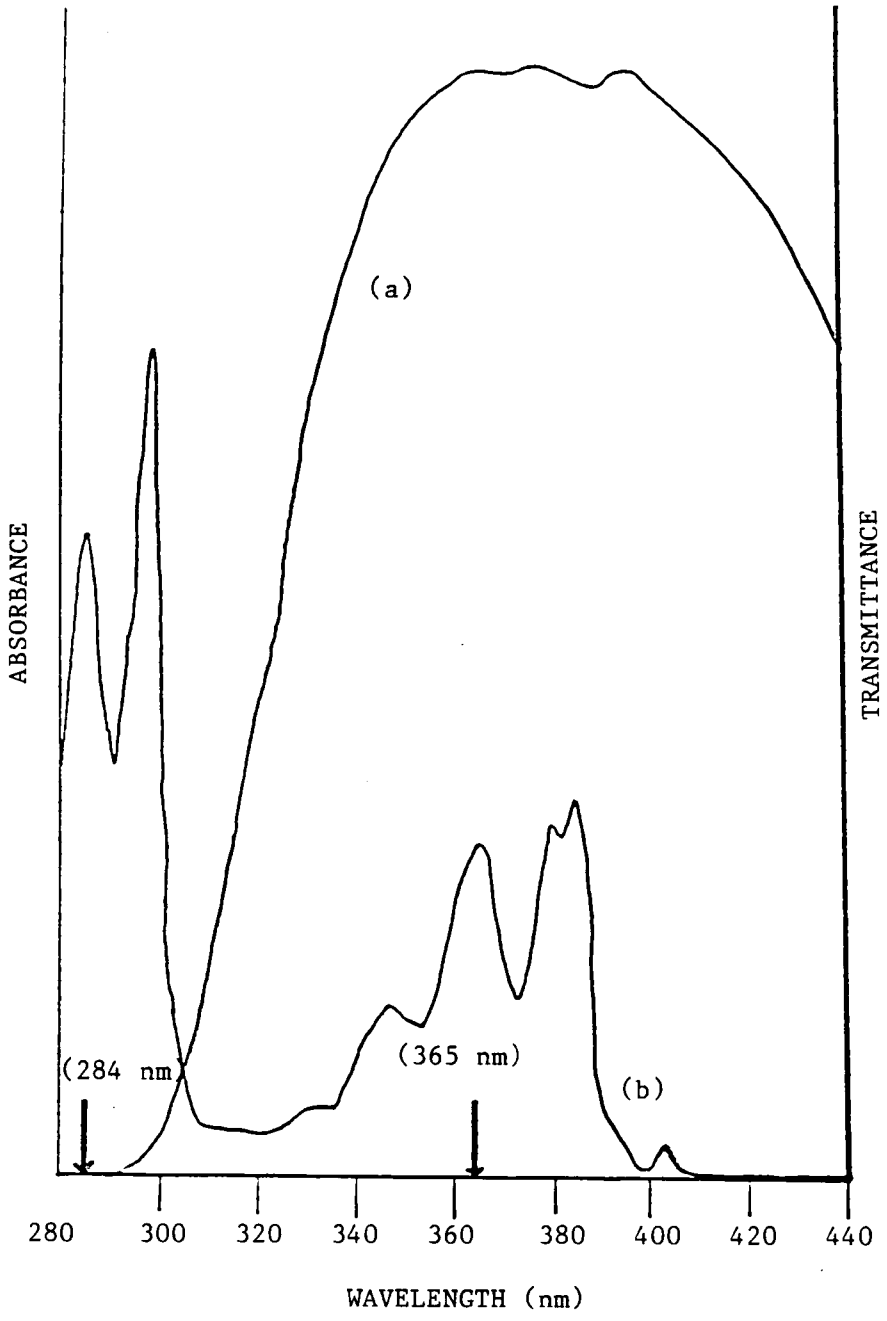



Figure 35. (a) Transmittance Spectrum of a Cobalt Glass Plate (2 mm thick that had not been pulverized) and, (b) Absorption Spectrum of Benzo(a)pyrene Dissolved in Methanol. Arrows refer to the two wavelengths used in the Selected Wavelength Irradiation Experiment.

dissolved in methanol. Assuming that benzo(a)pyrene adsorbed on glass exhibits an absorption spectrum similar to that observed in methanolic solution, one can see from this figure that the possibility existed for illumination at wavelengths at which benzo(a)pyrene absorbed, but also at wavelengths at which the cobalt glass plate substrate was transparent (365 nm) and absorptive (284 nm). The sharp wavelength cutoff of the transmittance spectrum of the cobalt glass was a characteristic not exhibited by any of the other substrates examined in this study. This experiment was quite logical in its attempt to evaluate the influence of the inner-filter effect (if any). If photochemical transformations of benzo(a)pyrene adsorbed on the (pulverized) cobalt glass occurred upon illumination at 365 nm but not at 284 nm, then one could conclude with high reliability that the influence of the inner-filter effect was significant. In the region in which the substrate was absorptive (284 nm), the incident radiation presumably would be attenuated before reaching benzo(a)pyrene molecules that were adsorbed in the pores of the substrate. In the region in which the substrate was transparent (365 nm), the incident radiation would not be attenuated significantly before reaching benzo(a)pyrene molecules that were adsorbed in the pores of the substrate and photochemical transformations should occur.

As discussed in Section II-L, benzo(a)pyrene was vapor-deposited onto the surface of a cobalt glass plate sample that had been pulverized, sieved to $\leq$ 45 μm, then etched with 5% HF to increase the surface area for adsorption. Initial vapor-adsorption experiments with unetched cobalt glass plate substrates were unsuccessful because the

quantity of benzo(a)pyrene "coated" onto this sample was below the detection limits of the technique (ultraviolet absorption spectroscopy) used to quantify the micro-soxhlet extracts. Several attempts to vapor-deposit benzo(a)pyrene onto this substrate were unsuccessful, even when the PAH generator in the first oven of the vapor-adsorption apparatus was allowed to remain operative for three days. These unsuccessful attempts to "coat" the cobalt glass plate substrate with benzo(a)pyrene led to the idea of increasing the surface area of the substrate by etching with HF.

The initial vapor-deposition experiment with etched cobalt glass was also unsuccessful, for two reasons. First of all, the sample was quantified to contain only 13 ± 10 μg of benzo(a)pyrene per g of cobalt glass. Secondly, the benzo(a)pyrene either underwent a rapid non-photochemical transformation or evaporated from the surface and could not be detected, after micro-soxhlet extraction, by ultraviolet absorption spectroscopy after storage for only four days. The very low "coating" level signified that, even had the "loss" of deposited benzo(a)pyrene not taken place, reliable results in photochemical experiments would not have been obtained.

Another attempt to obtain useful information from this experiment was made by depositing benzo(a)pyrene from solution, rather than the vapor phase, onto the surface of the etched cobalt glass plate sample. It was desired to obtain a benzo(a)pyrene concentration such that, after illumination, reliable data could be obtained and compared with the results for an unirradiated sample. For this reason, an aliquot portion of the cobalt glass was spiked with 3 ml of a benzo(a)pyrene

standard (48 µg/ml) dissolved in methanol. The expected concentration by spiking in this manner was 93 µg/g since 144 µg of benzo(a)pyrene was deposited onto 1.55 g of substrate. Table 45 shows the benzo(a)pyrene content of this sample, after micro-soxhlet extraction, to have been 58 ± 15 µg/g. After four days another aliquot portion of the "coated" cobalt glass was subjected to micro-soxhlet extraction was quantified to contain 57 ± 12 µg of benzo(a)pyrene per g of glass. These data tend to indicate that no severe non-photochemical transformations (or evaporation) were occurring so the selected wavelength irradiation experiment described above was attempted using this sample.

The results of irradiating the solution-deposited sample (benzo-(a)pyrene/cobalt glass) at 365 and 284 nm, as determined by micro-soxhlet extraction, can be seen in Table 45. The data shown in Table 45 indicate that no photochemical transformations appeared to occur at either irradiation wavelength. This result was unanticipated. Therefore, in an attempt to evaluate whether or not there was a defect in the design of the selected wavelength irradiation experiment, "benzo(a)pyrene-coated" controlled porosity glass was also irradiated at these same two wavelengths. This is a system in which it was known, from previous studies, that benzo(a)pyrene exhibits efficient photodecomposition (Table 22, p 92).

The results of irradiating "benzo(a)pyrene-coated" controlled pore glass suggest that the choice of wavelength and the photon flux of the 2500 W xenon lamp as dispersed by the excitation monochromator (only a small spectral region is available in these experiments: ± 10 nm) at these particular wavelengths was sufficient to induce

TABLE 45

THE RESULTS OF MICRO-SOXHLET EXTRACTION RESULTS FOR "BENZO(a)PYRENE-COATED" COBALT GLASS AND CONTROLLED POROSITY GLASS SUBSTRATES BEFORE AND AFTER ILLUMINATION AT 365 AND 284 NANOMETERS

| Substrate | Unirradiated Extract | Irradiation at (24 hr) 365 nm | 284 nm |
|---|---|---|---|
| Cobalt Glass | *58 ± 15 | 57 ± 11 | 47 ± 13 |
| Controlled Porosity Glass | 233 ± 7 | 100 ± 11 | 112 ± 8 |

*Micrograms benzo(a)pyrene per gram of glass.

photochemical transformations on controlled pore glass (Table 45, p 164). This result implies that the cobalt glass substrate stabilizes benzo(a)pyrene with respect to photodecomposition, even when illumination is performed at a wavelength at which cobalt glass is transparent. Thus, whatever mechanism(s) for PAH stabilization may be operative in this particular case, the inner-filter effect appears to be of no discernible significance. Hence, the objective of the experiment (to attempt to assess the validity of the inner-filter effect mechanism for PAHs deposited on fly ash) was not attained.

Whether or not the Cermax lamp, as discussed in Section II-D, could induce photochemical transformations of benzo(a)pyrene, adsorbed on the cobalt glass substrate, from the vapor phase, has not been determined (due to the difficulty of vapor-depositing PAHs onto this substrate). A solution-deposited sample of "benzo(a)pyrene-coated" cobalt glass was irradiated by the Cermax lamp for 24 hr and these results indicate that benzo(a)pyrene does undergo photodecomposition under these conditions (106 ± 21 μg and 72 ± 5 μg/g, before and after 24 hr illumination, respectively).

The cobalt glass plate substrate was not subjected to the BET gas adsorption procedure so the specific surface area, porosity, and suspected pore shapes were not determined. If the cobalt glass was anything like the brown glass bottle, then it was of low specific surface area and had a pore size distribution of 100 to 1000 Å. However, these two substrates were quite different in some respects (e.g., carbon content and color) and may have also had quite different surface characteristics. If photochemical transformations had occurred

upon irradiation of "benzo(a)pyrene-coated" cobalt glass, it would have been necessary to subject this substrate to the BET gas adsorption procedure.

The extent to which the solid glass plate resembled the optical absorption characteristics of the powdered cobalt glass also is questionable. The diffuse reflectance spectrum of powdered cobalt glass (see Table 40, p 127) suggests that the cobalt glass substrate may be nearly transparent all the way down to 275 nm, which is considerably different from the transmission spectrum shown in Figure 35 (p 160).

The results obtained from the selected wavelength irradiation experiment unfortunately cannot be used to infer, one way or the other, the influence of the inner-filter effect upon the photochemical behavior of coal fly ash-associated PAHs. Thus, no further studies of this particular system were attempted.

# CHAPTER IV

## INTERACTIONS OF PARTICULATE-ASSOCIATED PAH WITH GASEOUS $NO_2$

### A. Non-Photochemical Reactions of Pyrene With $NO_2$

Using the experimental photoreactor apparatus (Figure 19, p 60), several "pyrene-coated" substrates were exposed to 95 ppm $NO_2$ in $N_2$ for 20 min in the dark. The concentration of $NO_2$ (95 ppm) was measured and certified by the Linde Gas Company (Birmingham, Alabama) using chemiluminescence techniques. The photoreactor was covered with aluminum foil to minimize any photochemical reactions that might possibly occur, and the flow rate was typically about 0.5 L/min. The stainless steel filter holders (p 47) contained nylon filters, but no other precautions were taken to remove nitric acid ($HNO_3$) presumed to be present as an impurity in the $NO_2$ gas cylinder. After the 20 min exposure to $NO_2$, aliquot samples of each substrate were then subjected to micro-soxhlet extraction and direct-probe mass spectrometry (DP-MS).

The results of the micro-soxhlet extractions are listed in Table 46. It can be seen from these data that the pyrene concentrations were considerably decreased after exposure to $NO_2$ in the dark. The concentration of $HNO_3$ (as $NO_3^-$) found on each nylon filter (using the procedure described in Section II-K), after the 20 min exposure experiment, was typically about 400 μg $NO_3^-$ per filter. Since each filter contained approximately the same quantity of $HNO_3$, it appeared likely that the nylon filters were becoming saturated with $HNO_3$ and that $HNO_3$ was passing into the photoreactor. It has been reported that $HNO_3$, as an impurity in $NO_2$ gas cylinders, may be responsible for catalyzing

TABLE 46

RESULTS OF MICRO-SOXHLET EXTRACTIONS OF "PAH-COATED" SUBSTRATES BEFORE AND AFTER EXPOSURE TO 95 ppm $NO_2$ ($HNO_3$ PRESENT) FOR 20 MINUTES

| PAH/Substrate | Before $NO_2$ Exposure | After $NO_2$ Exposure |
|---|---|---|
| Pyrene/Texas Lignite Coal Fly Ash | 472 ± 9 µg/g | 139 ± 2 |
| Pyrene/Kaneb Coal Fly Ash | 1074 ± 40 | 102 ± 11 |
| Pyrene/Silica Gel | 140 ± 6 | ND |
| Benzo(a)pyrene/Kaneb Coal Fly Ash | 5 ± 1 | ND |
| Benzo(a)pyrene/Silica Gel | 73 ± 12 | ND |

ND = Not Detected.

nitration reactions of benzo(a)pyrene with $NO_2$.[83,84] Furthermore, it has been reported that the $HNO_3$ capacity of a single nylon filter may vary from 20 to 3000 μg $NO_3^-$ per filter although the nylon filters used in this work never exceeded 400 μg $NO_3^-$ per filter.[113]

Table 47 shows the result of a DP-MS experiment for the "pyrene-coated" Texas lignite coal fly ash. The data in this table show the mass and the relative abundance of ions of that particular mass. It can also be seen that $H_2O$ (mass 18), $N_2$ and/or CO (mass 28), and $CO_2$ (mass 44) were adsorbed on the surface of the substrate.

The data for some of the ions of interest shown in Table 47 can be seen in Table 48 as calculated isotopic abundances. These data indicate that the peaks at 202, 247, and 292, respectively, have the correct isotopic percentages for compounds containing 16 carbon atoms (202; pyrene), 16 carbon atoms and 1 nitrogen atom (247; mononitropyrene), and 16 carbon atoms and 2 nitrogen atoms (292; dinitropyrene). In a study of this type, the isotopic percentages are acceptable as long as the experimental values are within ± 10% of the calculated values which can be obtained from mass spectral isotopic abundance tables.[114] The A + 2 isotopic contributions from carbon were too small to show up under the parameters used in this particular mass spectrometric experiment.

Tables 49 and 50 show the mass and relative abundance of each ion observed in the mass spectra of samples of 1-nitropyrene and 3-nitropyrene, respectively. It can be seen from these data that many of the ions that appear in the mass spectra of the two nitropyrenes also appear in the mass spectrum of the "pyrene-coated" Texas lignite coal

TABLE 47

MASS VERSUS RELATIVE ABUNDANCE DATA OBTAINED FROM THE MASS SPECTRUM OF "PYRENE-COATED" TEXAS LIGNITE COAL FLY ASH AFTER EXPOSURE TO $NO_2$ ($HNO_3$ PRESENT)

| MASS | ABUND | MASS | ABUND | MASS | ABUND | MASS | ABUND |
|---|---|---|---|---|---|---|---|
| 17 | 9.0 | 84 | 4.0 | 127 | 3.3 | 201 | 100.0 |
| 18 | 39.9 | 85 | 29.0 | 131 | 4.2 | | |
| 28 | 26.4 | | | 133 | 2.1 | 203 | 7.8 |
| 30 | 3.3 | 93 | 3.3 | 135 | 2.1 | 204 | 2.8 |
| 32 | 6.1 | 94 | 5.2 | 137 | 5.4 | 207 | 2.4 |
| | | 95 | 19.1 | 139 | 5.0 | | |
| 41 | 2.4 | 96 | 10.1 | | | 216 | 5.2 |
| 43 | 13.9 | 97 | 34.2 | 149 | 4.0 | 217 | 27.8 |
| 44 | 40.8 | 98 | 6.6 | 150 | 4.5 | 218 | 5.2 |
| | | 99 | 20.5 | 151 | 7.3 | 219 | 4.5 |
| 48 | 2.8 | 100 | 37.0 | | | | |
| 51 | 2.6 | | | 165 | 2.6 | 231 | 2.1 |
| 55 | 13.2 | 105 | 1.9 | 167 | 1.9 | 232 | 2.6 |
| 56 | 5.4 | 107 | 2.1 | 169 | 4.0 | | |
| 57 | 38.7 | 109 | 13.2 | | | 247 | 82.8 |
| | | 110 | 5.7 | 174 | 8.4 | 248 | 13.7 |
| 64 | 12.7 | 111 | 23.1 | 175 | 4.5 | | |
| 67 | 7.5 | 112 | 2.4 | 187 | 10.1 | 292 | 23.6 |
| 68 | 3.5 | 113 | 5.7 | | | 293 | 4.2 |
| 69 | 26.4 | | | 188 | 9.7 | | |
| 70 | 6.8 | 119 | 5.2 | 189 | 42.2 | | |
| 71 | 33.7 | 121 | 2.8 | 190 | 9.4 | | |
| | | 123 | 9.2 | 191 | 7.3 | | |
| 81 | 18.2 | 124 | 2.8 | 198 | 13.2 | | |
| 82 | 9.0 | 125 | 11.1 | 199 | 22.2 | | |
| 83 | 30.4 | 126 | 1.9 | 200 | 90.3 | | |

TABLE 48

ISOTOPIC ABUNDANCE CALCULATIONS FOR SELECTED DATA FROM THE MASS SPECTRUM OF "PYRENE-COATED" TEXAS LIGNITE COAL FLY ASH THAT HAD BEEN EXPOSED TO 95 ppm $NO_2$ ($HNO_3$ PRESENT) FOR 20 MINUTES

| Mass | Experimental Relative Abundance | Experimental, Normalized | Carbon | Nitrogen |
|---|---|---|---|---|
| 202 | 44.3 | 100 | 100 | |
| 203 | 7.8 | 17.6 | 18 | |
| 247 | 82.8 | 100 | 100 | |
| 248 | 13.7 | 16.5 | 18 | 0.37 |
| 292 | 23.6 | 100 | 100 | |
| 293 | 4.2 | 17.8 | 18 | 0.74 |

TABLE 49

THE MASS AND RELATIVE ABUNDANCE DATA OBTAINED FROM THE MASS SPECTRUM OF PURE 1-NITROPYRENE

| MASS | ABUND | MASS | ABUND |
|---|---|---|---|
| 40 | 2.9 | 202 | 15.4 |
| 44 | 3.1 | | |
| | | 217 | 33.9 |
| 74 | 1.9 | 218 | 4.8 |
| 75 | 1.2 | | |
| | | 247 | 81.2 |
| 87 | 10.6 | 248 | 12.5 |
| 94 | 1.7 | | |
| 95 | 1.9 | | |
| 98 | 2.2 | | |
| 100 | 54.1 | | |
| 150 | 2.6 | | |
| 174 | 4.8 | | |
| 175 | 2.2 | | |
| 187 | 5.3 | | |
| 188 | 4.1 | | |
| 190 | 47.4 | | |
| 190 | 8.2 | | |
| 191 | 7.0 | | |
| 198 | 9.6 | | |
| 199 | 13.7 | | |
| 200 | 77.6 | | |
| 201 | 100.0 | | |

TABLE 50

THE MASS AND RELATIVE ABUNDANCE DATA OBTAINED FROM THE MASS SPECTRUM OF PURE 3-NITROPYRENE

| MASS | ABUND | MASS | ABUND | MASS | ABUND |
|---|---|---|---|---|---|
| 50 | .3 | 135 | .4 | 202 | 20.8 |
| 51 | .4 | | | 203 | 2.6 |
| | | 148 | .2 | 207 | 1.0 |
| 62 | .6 | 149 | 2.2 | 214 | 1.0 |
| 63 | 1.2 | 150 | 4.8 | | |
| 74 | 3.3 | 151 | 2.2 | 217 | 39.3 |
| 75 | 2.3 | | | 218 | 6.5 |
| | | 161 | .7 | 219 | 1.5 |
| 76 | .7 | 162 | 1.1 | 223 | .5 |
| 82 | .3 | 163 | 2.3 | | |
| 86 | 1.8 | 173 | 1.5 | 231 | .5 |
| 87 | 7.8 | | | | |
| | | 174 | 8.0 | 247 | 100.0 |
| 94 | 2.2 | 175 | 4.1 | 248 | 18.7 |
| 98 | 2.5 | 176 | .6 | 249 | 1.6 |
| 100 | 35.8 | 185 | .2 | 253 | 1.5 |
| | | 186 | 1.2 | | |
| 110 | 1.0 | 187 | 7.2 | | |
| 111 | 1.2 | | | | |
| | | 189 | 50.4 | | |
| 122 | 1.4 | 190 | 8.6 | | |
| 123 | 1.1 | 191 | 10.1 | | |
| 124 | .4 | 192 | 1.3 | | |
| 125 | .2 | 198 | 12.0 | | |
| 126 | .3 | 199 | 19.9 | | |
| | | 201 | 90.5 | | |
| 134 | .2 | | | | |

fly ash sample. Some of the masses (and relative abundances) of ions of interest that appear in all three of these mass spectra are shown in Table 51. From these data it appears that either one or both of the mononitropyrenes were present on the Texas lignite coal fly ash. Furthermore, according to the "nitrogen rule",[114] the ion responsible for the peak at 247 can only contain an odd number of nitrogen atoms, and that responsible for the peak at 292 can only contain an even number of nitrogen atoms (or zero nitrogen atoms). Figures 36(a,b, and c) shows the bar graphs obtained when DP-MS spectra were collected on "pyrene-coated" Texas lignite coal fly ash after exposure to 95 ppm $NO_2$ for 20 min in the dark ($HNO_3$ probably present), 1-nitropyrene, and 3-nitropyrene, respectively. This figure demonstrates the similarity of these three spectra. Dinitropyrene standards were not available for these studies but strong peaks at mass 292 and 293 having the correct isotopic abundance provide evidence that these compounds were also present.

Evidence for the presence of mononitropyrenes and dinitropyrenes was detected for several other "pyrene-coated" substrates exposed to $NO_2$ and $HNO_3$ in the dark by DP-MS. These substrates included silica gel and Texas lignite, Kaneb, and Illinois bituminous coal fly ashes.

Further evidence for the presence of 1-nitropyrene and/or 3-nitropyrene was obtained by analyzing micro-soxhlet extracts of "pyrene-coated" substrates that had been exposed to $NO_2$ and $HNO_3$ in the dark by ultraviolet absorption spectroscopy. Figure 37 shows the UV-visible absorption spectrum of the micro-soxhlet extract of "pyrene-coated" Texas lignite coal fly ash after such an $NO_2$ exposure

TABLE 51

MASS AND RELATIVE ABUNDANCE OF IONS OF INTEREST FROM THE MASS SPECTRA OF "PYRENE-COATED" TEXAS LIGNITE COAL FLY ASH, 1-NITROPYRENE, AND 3-NITROPYRENE

| "PYRENE-COATED" TEXAS LIGNITE COAL FLY ASH | 1-NITROPYRENE | 3-NITRO |
|---|---|---|
| *292 (23.6) | | |
| 247 (82.8) | 247 (81.2) | 247 (100) |
| 217 (27.8) | 217 (33.9) | 217 (39.3) |
| 202 (44.3) | 202 (15.4) | 202 (20.8) |
| 201 (100) | 201 (100) | 201 (90.5) |
| 200 (90.3) | 200 (77.6) | 200 (ND)** |
| 199 (22.2) | 199 (13.7) | 199 (19.9) |
| 189 (42.2) | 189 (47.4) | 189 (50.4) |
| 100 (37.0) | 100 (54.1) | 100 (35.8) |
| 87 (7.1) | 87 (10.6) | 87 (7.8) |

*Mass (Relative Abundance)

**ND = Not Detected.

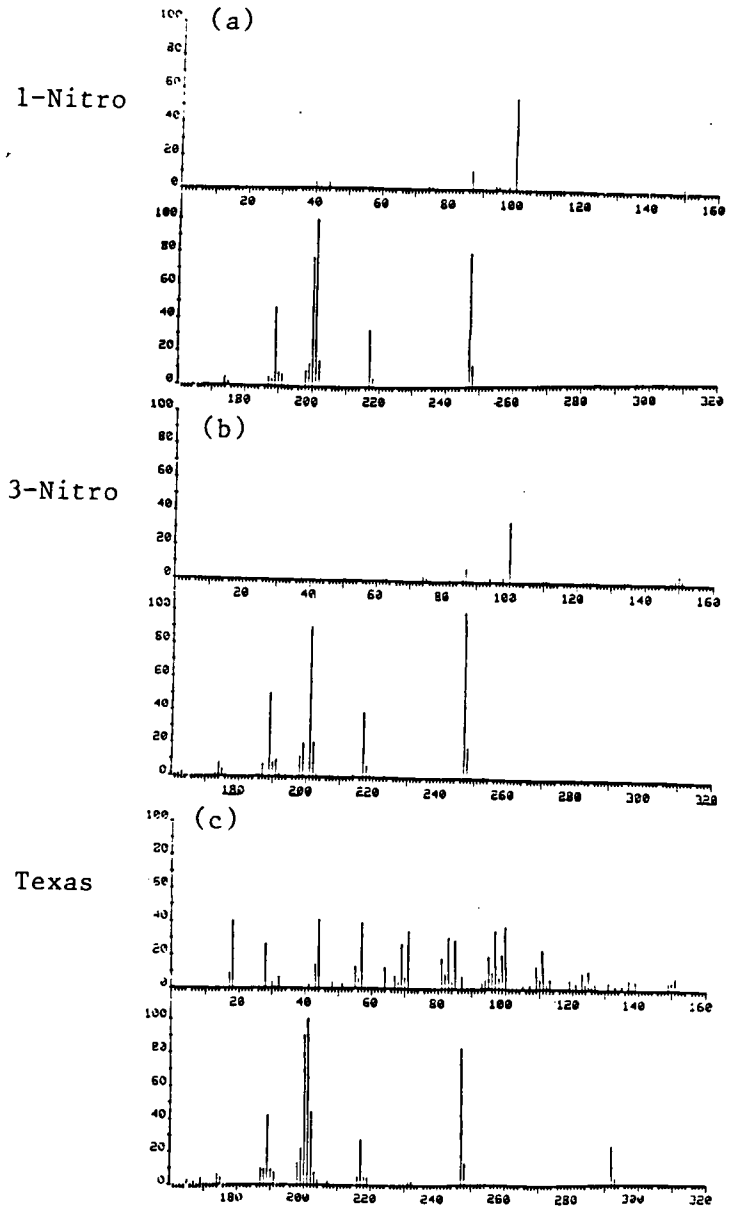



Figure 36. Bar Graph of Direct-Probe Mass Spectral Date (From Mass 10 to Mass 320) Collected for (a) 1-Nitropyrene, (b) 3-Nitropyrene and, (c) "Pyrene-Coated" Texas Lignite Coal Fly Ash after exposure to 95 ppm $NO_2$ ($HNO_3$ Present) for 20 min in the dark.

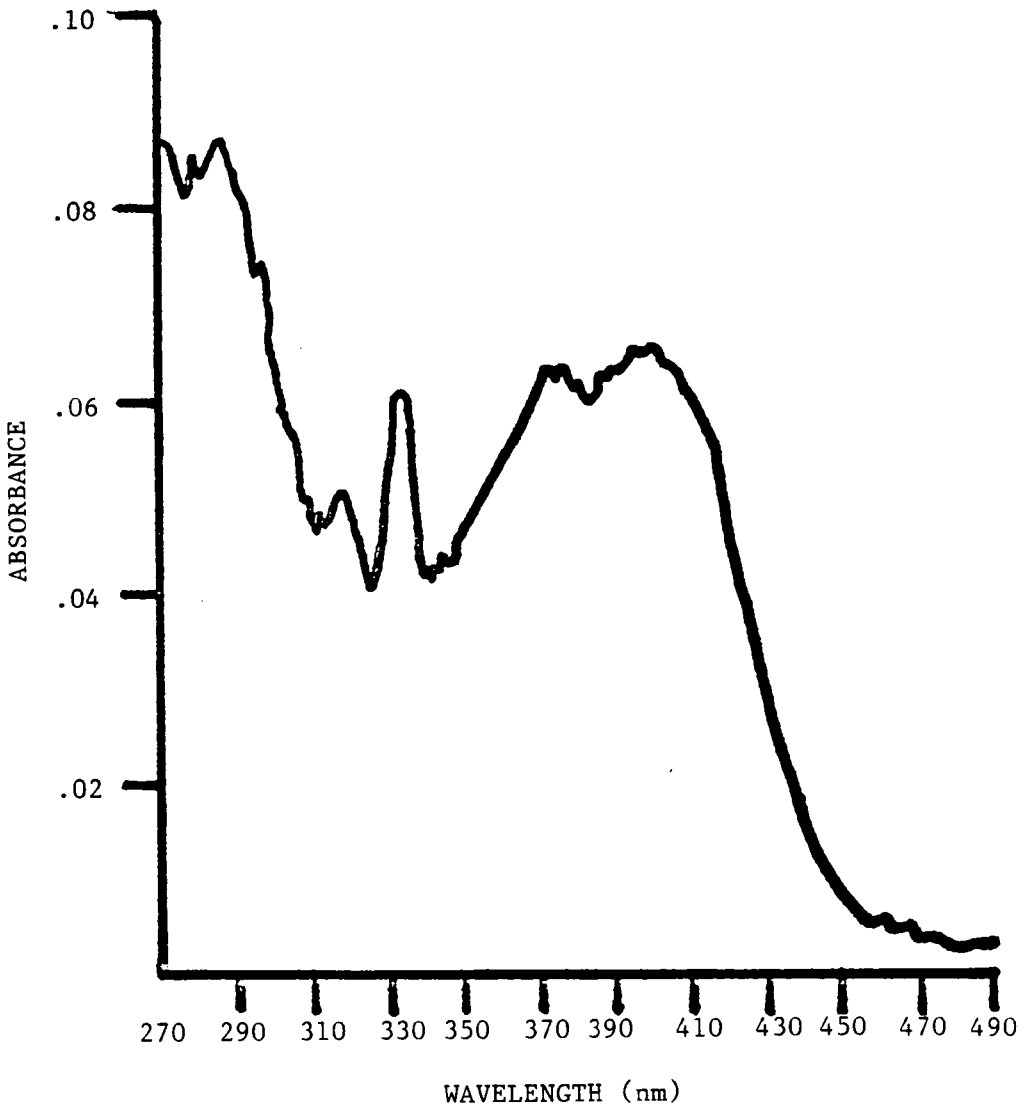



Figure 37. Absorption Spectrum of a Micro-Soxhlet Extract of "Pyrene-Coated" Texas Lignite Coal Fly Ash after a 20 min exposure to $NO_2$ and $HNO_3$.

experiment. Comparison of Figure 37 with the absorption spectrum of pyrene (Figure 14, p 51) showed that, upon exposure of the sample to $NO_2$ and $HNO_3$, new broad peaks had appeared in the 450 to 340 nm region and the 320 to 270 nm region. The ultraviolet absorption spectra of 1-nitropyrene and 3-nitropyrene, each dissolved in methanol, are shown in Figures 38 and 39, respectively. One can see from these figures that the new broad bands that appear in the extract of Texas lignite coal fly ash exposed to $NO_2$ and $HNO_3$ were very similar to the bands present in the spectra of the nitropyrene standards. These spectra provide additional evidence for the production of mononitropyrenes by exposure of pyrene adsorbed on Texas lignite coal fly ash to $NO_2$ in the presence of $HNO_3$ in the dark. These absorption features were also present in the micro-soxhlet extracts of the other "pyrene-coated" substrates (treated similarly) that are listed in Table 46 (p 168).

Several experiments, using the photoreactor covered with aluminum foil, were performed by packing nylon wool[99] into a tube that had been incorporated into the photoreactor apparatus, so that the $HNO_3$ would be adsorbed. This was done to determine if $HNO_3$ was indeed responsible for catalyzing the nitration reactions. To insure that $NO_2$ was still passing through the nylon wool, the procedure described in Section II-K was utilized to determine qualitatively if $NO_2$ was present in the photoreactor. Other workers[113] have reported the $NO_2$ retention on nylon filters to be $< 0.3\%$, expressed as $\mu g/m^3$ $NO_3^-$. Since the $NO_2$, in the experiments discussed in this section, was passing through a relatively large amount of nylon wool (compared to the small nylon filters), it was necessary to measure the $NO_2$ exiting the

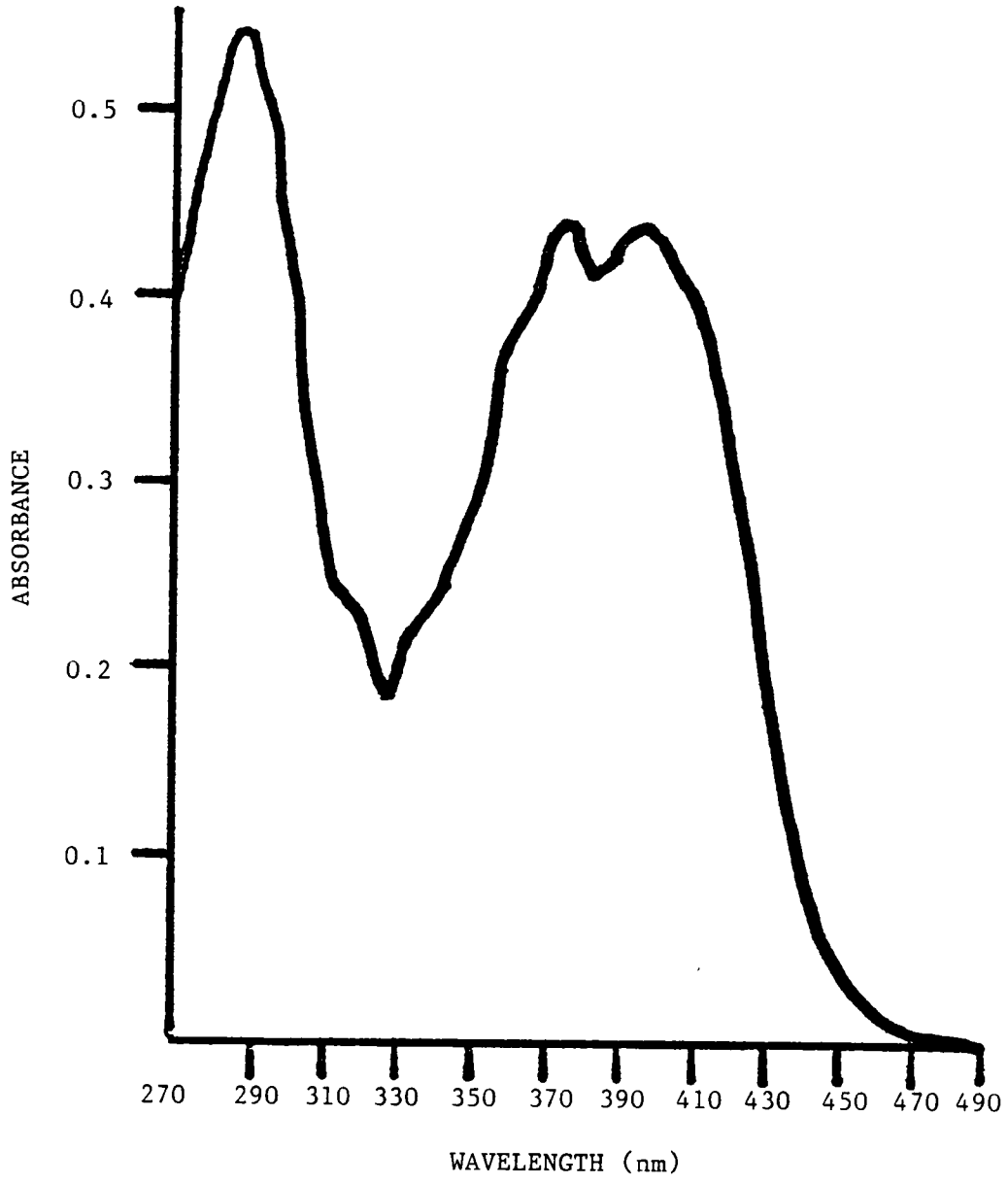



Figure 38. Absorption Spectrum of 1-Nitropyrene Dissolved in Methanol (about 14 ppm).

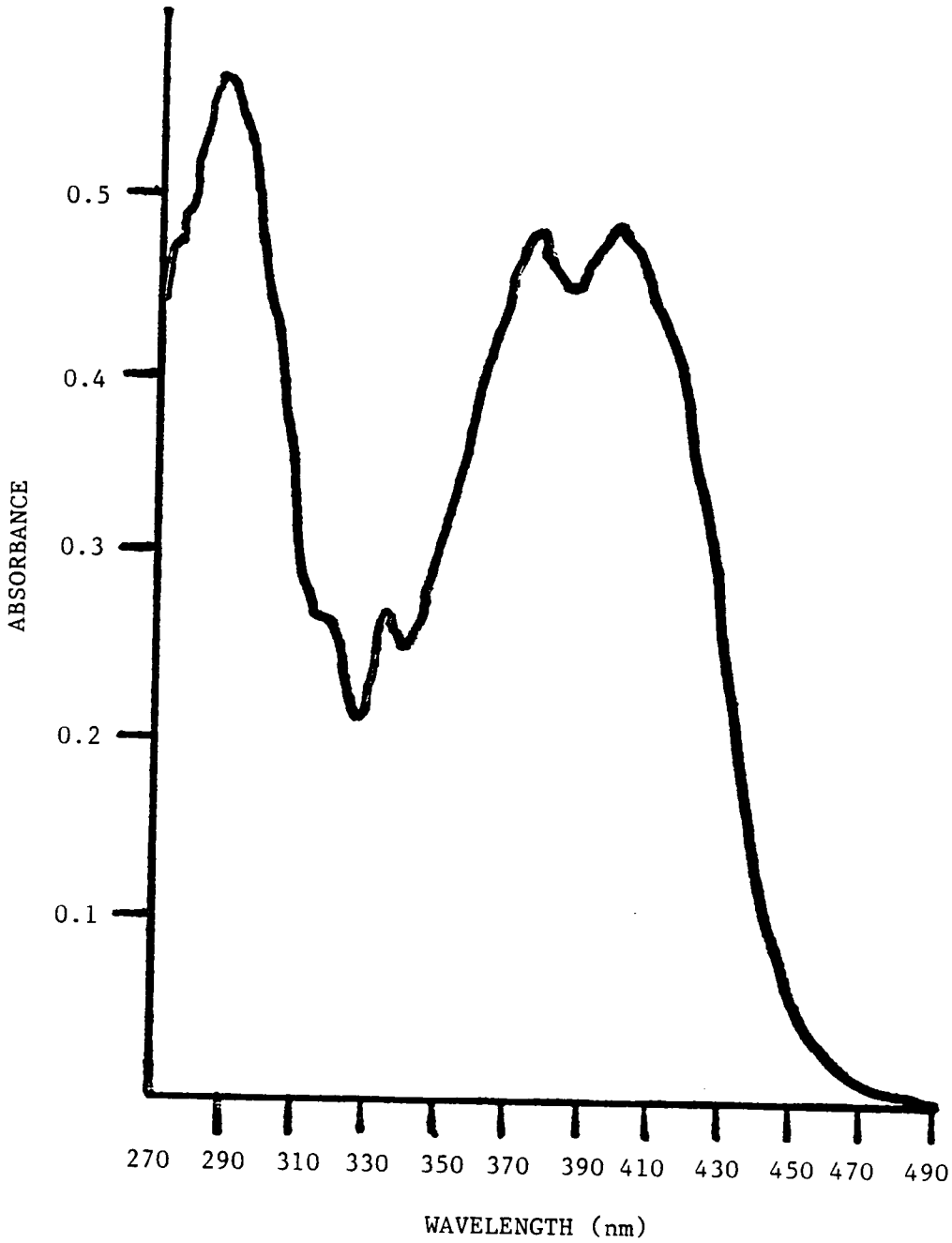



Figure 39. Absorption Spectrum of 3-Nitropyrene Dissolved in Methanol (about 15 ppm).

photoreactor. The $NO_2$ measurement was made at two points in the photoreactor apparatus. The first measurement was made at the regulator outlet of the $NO_2/N_2$ gas cylinder and the second measurement was made between the photoreactor and the charcoal filter. In both cases a pink color (indicating the presence of $NO_2$) developed within about 5 s. This tends to indicate that any retention of $NO_2$ by the nylon wool that might have occurred was not sufficient to prevent $NO_2$ from passing into the reactor.

Nylon filters were placed into the stainless steel filter holders and these filters were analyzed, after an experiment, by the procedure described in Section II-K. The results of the analyses of the nylon filters for experiments involving both pyrene and benzo(a)pyrene as adsorbates, shown in Table 52, indicate that only extremely small quantities of $HNO_3$ could have been passing through the second nylon filter into the photoreactor. Several analyses were performed on nylon filters that had not been exposed to $NO_2$ in the photoreactor and these were used as blanks, and the results of these analyses are shown in Table 53. Comparing the data in Tables 52 and 53 appears to indicate that the nylon wool succeeded in absorbing virtually all of the $HNO_3$ present as an impurity in the $NO_2$, so that most of the experiments were performed in nearly $HNO_3$-free carrier gas. The analyses of blank nylon filters (Table 53) resulted in $HNO_3$ concentrations (as $NO_3^-$) that ranged from 3 to 14 μg per filter and it can also be seen in Table 52 that many of the nylon filters, after exposure to 95 ppm $NO_2$, were also found to be in this concentration range. The one clear exception to this statement is the first experiment using pyrene on Illinois

TABLE 52

RESULTS OF EXTRACTING AND ANALYZING NYLON FILTERS FOR THE PRESENCE OF NITRATE AFTER A ONE HOUR EXPOSURE TO 95 ppm $NO_2$

| | $NO_3^-$ Detected on Filter |
|---|---|
| Benzo(a)pyrene Adsorbed on Various Substrates | |
| Eastern Appalachian Coal/Filter #1 | 10 µg/filter |
| Eastern Appalachian Coal/Filter #2 | 10 |
| Commercial Fly Ash (720-1)/Filter #1 | 10 |
| Commercial Fly Ash (720-1) | 9 |
| Silica Gel/Filter #1 | 3 |
| Silica Gel/Filter #2 | 2 |
| Silica Gel/Filter #1 | 11 |
| Silica Gel/Filter #2 | 11 |
| Texas Lignite/Filter #1 | 7 |
| Texas Lignite/Filter #2 | 12 |
| Illinois Bituminous/Filter #1 | 11 |
| Illinois Bituminous/Filter #2 | 14 |
| Kaneb/Filter #1 | 5 |
| Kaneb/Filter #2 | 5 |
| Pyrene Adsorbed on Various Substrates | |
| Silica Gel/Filter #1 | 4 |
| Silica Gel/Filter #2 | 6 |
| Illinois/Filter #1 | 16 |
| Illinois/Filter #2 | 2 |
| Illinois/Filter #1 | 23 |
| Illinois/Filter #2 | 16 |

Filter Number 1 = Nylon Filter Near the $NO_2$ Source.

Filter Number 2 = Nylon Filter Near the Photoreactor.

TABLE 53

RESULTS OF EXTRACTING AND ANALYZING NYLON FILTERS THAT HAVE NOT BEEN EXPOSED TO $NO_2$

| Nylon Filter | Amount of $NO_3^-$ Detected on Filter |
|---|---|
| Blank | 4 µg/filter |
| Blank | 5 |
| Blank | 7 |
| Blank | 7 |
| Blank | 3 |
| Blank | 4 |
| Blank | 14 |
| Blank | 12 |
| Blank | 8 |
| Blank | 11 |

bituminous coal fly ash, wherein the quantity of $NO_3^-$ detected on the nylon filter (23 μg) significantly exceeded that observed for filter blanks, suggesting that some $HNO_3$ may have come into contact with the sample in this experiment.

Table 54 shows the results of micro-soxhlet extraction of various substrates, before and after exposure to 95 ppm $NO_2$ (nylon wool used; $HNO_3$ presumably absent) for 1 hr. These results appear to indicate that pyrene adsorbed on the surface of these substrates was not undergoing detectable non-photochemical reaction with $NO_2$. Subjecting the "pyrene-coated" substrates to DP-MS, after exposure to $NO_2$, did not reveal any peaks (or ions) higher in mass than the parent ion (pyrene: 202); therefore, it did not appear that detectable quantities of any nitropyrenes were being formed. The ultraviolet absorption spectra of concentrated (50 ml to 5 ml) micro-soxhlet extracts did not reveal any new absorption features not present in the spectrum of pyrene.

B. Non-Photochemical Reactions of Benzo(a)pyrene With $NO_2$

"Benzo(a)pyrene-coated" substrates were also exposed to 95 ppm $NO_2$ by using the experimental apparatus (Figure 19, p 60). Once again the photoreactor was covered with aluminum foil to minimize any photochemical reactions that might possibly occur, and the flow rate of $NO_2$ was typically about 0.5 L/min.

Experiments were first performed without the use of nylon wool, and the results of the micro-soxhlet extractions are listed in Table 46 (p 168). Although the benzo(a)pyrene concentration was observed to decrease (as determined by micro-soxhlet extraction) after exposure to

TABLE 54

MICRO-SOXHLET EXTRACTION RESULTS OF "PAH-COATED" SUBSTRATES BEFORE AND AFTER EXPOSURE TO 95 ppm $NO_2$ ($HNO_3$ ABSENT) IN THE DARK FOR ONE HOUR

| PAH/Substrate | Before $NO_2$ Exposure | After $NO_2$ Exposure |
|---|---|---|
| Pyrene/Texas Lignite Coal Fly Ash | 474 ± 10 μg/g | 466 ± 14 |
| Pyrene/Alumina | 720 ± 31 | 717 ± 6 |
| Pyrene/Silica Gel | 132 ± 30 | 116 ± 12 |
| Pyrene/Illinois Bituminous Coal Fly Ash | 39 ± 3 | 41 ± 3 |
| Benzo(a)pyrene/Silica Gel | 73 ± 12 | 61 ± 10 |
| Benzo(a)pyrene/Eastern Appalachian Coal Fly Ash | 119 ± 8 | 127 ± 5 |
| Benzo(a)pyrene/Commercial Fly Ash (Lot no. 720-1) | 56 ± 1 | 57 ± 6 |

95 ppm $NO_2$ (and $HNO_3$) for 20 min, the mass spectra of these "benzo(a)-pyrene-coated" substrates revealed no peaks higher in mass than the parent ion (benzo(a)pyrene; 252). Thus, mononitrobenzo(a)pyrenes and/or dinitrobenzo(a)pyrenes were not present on these substrates at detectable levels. Nitrobenzo(a)pyrene standards are not commercially available and could not be obtained from other sources, so no comparisons could be made between the mass spectra of standards and the "benzo(a)pyrene-coated" substrates used in this study. The ultraviolet absorption features of concentrated (from 50 ml to about 5 ml) micro-soxhlet extracts did not show any new peaks not present in the ultraviolet spectrum of benzo(a)pyrene.

Table 54 (p 185) shows the results of micro-soxhlet extraction of "PAH-coated" substrates, before and after exposure to 95 ppm $NO_2$ for 1 hr. In these experiments, nylon wool was once again incorporated into the photoreactor apparatus by packing the wool into the same tube as discussed in the previous section. These results appear to indicate that benzo(a)pyrene adsorbed on the surface of these substrates was not undergoing detectable reaction with $NO_2$ (when $HNO_3$ was presumably absent). Subjecting the "benzo(a)pyrene-coated" substrates to DP-MS did not reveal any peaks (or ions) higher in mass than that of benzo-(a)pyrene (252). The ultraviolet absorption spectra of concentrated micro-soxhlet extracts did not reveal any new features not present in the spectrum of benzo(a)pyrene. These data appear to indicate that detectable quantities of nitrobenzo(a)pyrenes were not being formed.

The results of these experiments tend to suggest that, in the absence of illumination, the presence of $HNO_3$ is necessary to catalyze

nitration reactions (or actually be a reactant) of pyrene and benzo(a)-pyrene with gaseous $NO_2$. Other workers[77] have observed similar results when solution-deposited samples (PAHs) of coal fly ash were exposed to $NO_2$. In other words, when $HNO_3$ was present, nitration reactions were observed; when $HNO_3$ was purged from the system, nitration reactions were not observed.

It is difficult to estimate how much $HNO_3$ might possibly have been passing through the nylon filters into the photoreactor in the presence of nylon wool since the analytical results for blank or unexposed nylon filters varied from 3 to 14 μg $NO_3^-$ per filter. It must be noted in Table 52 (p 182), however, that in most cases the analytical results for the filter nearest to the $NO_2/N_2$ gas regulator (#1) and the filter nearest to the photoreactor (#2) were very similar as far as the quantity of $NO_3^-$ measured. If a substantial quantity of $HNO_3$ was adsorbed by the #1 filter then one would expect the #2 filter to be considerably lower as far as the amount of $NO_3^-$ detected. This observation tends to suggest that only extremely low $HNO_3$ levels were present after the gases passed through the #2 filter when nylon wool was used.

Only for the "pyrene-coated" Illinois bituminous coal fly ash experiments did the quantity of $NO_3^-$ detected on the two nylon filters significantly differ; in that case, the #1 filter contained 23 μg of $NO_3^-$ and the #2 filter contained 16 μg $NO_3^-$. This could mean that some of the blank filters were quite high in $NO_3^-$ and that the amount of $HNO_3$ passing through the #2 filter was quite small or virtually zero. It could also mean that some $HNO_3$ was passing the #2 filter and thus

coming into contact with the sample. Without knowing the quantity of $NO_3^-$ present on the filters before exposure to $NO_2$, one could not know for certain whether or not a significant quantity of $HNO_3$ had passed through the filters or was almost totally adsorbed by the filters. The blank filter analyses averaged about 8 μg $NO_3^-$ per filter. If one assumes that each filter contained 8 μg $NO_3^-$ before exposure to $NO_2$ then the #1 filter adsorbed 15 μg of $HNO_3$. This figure is far below the 400 μg per filter quantities of $NO_3^-$ measured when nylon wool was not used in the experiments. This tends to suggest that the #1 filter was not saturated in the Illinois ash experiments. The #2 filter was the only #2 filter analyzed, out of many, that contained more $NO_3^-$ than the blank filters. This tends to suggest that if enough unexposed filters were analyzed, some might have $NO_3^-$ quantities higher than 14 μg. If 1 μg of $HNO_3$ passed through the #2 filter, however, at a flow rate of 0.5 L/min for 1 hr, then this would correspond to a vapor phase concentration of 18 ppb.

Table 2 (p 7) shows $HNO_3$ concentrations, in ambient Southern California air, for mild to severe air pollution episodes. These concentrations range from 1 to 50 ppb $HNO_3$.[23] Other workers[115] reported the average ambient concentration of $HNO_3$ in Warren, Michigan to range from 0.30 (Fall) to 0.51 (Winter) to 1.33 ppb (Spring). The data reported in this work tend to suggest that low level (ppb) $HNO_3$ concentrations may be sufficient for catalyzing (or directly reacting in) nitration reactions between $NO_2$ and airborne particulate-associated PAHs.

## C. Photochemical Reactions of Adsorbed PAHs in the Presence of Gaseous $NO_2$

Some of the "pyrene-coated" substrates were exposed to 12 ppm $NO_2$ in $N_2$, using the photoreactor apparatus (Figure 19, p 60) while being illuminated by the Cermax lamp (described in Section II-D) for 24 hr. The flow rate of $NO_2/N_2$ in these experiments was increased from 0.5 L/min to 1.15 L/min to insure that the substrate was suspended in the quartz region of the photoreactor. The stainless steel filter holders contained nylon filters and nylon wool was incorporated into the system to consume $HNO_3$ as discussed in the previous section. After 24 hr the substrate was removed from the photoreactor and then subjected to micro-soxhlet extraction.

Table 55 shows the results of micro-soxhlet extraction of "pyrene-coated" substrates, before and after exposure to 12 ppm $NO_2$ ($HNO_3$ absent) and illumination. It appears from these data that exposure to 12 ppm $NO_2$ ($HNO_3$ absent) during illumination of "pyrene-coated" East Tennessee and Illinois bituminous coal fly ashes resulted in essentially no change in pyrene concentration, as determined by micro-soxhlet extraction. The "pyrene-coated" silica gel and Texas lignite coal fly ash samples, after illumination and exposure to 12 ppm $NO_2$ ($HNO_3$ absent), however, showed relatively small decreases in pyrene concentration. This was not unexpected since pyrene, adsorbed on these substrates, had undergone photochemical transformations in the irradiation experiments discussed in Section III-C. Furthermore, if one compares the data in Table 55 with the non-photochemical data in Table 54 (p 185), one can see that the illumination of these "pyrene-coated"

TABLE 55

RESULTS OF MICRO-SOXHLET EXTRACTION OF "PYRENE-COATED" SUBSTRATES BEFORE AND AFTER EXPOSURE TO 12 ppm $NO_2$ ($HNO_3$ ABSENT) AND ILLUMINATION FOR 24 HOURS

| Substrate | Before Illumination | After Illumination |
|---|---|---|
| Silica Gel | 833 ± 36 µg/g | 632 ± 66 µg/g |
| Texas Lignite Coal Fly Ash | 1321 ± 16 | 1074 ± 66 |
| East Tennessee Bituminous Coal Fly Ash | 187 ± 10 | 165 ± 7 |
| Illinois Bituminous Coal Fly Ash | 39 ± 3 | 43 ± 3 |

substrates was responsible for the observed decreases in pyrene concentrations, since non-photochemical reactions, even in the presence of $NO_2$ ($HNO_3$ presumably not present), were not observed.

All four of the "pyrene-coated" substrates listed in Table 55 were subjected to DP-MS. The mass spectra of the three "pyrene-coated" coal fly ashes did not reveal any peaks higher in mass than the parent ion (pyrene: mass 202). The mass spectral and micro-soxhlet extraction results of these three samples suggest that the illumination of pyrene adsorbed on the surface of Texas lignite and East Tennessee bituminous coal fly ashes, in the presence of $NO_2$ ($HNO_3$ absent), does not lead to nitration reactions.

When the "pyrene-coated" silica gel sample that had been illuminated in the presence of $NO_2$, from which precautions were exercised to remove $HNO_3$, was subjected to DP-MS, however, many new peaks appeared in the mass spectrum that were not present in the mass spectrum of an unirradiated sample. The mass and relative abundance of each ion obtained by subjecting the irradiated sample to DP-MS are shown in Table 56. These data as well as the yellow color in the micro-soxhlet extracts tend to indicate the presence of nitro- and dinitropyrenes on the surface of the silica gel sample. These data suggest that the illumination of "pyrene-coated" silica gel in the presence of $NO_2$ leads to nitration products even when $HNO_3$ is purged from the system.

However, it was found that, in these experiments, the nylon wool had become saturated with $HNO_3$, allowing $HNO_3$ to pass into the photoreactor and to come into contact with the sample. For the 1 hr non-photochemical experiments, saturation of the nylon wool was not

TABLE 56

THE MASS AND RELATIVE ABUNDANCE OF EACH ION OBTAINED FROM THE MASS SPECTRUM OF IRRADIATED "PYRENE-COATED" SILICA GEL EXPOSED TO 12 ppm $NO_2$ ($HNO_3$ THOUGHT NOT TO BE PRESENT)

| MASS | ABUND | MASS | ABUND | MASS | ABUND | MASS | ABUND |
|---|---|---|---|---|---|---|---|
| 36 | .6 | 69 | 61.7 | 97 | 84.9 | 124 | 9.0 |
| 39 | 2.3 | 70 | 19.7 | 98 | 18.3 | 125 | 26.6 |
| 40 | 3.1 | 71 | 77.2 | 99 | 24.1 | 126 | 5.5 |
| 41 | 11.4 | 72 | 4.3 | 100 | 11.6 | 127 | 9.4 |
| 42 | 4.6 | 73 | 6.5 | 101 | 10.7 | 128 | 1.8 |
| 43 | 37.1 | 74 | 1.3 | 103 | .5 | 129 | 3.7 |
| 44 | 62.9 | 75 | .6 | | | 130 | 1.0 |
| 45 | 3.0 | | | 104 | 1.8 | 131 | 6.4 |
| 46 | .4 | 77 | 2.8 | 105 | 9.2 | | |
| | | 78 | 1.2 | 106 | 3.3 | 132 | 1.3 |
| 48 | 2.3 | 79 | 6.1 | 107 | 6.4 | 133 | 7.7 |
| 50 | .6 | 80 | 6.2 | 108 | 5.0 | 134 | 2.2 |
| 51 | 2.2 | 81 | 41.7 | 109 | 33.5 | 135 | 7.7 |
| 53 | 1.2 | 82 | 21.1 | 110 | 13.7 | 136 | 3.3 |
| 54 | 2.4 | 83 | 77.7 | 111 | 50.8 | 137 | 13.5 |
| 55 | 39.6 | 84 | 16.8 | 112 | 9.2 | 138 | 5.8 |
| 56 | 16.3 | 85 | 62.1 | 113 | 13.9 | 139 | 12.4 |
| 57 | 100.0 | 86 | 3.7 | 114 | 1.3 | 140 | 3.2 |
| 58 | 4.7 | 87 | 3.5 | 115 | 2.4 | 141 | 7.2 |
| 60 | 5.0 | 88 | 3.8 | 117 | 2.2 | 142 | 1.1 |
| | | | | | | 143 | 2.3 |
| 63 | .5 | 91 | 5.8 | 118 | 1.2 | 144 | 1.1 |
| 64 | 10.0 | 92 | 1.8 | 119 | 10.7 | 145 | 5.5 |
| 65 | .9 | 93 | 6.6 | 120 | 3.3 | | |
| 66 | 1.6 | 94 | 7.8 | 121 | 8.1 | 146 | 1.4 |
| 67 | 19.3 | 95 | 51.5 | 122 | 4.8 | 147 | 4.1 |
| 68 | 8.1 | 96 | 22.8 | 123 | 21.9 | 148 | 1.4 |

TABLE 56 (Continued)

| MASS | ABUND | MASS | ABUND | MASS | ABUND | MASS | ABUND |
|---|---|---|---|---|---|---|---|
| 149 | 7.2 | 175 | 3.4 | 202 | 60.9 | 235 | 2.1 |
| 150 | 3.7 | 176 | .8 | 203 | 11.4 | 236 | 1.1 |
| 151 | 10.1 | 177 | 3.3 | 204 | 2.1 | 237 | 1.4 |
| 152 | 4.2 | 178 | 1.3 | 205 | 2.5 | 239 | .5 |
| 153 | 8.0 | 179 | 5.7 | 206 | 1.1 | 238 | 1.6 |
| 154 | 2.1 | 180 | 2.1 | 207 | 4.2 | 243 | .5 |
| 155 | 6.3 | 181 | 5.4 | 208 | 2.8 | | |
| 156 | .6 | 182 | 1.4 | 209 | 3.5 | 245 | .6 |
| 157 | 2.2 | 183 | 4.8 | 210 | 1.0 | 247 | 1.3 |
| 158 | .7 | 184 | .8 | 211 | 2.8 | 248 | .6 |
| 159 | 5.1 | 185 | 2.1 | 213 | 1.1 | 249 | 1.8 |
| | | 187 | 1.7 | 215 | .9 | 250 | 1.1 |
| 160 | .9 | | | | | 251 | 1.3 |
| 161 | 3.2 | 189 | 2.2 | 217 | 1.3 | 252 | .5 |
| 162 | 1.1 | 190 | .6 | 218 | .7 | 253 | 1.1 |
| 163 | 5.5 | 191 | 3.1 | 219 | 1.8 | 257 | .6 |
| 164 | 1.9 | 192 | 1.0 | 220 | .9 | | |
| 165 | 6.6 | 193 | 4.8 | 221 | 2.6 | 259 | .5 |
| 166 | 2.7 | 194 | 2.2 | 222 | 1.3 | 261 | .8 |
| 167 | 5.9 | 195 | 3.8 | 223 | 2.5 | 263 | 1.3 |
| 168 | 2.4 | 196 | 1.8 | 224 | 1.1 | 264 | .6 |
| 169 | 6.0 | 197 | 3.4 | 225 | 1.5 | 265 | .7 |
| 170 | 1.1 | 198 | 2.4 | 227 | .6 | 266 | .5 |
| 171 | 2.0 | 199 | 4.0 | 229 | .5 | 267 | .9 |
| 173 | 2.9 | 200 | 13.4 | | | | |
| | | 201 | 12.5 | 231 | 1.2 | 275 | .6 |
| 174 | 1.6 | | | 233 | 1.7 | 277 | 1.1 |

TABLE 56 (Continued)

| MASS | ABUND | MASS | ABUND | MASS | ABUND | MASS | ABUND |
|---|---|---|---|---|---|---|---|
| 279 | .7 | | | | | | |
| 280 | .4 | | | | | | |
| 280 | .7 | | | | | | |
| 291 | .9 | | | | | | |
| 292 | .6 | | | | | | |
| 293 | .9 | | | | | | |
| 295 | .6 | | | | | | |
| 304 | .7 | | | | | | |
| 306 | .5 | | | | | | |

thought to be a problem since the total time in which sample exposure to $NO_2$ occurred was only about 7 hr (7 analyses as shown in Table 54, p 185) even though the $NO_2$ concentration was 95 ppm at a flow rate of 0.5 l/min. However, for one photochemical experiment which took 24 hr (at 12 ppm $NO_2$ at a flow rate of 1.15 l/min), a much higher quantity of $HNO_3$ was absorbed by the nylon wool.

To determine the capacity of nylon wool for "scrubbing" $HNO_3$ from the $NO_2$ system, swabs of nylon wool were extracted and analyzed, before and after exposure to 95 ppm $NO_2$ for 1 hr at a flow rate of 0.5 l/min, by the same procedure used to determine the $NO_3^-$ content of the nylon filters (Section II-J). These results indicated that 1 g of nylon wool had a capacity of about 30 μg $NO_3^-$. Since approximately 60 g of nylon wool was used in each experiment, the capacity of the nylon wool-packed tube was about 1800 μg $NO_3^-$. The nylon filters, as discussed in Section IV-A, contained 400 μg $NO_3^-$ per filter after a 20 min exposure to 95 ppm $NO_2$ at a flow rate of 0.5 l/min when nylon wool was not in the system. However, nylon filter analyses, after the nylon wool was in the system, revealed that the $NO_3^-$content of each nylon filter was within the levels detected on new, unused filters. The overall conclusion obtained from these results is that the nylon wool is quite effective for purging $HNO_3$ from the gas stream but must be replaced regularly when performing photochemical experiments that require passage of $NO_2$ through the photoreactor for long (24 hr) periods of time.

When "pyrene-coated" silica gel was illuminated in the presence of 12 ppm $NO_2$ ($HNO_3$ removed) at a flow rate of 1.15 l/min, micro-soxhlet extraction still showed a decrease in pyrene concentration.

The extracts were colorless, however, and no nitropyrenes were detected after subjecting the sample to DP-MS, as shown in Table 57.

Table 58 shows the micro-soxhlet extraction results for "benzo-(a)pyrene-coated" substrates, before and after exposure to 12 ppm $NO_2$ ($HNO_3$ removed) and illumination for 24 hr. These results are similar to the "pyrene-coated" substrate results discussed in the preceding paragraph, in that the concentration of the PAH adsorbed on the surface of silica gel and Texas lignite coal fly ash decreased, whereas the concentration of PAH on the surface of East Tennessee and Illinois bituminous coal fly ash did not show any apparent change, as determined by micro-soxhlet extraction. After subjecting these four samples to DP-MS, no peaks greater in mass than the parent ion (benzo(a)pyrene; mass 252), were observed in their mass spectra. When the photoreactor apparatus was purged of $HNO_3$, the micro-soxhlet extracts of "benzo(a)-pyrene-coated" silica gel illuminated in the presence of $NO_2$ were colorless (these extracts had a yellow coloration when the PAH was pyrene and $HNO_3$ had not been completely removed).

These data tend to suggest that illumination (by sunlight) of airborne particulate matter, such as coal fly ash, on which pyrene and/or benzo(a)pyrene are adsorbed, will not lead to nitration reactions with these particular PAHs when the atmospheric concentration of $HNO_3$ is very low. The overall results of the $NO_2$ pollutant gas experiments appear to indicate that $HNO_3$ is a necessary participant in nitration reactions of PAHs, either as a catalyst or as a reactant, when the PAHs are associated with coal fly ash. Whether or not

TABLE 57

THE MASS AND RELATIVE ABUNDANCE OF EACH ION OBTAINED FROM THE MASS SPECTRUM OF ILLUMINATED "PYRENE-COATED" SILICA GEL IN THE PRESENCE OF 12 ppm $NO_2$ (FRESH NYLON WOOL SO $HNO_3$ IS NOT PRESENT)

| MASS | ABUND | MASS | ABUND | MASS | ABUND | MASS | ABUND |
|---|---|---|---|---|---|---|---|
| 40 | 4.9 | 84 | 2.3 | 124 | 1.2 | 177 | .6 |
| 41 | 3.2 | 85 | 13.6 | 125 | 5.4 | 179 | .5 |
| 42 | 1.6 | 87 | 1.9 | 126 | 1.0 | 181 | 1.0 |
| 43 | 14.3 | 88 | 3.0 | 127 | 1.6 | 183 | .5 |
| 44 | 11.3 | | | 130 | .5 | | |
| | | 93 | .6 | 131 | .9 | 197 | .5 |
| 48 | .9 | 94 | 1.2 | | | 198 | 2.6 |
| 55 | 10.5 | 95 | 10.1 | 133 | .7 | 199 | 4.2 |
| 56 | 3.4 | 96 | 4.3 | 135 | 1.0 | 200 | 22.8 |
| 57 | 23.6 | 97 | 18.9 | 137 | 1.9 | 201 | 20.1 |
| 58 | 1.4 | 98 | 3.7 | 138 | 1.0 | | |
| | | 99 | 7.0 | 139 | 2.4 | 202 | 100.0 |
| 64 | 2.6 | 100 | 9.1 | 141 | 1.1 | 203 | 15.2 |
| 67 | 4.5 | 101 | 11.7 | | | 204 | .7 |
| 68 | 1.2 | | | 149 | 1.7 | 208 | 1.8 |
| 69 | 15.4 | 105 | 1.7 | 150 | 2.3 | 209 | .9 |
| 70 | 3.4 | 107 | .7 | 151 | 2.8 | | |
| 71 | 18.7 | 109 | 5.8 | 152 | 1.0 | | |
| 72 | .7 | 110 | 1.9 | 153 | 11.1 | | |
| 74 | .5 | 111 | 12.1 | 155 | .6 | | |
| 75 | .5 | 112 | 1.1 | | | | |
| | | 113 | 2.1 | 163 | .9 | | |
| 77 | .7 | | | 165 | .5 | | |
| 80 | .5 | 119 | 2.4 | 169 | 1.1 | | |
| 81 | 10.0 | 121 | 1.8 | | | | |
| 82 | 5.2 | 122 | 1.1 | 174 | 2.7 | | |
| 83 | 16.6 | 123 | 4.5 | 175 | 1.1 | | |

TABLE 58

THE RESULTS OF MICRO-SOXHLET EXTRACTION OF "BENZO(a)PYRENE-COATED" SUBSTRATES BEFORE AND AFTER EXPOSURE TO 12 ppm $NO_2$ ($HNO_3$ ABSENT) AND ILLUMINATION FOR 24 HOURS

| Substrate | Before Illumination | After Illumination |
|---|---|---|
| Silica Gel | 73 ± 12 | ND |
| Texas Lignite Coal Fly Ash | 342 ± 1 | 266 ± 10 |
| East Tennessee Bituminous Coal Fly Ash | 26 ± 2 | 28 ± 4 |
| Illinois Bituminous Coal Fly Ash | 28 ± 2 | 33 ± 2 |

*Concentration in micrograms of benzo(a)pyrene per gram to substrate.

ND = Not Detected.

illumination can enhance nitration reactions between PAHs and $NO_2$ (when $HNO_3$ is present) cannot be conclusively deduced from these results.

Again, as in the case of photochemical reactions of adsorbed PAHs in the absence of $NO_2$, adsorption of PAHs on coal fly ash surfaces stabilizes the adsorbates to photodecomposition, as compared with the behavior observed on silica surfaces. The East Tennessee and Illinois bituminous coal fly ashes stabilize surface-adsorbed pyrene and benzo-(a)pyrene from photochemical transformations in the presence or absence of $NO_2$. Texas lignite coal fly ash, however, does not stabilize pyrene and benzo(a)pyrene from photochemical transformations to the same extent as does East Tennessee and Illinois bituminous coal fly ash, but does stabilize these compounds to a greater extent than silica gel. In other words, the observed photochemical behavior in the absence of $NO_2$ tends to parallel the observed photochemical behavior in the presence of $NO_2$. It is quite conceivable that $NO_2$ has no appreciable effect on the stability (photochemical or non-photochemical) of adsorbed PAHs, so long as $HNO_3$ is absent. The formation of nitro-PAHs is observed (photochemically or non-photochemically) only when $HNO_3$ is present.

# CHAPTER V

## SUMMARY AND CONCLUSIONS

The expected increases for electrical power demand combined with the availability of native coal has assured a key role for the combustion of coal as a power source for many years to come. Proven carcinogens, such as some of the PAHs, as well as many other organic species, are likely to be adsorbed on the surface of coal fly ashes that are emitted from the stacks of coal-fired power plants, and the ultimate environmental fate of these species is a topic of much research and debate. Most of the atmospheric PAHs are associated with airborne particulate matter, such as coal fly ash, rather than existing in the vapor phase and the evidence to date suggests that the mutagenic activity (Ames test) is associated with organic extracts of coal fly ash rather than the inorganic matrix of the fly ash itself. Furthermore, it appears that the activity can be accounted for by the presence of PAHs, aromatic nitrogen heterocycles, and nitro-substituted PAHs adsorbed on coal fly ash.[116]

Two types of reactions appear to be possible with PAHs associated with airborne coal fly ash. The first type of reaction involves the photochemical and non-photochemical oxidation of PAHs and the second involves particle-associated PAH reactions with pollutant gases such as $NO_2$. Adsorption of pyrene or benzo(a)pyrene on coal fly ash results in stabilization of these compounds against photochemical decomposition, as compared with these same compounds adsorbed on silica gel, alumina, and glass. Some PAHs (e.g., fluorene) undergo non-photochemical

oxidation to quinones or ketones, but this behavior has not been observed when the PAH was adsorbed on silica gel, alumina, or glass.[117]

Reactions of glass fiber-filter associated PAHs with $NO_2$ leads to increased mutagenic activity in the Ames test. Some compounds such as perylene, are relatively non-mutagenic until exposed to $NO_2$ when the compound is adsorbed on glass fiber-filters.[117] Clearly, a better understanding of these reactions, and how adsorption of PAHs on coal fly ash affects these reactions, must be acquired before reasonable predictions of atmospheric residence times of particle-bound organic compounds can be made.

Conclusions that can be drawn from the work discussed in this dissertation include the following:

1) PAHs tend to be more resistant to photochemical reactions when adsorbed on coal fly ash than when adsorbed on substrates such as silica gel, alumina, or glass. Other workers[63] have reported similar results. In this work, however, some coal fly ashes were found to be associated with PAH photochemical transformations, although not nearly to the same extent as PAHs adsorbed on silica gel, alumina, or glass.

2) There does not appear to be any relationship between the aqueous extract pH of coal fly ash and the observed photochemical behavior. Other workers[118] had suggested that acidic sites on the surface of coal fly ash may be responsible for the observed photochemical behavior; however,

in this work there did not appear to be any such relationship.

3) There appears to be some degree of negative relationship between the total carbon content of coal fly ash and the observed photochemical behavior. Much of the data reported in this work shows that, as the percentage of carbon in the coal fly ash increases, the PAHs adsorbed on coal fly ash tend to resist photochemical decomposition. Moreover, no photodecomposition was observed for pyrene or benzo(a)pyrene adsorbed on pure carbon (graphite). There are exceptions, however, to this trend which suggest that one or more other factors are also operative.

4) There appears to be a relationship between the absorbance (or color) of coal fly ash and the observed photochemical behavior, but again, there are exceptions. Most of the substrates associated with high photochemical reactivity are substrates of low absorbance over the 375 to 250 nanometer wavelength region. Substrates associated with little or no photochemical reactivity tend to exhibit high absorbance over the 375 to 250 nanometer wavelength region. This observation suggests that "inner-filter" absorption of incident light by the substrate may be an important mechanism by which fly ashes stabilize PAHs to photodecomposition.

5) There does not appear to be any obvious relationship between the surface area of coal fly ash and the observed photochemical behavior. Of course, as the specific surface area

increases, the probability increases that high concentrations of PAHs will be adsorbed on the substrate.

6) It appears that most coal fly ashes have somewhat similar pore volumes and pore size distributions. This suggests that the observed photochemical behavior is not dependent on whether or not PAH molecules can deposit inside pores and thus be shielded from incident radiation. It appears that even molecules that deposit inside pores may undergo photochemical transformations if the substrate on which the PAH is adsorbed is transparent to the incident radiation in the spectral region in which the PAH is absorptive.

7) Non-photochemical transformations of coal fly ash-associated pyrene and benzo(a)pyrene appear to be so slow that their environmental significance is negligible.

8) It appears that the nitration of coal fly ash-associated PAHs is dependent on the atmospheric concentration of $HNO_3$, rather than that of $NO_2$. The results discussed in this work are similar to those reported by other workers.[84] Whether or not $HNO_3$ behaves as a reactant or as a catalyst for PAH reaction with $NO_2$ cannot be deduced from this work. The nitration of coal fly ash-associated PAHs, however, does not appear to require illumination. The presence of $HNO_3$ appears to be necessary for nitration reactions of PAHs adsorbed on coal fly ash, similar to the observed results for nitration reactions in solution.[119] Of course, other atmospheric equilibria are taking place that involve $NO_2$. The species NO

> tends to slowly oxidize to $NO_2$; and $NO_2$ itself is reactive photochemically according to $NO_2 + h\nu \rightarrow NO + O$. The highly active monatomic oxygen (O) combines with $O_2$ (in the presence of a third body) to form $O_3$. Then, $O_3$ oxidizes NO to $NO_2$. The result is a low steady state level of $O_3$.[120]

Because of the extreme mutagenicity associated with nitro-PAHs, the formation of these compounds on airborne coal fly ash is most alarming. This work suggests that low level concentrations (such as those present in ambient air) of $HNO_3$ are sufficient for nitration of coal fly ash-associated PAHs. Work is presently underway[121] to design the control technology necessary to reduce $NO_x$ emissions from coal combustion.

This work demonstrates that PAHs are stabilized against photodecomposition when the PAHs are adsorbed on most (but not all) coal fly ashes. When one considers the higher specific surface area and longer residence times of submicrometer size particles versus particles greater than one micrometer in size, then it becomes clear that considerable quantities of particulate-associated PAHs are remaining in the atmosphere for longer time periods than had been previously thought. Whether or not PAHs are being photooxidized to compounds believed to be more carcinogenic and/or mutagenic than the parent PAH cannot be conclusively deduced from this work since attempts to identify photochemical products were unsuccessful.

Obviously, the work presented here has introduced new questions. Experiments must be designed to accurately evaluate the delicate balance between coal fly ash carbon content (and how this affects

substrate color) and inner-filter effects and how these factors affect the photochemistry of coal fly ash-associated PAHs. Furthermore, the study of coal fly ash-associated PAH reactions with other gaseous pollutants, such as $SO_2$ and $O_3$, must be examined.

Ultimately, the use of "in-situ" techniques may be required before mechanisms of bonding (whether physical, chemical, or both) between coal fly ash and adsorbed PAHs can be correctly elucidated. Experiments of this type may require the separation of coal fly ash into its various phases since it is quite obvious that different phases will affect adsorbed PAHs differently. The use of electron spectroscopy for chemical analysis (ESCA) may provide information regarding bonding and secondary ion mass spectrometry (SIMS) may ultimately be used to obtain photochemical product identification. The use of SIMS may eventually allow the analysis of coal fly ash samples of greater environmental relevance than those employed in this work, since this work required vapor-deposition of PAHs onto the surfaces of coal fly ash at concentrations that are probably much greater than those found on "real" airborne coal fly ash.

A technique that may be useful for studying particulate-associated PAHs is the use of carbon-14 labeled PAHs. By "coating" the coal fly ashes with, e.g., carbon-14 labeled pyrene, one could measure the activity on the coal fly ash and determine the concentration of the pyrene. This information would help determine micro-soxhlet extraction efficiencies as well as serve as an aid for evaluation of photochemical and non-photochemical transformation data.

# LIST OF REFERENCES

# LIST OF REFERENCES


1. D. Hoffman and E. L. Wynder, in "Chemical Carcinogens", C. E. Searle, Ed., ACS Monograph 173, American Chemical Society, Washington, D.C., (1976) p 343.

2. Division of Medical Sciences, National Research Council, "Particulate Polycyclic Organic Matter", 13 (1972).

3. G. M. Badger, Nat. Cancer Inst. Monogr., 9, 1 (1962).

4. I. E. Burrows and A. J. Lindsey, Chem. Ind., 1395 (1961).

5. P. Pott, Chirurgical Observations (1775); Reprinted in Nat. Cancer Monogr., 10, 7 (1963).

6. D. M. Jerina, J. W. Daly, B. Witkop, P. Zaltzmann-Nivenberg, and S. Udenfriend, J. Am. Chem. Soc., 90, 6525 (1968).

7. P. Sims, P. L. Grover, A. Swaisland, K. Pal, and A. Hewer, Nature (London), 252, 326 (1974).

8. A. Dipple, P. D. Lawley, and P. Brooks, Eur. J. Cancer, 4, 493 (1968).

9. A. Dipple, Cancer Res., 43, 2422 (1983).

10. P. G. Wislocki, A. W. Wood, R. L. Chang, W. Levin, H. Yagi, O. Hernandez, P. M. Dansette, D. M. Jerina, and A. H. Conney, Cancer Res., 36, 3350 (1976).

11. J. N. Pitts, Jr., D. M. Lokensgard, P. S. Ripley, K. A. van Cauwenberghe, L. van Vaeck, S. D. Shaffer, A. J. Thill, and W. L. Belser, Science, 210, 1347 (1980).

12. M. A. Fox and S. Olive, Science, 205, 582 (1979).

13. E. McCoy and H. Rosenkranz, Cancer Lett., 9, 35 (1980).

14. K. van Cauwenberghe and L. van Vaeck, Mutat. Res., 116, 1 (1983).

15. T. Nielsen, T. Ramdahl, and A. Bjϕrseth, Environ. Health Perspect., 47, 103 (1983).

16. National Academy of Sciences, Polycyclic Aromatic Hydrocarbons: Evaluation of Sources and Effects, National Academy Press, Washington, D.C. (1983).

17. H. Tokiwa, H. Takeyoshi, K. Morita, K. Takahashi, N. Saruta, and Y. Ohnishi, Mutat. Res., 38, 351 (1976).

18. J. N. Pitts, Jr., D. Grosjean, T. M. Mischke, V. F. Simmon, and D. Poole, Toxicol. Lett., 1, 65 (1977).

19. C. E. Chrisp and G. L. Fisher, Mutat. Res., 76, 143 (1980).

20. Committee on Biological Effects of Atmospheric Pollutants, National Academy of Sciences, Particulate Polycyclic Organic Matter, Washington, D.C., (1972).

21. H. V. Gelboin and P. O. P. T'so, Eds., in "Polycyclic Hydrocarbons and Cancer", Academic Press, New York, 15 (1978).

22. R. C. Lao, R. S. Thomas, and J. L. Monkman, J. Chromatogr., 112, 681 (1975).

23. J. N. Pitts, Jr., Environ. Health Perspect., 47, 115 (1983).

24. M. W. McElroy, R. C. Carr, D. S. Ensor, and G. R. Markowski, Science, 215, 13 (1982).

25. R. A. Hites, R. E. LaFlamme, and J. W. Farrington, Science, 198, 829 (1977).

26. B. T. Commins, Natl. Cancer Inst. Monogr., 9, 225 (1962).

27. G. A. Eiceman and V. J. Vandiver, Atmos. Environ., 17, 461 (1983).

28. R. J. Charlston, D. S. Covert, T. V. Larson, and A. P. Waggoner, Atmos. Environ., 12, 39 (1978).

29. H. S. Stoker and S. L. Seager, in "Environmental Chemistry: Air and Water Pollution", Scott Foresman, Publisher, Dallas, Texas, (1976) p. 2.

30. N. A. Esmen and M. Corn, Atmos. Environ., 5, 571 (1971).

31. D. F. S. Natusch and J. R. Wallace, Science, 186, 695 (1974).

32. H. A. Schroeder, Environment (St. Louis), 13, 18 (1971).

33. P. E. Morrow, Am. Ind. Hyg. Assoc. J., 25, 213 (1965).

34. W. D. Ruckelstein, Chem. Eng., 62, 6 (1984).

35. L. D. Hulett and A. J. Weinberger, Environ. Sci. Technol., 14, 965 (1980).

36. W. S. Lyon, Environ. Sci. Technol., 9, 973 (1975).

37. G. L. Fisher, B. A. Prentice, D. Silberman, J. M. Ondov, A. H. Biermann, R. C. Ragaini, and A. R. MacFarland, Environ. Sci. Technol., 12, 447 (1978).

38. R. E. Bickelhaupt, J. Air Pollut. Control Assoc., 25, 148 (1975).

39. P. Ditl and R. W. Caughlin, Environ. Sci. Technol., 11, 701 (1977).

40. T. L. Theis and J. L. Wirth, Environ. Sci. Technol., 11, 1096 (1977).

41. J. A. Campbell, J. C. Laul, K. K. Nielson, and R. D. Smith, Anal. Chem., 50, 1032 (1978).

42. R. D. Smith, J. A. Campbell, and K. K. Nielson, Atmos. Environ., 13, 607 (1979).

43. R. L. Davison, D. F. S. Natusch, J. R. Wallace, and C. A. Evans, Jr., Environ. Sci. Technol., 8, 1107 (1974).

44. D. M. Hercules, Anal. Chem., 50, 734A (1978).

45. T. R. Keyser, D. F. S. Natusch, C. A. Evans, Jr., and R. W. Linton, Environ. Sci. Technol., 12, 768 (1978).

46. J. A. Campbell, R. D. Smith, L. E. Davis, and K. L. Smith, Sci. Total Environ., 12, 75 (1979).

47. J. A. Campbell, R. D. Smith, and L. E. Davis, Appl. Spectrosc., 32, 316 (1978).

48. R. W. Linton, P. Williams, C. A. Evans, Jr., and D. F. S. Natusch, Anal. Chem., 49, 1514 (1977).

49. R. E. Lee, Jr. and D. J. von Lehmden, J. Air Pollut. Control Assoc., 23, 853 (1973).

50. R. C. Lao, R. S. Thomas, H. Oja, and L. Dubois, Anal. Chem., 45, 908 (1973).

51. W. Cautreels and K. Van Cauwenberghe, Atmos. Environ., 10, 447 (1976).

52. W. Cautreels and K. Van Cauwenberghe, J. Chromatogr., 131, 253 (1977).

53. M. A. Fox and S. W. Staley, Anal. Chem., 48, 992 (1976).

54. W. Giger and C. Schaffner, Anal. Chem., 50, 243 (1978).

55. E. J. Bowen, in "The Photochemistry of Aromatic Hydrocarbon Solutions", Advances in Photochemistry, 1, 23 (1963), W. A. Noyes, Jr., G. S. Hammond, and J. N. Pitts, Jr., Eds., Interscience, New York.

56. Y. Masuda and M. Kuratsune, Int. J. Air Water Pollut., 10, 805 (1966).

57. E. J. Moriconi, B. Rakoczy, and W. F. O'Connor, J. Am. Chem. Soc., 83, 4618 (1961).

58. G. Kortüm and W. Braun, Ann. Chem., 632, 104 (1960).

59. D. P. Craig and P. C. Hobbins, J. Chem. Soc., 2309 (1955).

60. M. N. Inscoe, Anal. Chem., 36, 2505 (1964).

61. M. R. Cimberle, P. Bottino, and F. Valerio, Chemosphere, 12, 317 (1983).

62. L. Blau and H. Güsten, in "Polynuclear Aromatic Hydrocarbons," M. Cooke, A. J. Dennis, and G. L. Fisher, Eds., Battelle Press, Columbus, Ohio, (1981) p 133.

63. W. A. Korfmacher, E. L. Wehry, G. Mamantov, and D. F. S. Natusch, Environ. Sci. Technol., 14, 1094 (1980).

64. W. A. Korfmacher, D. F. S. Natusch, D. R. Taylor, G. Mamantov, and E. L. Wehry, Science, 207, 763 (1980).

65. W. A. Korfmacher, G. Mamantov, E. L. Wehry, D. F. S. Natusch, and T. Mauney, Environ. Sci. Technol., 15, 1370 (1981).

66. A. H. Miguel, W. A. Korfmacher, G. Mamantov, E. L. Wehry, and D. F. S. Natusch, Environ. Sci. Technol., 13, 1229 (1979).

67. P. F. Southern and W. A. Walters, J. Chem. Soc., 4340 (1960).

68. H. L. Falk, I. Markul, and P. Kotin, Arch. Ind. Health, 13, 13 (1956).

69. W. H. Griest and J. E. Caton, Proceedings of the Fifth International Symposium on Polycyclic Aromatic Hydrocarbons, (1980) p 99.

70. P. A. Soltys, "The Extraction Behavior of PAH from Coal Fly Ash", M.S. Thesis, Colorado State University, Fort Collins, Colorado, 1980.

71. P. S. Pedersen, J. Ingwersen, T. Nielsen, and E. Larson, Environ. Sci. Technol., 14, 71 (1980).

72. J. D. Butler, P. Crossley, and D. M. Colwill, Sci. Total Environ., 19, 179 (1981).

73. H. Rosen, T. Novakov, and B. A. Bodhaine, Atmos. Environ., 15, 1371 (1981).

74. R. Dlugi and H. Güsten, Atmos. Environ., 17, 1765 (1983).

75. D. A. Lane and M. Katz, in "Fate of Pollutants in the Air and Water Environments", Part 2, I. A. Suffet, Ed., Wiley-Interscience, New York, N.Y., pp. 137-154 (1977).

76. L. van Vaeck and K. van Cauwenberghe, Atmos. Environ., 18, 323 (1984).

77. D. Grosjean, K. Fung, and J. Harrison, Environ. Sci. Technol., 17, 673 (1983).

78. H. Vollmann, H. Becker, M. Corell, H. Streeck, and G. Langbein, Ann. Chem., 531, 1 (1937).

79. B. D. Tebbens, J. F. Thomas, and M. Mukai, Am. Ind. Hyg. Assoc. J., 27, 415 (1966).

80. J. D. Butler and P. Crossley, Atmos. Environ., 15, 91 (1981).

81. B. N. Ames, J. McCann, and E. Yamasaki, Mutat. Res., 31, 347 (1975).

82. A. Brorstrom, P. Greenfelt, and A. Lindskog, Atmos. Environ., 17, 601 (1983).

83. H. Tokiwa, R. Nakagawa, K. Morita, and Y. Ohnishi, Mutat. Res., 85, 195 (1981).

84. D. Grosjean, Environ. Sci. Technol., 17, 13 (1983).

85. O. L. Chapman, A. A. Griswold, E. Hogansen, G. Lenz, and J. Reasoner, Pure Appl. Chem., 9, 585 (1964).

86. J. N. Pitts, Jr. and Y. A. Katzenstein, Atmos. Environ., 15, 1782 (1981).

87. J. N. Pitts, Jr., K. A. van Cauwenberghe, D. Grosjean, J. P. Schmid, D. R. Fitz, W. L. Belser, Jr., G. Knudsen, and P. M. Hynds, Science, 202, 515 (1978).

88. P. Neta and L. M. Dorfman, in "Radiation Chemistry", Vol. 1 (Advances in Chemistry Series 81), American Chemical Society, Washington, D.C., pp. 222-230 (1968).

89. J. Jager and V. Hanus, J. Hyg. Epidemiol. Microbiol. Immunol., 24, 1 (1980).

90. R. Mermelstein, D. K. Kiriazides, M. Butler, and E. C. Rosenkranz, Mutat. Res., 89, 187 (1981).

91. Alpha Resources Inc., Stevensville, Michigan.

92. R. J. Lauf, "Application of Materials Characterization Techniques to Coal and Coal Wastes," Oak Ridge National Laboratory/TM-7663, (1981).

93. L. D. Hulett, A. J. Weinberger, N. M. Ferguson, K. J. Northcutt, and W. S. Lyon, Electric Power Research Institute, EA-1822, Project 1061 Final Report (1981).

94. A. H. Miguel and D. F. S. Natusch, Environ. Sci. Technol., 47, 1705 (1975).

95. A. H. Miguel, W. A. Korfmacher, E. L. Wehry, G. Mamantov, and D. F. S. Natusch, Environ. Sci. Technol., 13, 1229 (1979).

96. D. Dulln and T. Mill, Environ. Sci. Technol., 16, 815 (1982).

97. J. M. Daisey, C. G. Lewandowski, and M. Zorz, Environ. Sci. Technol., 16, 857 (1982).

98. J. B. Mullin and J. P. Riley, Anal. Chim. Acta, 12, 464 (1955).

99. E. Sanhueza, C. N. Plum, and J. N. Pitts, Jr., Atmos. Environ., 18, 1029 (1984).

100. J. F. Foster and G. H. Beatty, "Final Report on Interlaboratory Cooperative Study of the Precision and Accuracy of the Measurement of Nitrogen Dioxide Content in the Atmosphere Using ASTM Method D1607," American Society for Testing and Materials, Philadelphia, Pennsylvania, p. 75 (1974).

101. P. A. Flowers, unpublished work, University of Tennessee, 1982.

102. A. A. Garrison, unpublished work, University of Tennessee, 1982.

103. R. K. Bauer, P. deMayo, W. R. Ware, and K. C. Wu, J. Phys. Chem., 86, 3781 (1982).

104. R. K. Bauer, R. Borenstein, P. deMayo, K. Okada, M. Rafalska, W. R. Ware, and K. C. Wu, J. Am. Chem. Soc., 104, 4635 (1982).

105. R. K. Bauer, P. deMayo, K. Okada, W. R. Ware, and K. C. Wu, J. Phys. Chem., 87, 460 (1983).

106. K. S. W. Sing, Pure Appl. Chem., 54, 2201 (1982).

107. A. W. Adamson, "Physical Chemistry of Surfaces", John Wiley and Sons, 1976.

108. S. J. Gregg and K. S. W. Sing, "Adsorption, Surface Area, and Porosity," Academic Press, 1982.

109. B. C. Lippens and J. H. deBoer, J. Catal., 4, 319 (1965).

110. A. LeCloux and J. P. Pirard, J. Coll. Interface Sci., 70, 265 (1979).

111. W. H. Griest, L. B. Yeatts, and J. E. Caton, Anal. Chem., 52, 199 (1980).

112. M. R. Shure, Ph.D. Dissertation, Colorado State University, Fort Collins, Colorado, 1981.

113. B. R. Appel, S. M. Wall, Y. Tokiwa, and M. Haik, Atmos. Environ., 14, 549 (1980).

114. F. W. McLafferty, "Interpretation of Mass Spectra," University Science Books, Mill Valley, California, 1980.

115. S. H. Cadle, R. J. Countess, and N. A. Kelley, Atmos. Environ., 16, 2501 (1982).

116. L. D. Hansen, G. L. Fisher, C. E. Chrisp, and D. J. Eatough, "Polynuclear Aromatic Hydrocarbons," M. Cooke, A. J. Dennis, and G. L. Fisher, Eds., Battelle Press, Columbus, Ohio, p. 507,1981.

117. M. M. Hughes, D. F. S. Natusch, D. R. Taylor, and M. V. Zeller, "Polynuclear Aromatic Hydrocarbons: Chemistry and Biological Effects," A. Bjørseth and A. J. Dennis, Eds., Battelle Press, Columbus, Ohio, p. 1, 1980.

118. R. Dlugi and H. Güsten, Atmos. Environ., 17, 1765 (1983).

119. T. Nielsen, Environ. Sci. Technol., 18, 157 (1984).

120. K. Wark and C. F. Warner, "Air Pollution; Its Origin and Control," Dun-Donnelley Publisher, (1976) p 399.

121. Chem. Eng. News, 62, 21 (1984).

# APPENDIX

# APPENDIX 1

## THE BRUNAUER-EMMETT-TELLER GAS ADSORPTION TECHNIQUE

The BET gas adsorption method is based on the original research on surface area measurements by gas adsorption as described by Brunauer, Emmett, and Teller (BET),[106] and the technique discussed here is an adaptation of the procedure used previously by the Analytical Chemistry Division at Oak Ridge National Laboratory. The method is completely automated, the instrument control and data acquisition being performed by a Hewlett-Packard 9835A desk-top computer. The program, written in BASIC, solves various equations for the variables that have been ascertained by various measurements during the experiment. The variables measured are:

$V_t$ = Total volume of gas in the manifold at STP.

$V_b$ = Amount of gas remaining in the manifold after sample-adsorbate equilibration.

$N_c$ = Correction for non-ideal behavior of $N_2$ at liquid $N_2$ temperature.

$V_s$ = Amount of gas at STP that fills the dead volume in the sample.

$V_a$ = Volume of gas adsorbed.

X = The reduced pressure.

$P_2$ = $N_2$ pressure after equilibrium is achieved.

$V_s = V_t - V_b$.

$V_a = V_t - (V_b + V_s)$.

$N_c = 1 + P_2\ (0.5/760)$.

An apparatus of special design is used which permits one to evacuate the sample container and allows measurement of the pressure, temperature, and volume of the gases used in the measurement (usually $N_2$ or He). A known mass of adsorbent is outgassed by heating and pumping and this is introduced into the sample container. The unoccupied volume of the container is then calibrated by means of He gas (under the conditions at which $N_2$ adsorbs, He is not adsorbed). The sample container is then placed in liquid $N_2$. After replacing the He used for calibrating the volume of the sample container with $N_2$, the volume of $N_2$ adsorbed at various pressures (after equilibration) is measured.

The evacuation system consists of a mechanical and an oil diffusion pump (evacuable to a pressure no greater than $2 \times 10^{-5}$ torr). The pumps are isolated from the system via a liquid nitrogen cold trap. Evacuation of the system can be achieved either through a pneumatic valve (for rapid evacuation) or through a needle valve (for controlled evacuation of powdered samples).

The Hewlett-Packard 9835A desk-top computer is interfaced through a 98032A 16-bit I/O interface card to a Hewlett-Packard multiprogrammer. This multiprogrammer is then interfaced to individual solenoid valves and to the heater control switch. The computer can activate or deactivate all of the solenoid valves in the system. Pneumatic valves are used to minimize temperature variations in the manifold and are controlled by solenoid valves. Pressure is measured by three pressure transducers. A switching device (to determine which pressure transducer to use depending on the pressure to be measured),

an amplifier, and a digital output device are also incorporated into the system. The digital output device is interfaced to the computer through a 98033A BCD input interface which allows the computer to read the pressure directly.

Three thermocouples (chromel-alumel) are connected to a Sanlab 102 ten-channel thermocouple scanner, and the scanner is interfaced to the multiprogrammer. This allows the computer to activate the scanner select, and read the thermocouple voltage. The first thermocouple is used to measure the manifold temperature, the second to measure the temperature of the sample cell, and the third to measure the degassing temperature.

The manifold system is constructed of 6.35 mm OD copper tubing and the necessary pneumatic valves. This system is also used as the calibration system.

The data collected (volume adsorbed versus adsorbate pressure) are used to calculate the specific surface area. Using the applicable equations, these same data can be used to calculate t-plots and porosity distribution information as well as adsorption isotherms.

Desorption isotherms are just the opposite of adsorption isotherms in that adsorption isotherms are obtained by experimentally starting with no gas (near zero pressure) and increasing the pressure in the appropriate increments. Desorption isotherms are obtained by starting a sample (after pressure equilibration) at a pressure near the saturation vapor pressure and then decreasing the pressure in increments.

# VITA

Robert Alonzo Yokley was born in Hohenwald, Tennessee, on September 10, 1946. After attending elementary schools and high schools in Indiana, Maryland, and Tennessee, he graduated from Lewis County High School, Hohenwald, Tennessee in May, 1964. He entered Middle Tennessee State University in 1966, left school for a tour of duty with the United States Marine Corps, and reentered Middle Tennessee State University in June, 1971. He graduated from that University in December, 1972 with a B.S. in Chemistry. From May, 1973 through December, 1979 he was employed with the Food and Drug Division, Tennessee Department of Agriculture, Nashville, Tennessee, as an Analytical Chemist. In January, 1980 he entered graduate school at The University of Tennessee, Knoxville.

The author is a member of the American Chemical Society, Analytical Division and the Society for Applied Spectroscopy. In June of 1972, he married Yvonne Carol Lee of McMinnville, Tennessee, and is the father of a daughter, Yasminda Lelanya, born in December 1973.

Mr. Yokley will be employed with the Coal Research Division, Conoco, Inc., in Library, Pennsylvania upon completion of his Ph.D. requirements.